

# VALIDATION OF A SCALABLE SOLAR SAILCRAFT\*

D. M. Murphy, ATK Space Systems, Goleta, California

## ABSTRACT

The NASA In-Space Propulsion (ISP) program sponsored intensive solar sail technology and systems design, development, and hardware demonstration activities over the past 3 years. Efforts to validate a scalable solar sail system by functional demonstration in relevant environments, together with test-analysis correlation activities on a scalable solar sail system have recently been successfully completed. A review of the program, with descriptions of the design, results of testing, and analytical model validations of component and assembly functional, strength, stiffness, shape, and dynamic behavior are discussed. The scaled performance of the validated system is projected to demonstrate the applicability to flight demonstration and important NASA road-map missions.

## INTRODUCTION

At the start of 2003, ABLE Engineering (now part of ATK Space Systems), in parallel with other activities<sup>1</sup> also under the purview of the ISP projects office at Marshall Space Flight Center (MSFC), began developing scalable analytical tools and advanced design technologies for a solar sail system, which led to 2 follow-on phases for System Ground Demonstrator (SGD) development and validation. These efforts, led by ATK, were performed with the assistance of the Systems Technology Group of SRS Technologies (sail assembly provider), the Langley Research Center (LaRC) for sail shape and dynamics modeling and test execution, Arizona State University (ASU) for attitude control modeling, Princeton Satellite Systems (PSS) for sailcraft control software, and the MSFC Space Environmental Effects (SEE) Laboratory (materials characterization and life evaluation).

In the first phase of the program (6 months) activities were focused on design and analysis refinement of the initial sail system concept<sup>2</sup> and refinement of plans for hardware development and demonstration<sup>3</sup> in Phases 2 and 3. The Phase 2 effort encompassed design, fabrication, and validation—through a series of component and system tests—of a 10-m Quadrant (1 sail, 2 masts). Validation activities culminated with the demonstration of deployment, and sail shape and system dynamics measurement in vacuum at LaRC in April of 2004.<sup>4</sup> Analytical correlation activities demonstrated that gossamer mast and sail subassembly and system behavior were predictable.<sup>5</sup>

In Phase 3 a larger and more complete sail system was designed, fabricated, and demonstrated,<sup>6</sup> first in ambient conditions at ATK-Goleta, and later at a large vacuum chamber facility in April and May of 2005. The 20-m hardware represents a flight-worthy full (4 sails, 4 masts) system including an instrument offset boom, additional mechanism dual-purposed for deployment and attitude control, tie-down/release hardware, solar panels, and launch vehicle interfaces, integrated together in a carbon-composite central assembly that also functions as a bus chassis.

Further descriptions of the hardware are provided herein, along with a review of some of the critical design developments important to the evolution and success of the SGD efforts. Lessons learned in the development of subsystem hardware on the 10-m Quadrant were integrated into design and analysis activities supporting the build and test of the full sail system. The evolution and integration of added systems in the 20-m sailcraft are described. Results of 20-m system validation activities are emphasized, followed by sail material life testing results, scaled performance discussion, and concluding remarks.

## TECHNOLOGY MATURATION

The ISP projects office at NASA headquarters prioritized the maturation of solar sail propulsion technology readiness in order to enable or enhance a variety of road-mapped space science missions.<sup>7,8</sup> Solar sails, especially as a system, present complex engineering challenges. In particular, the difficulty of validating modeling—through testing in a fully representative environment prior to flight—has thus far discouraged near-term mission planners from utilizing this enabling propulsion technology.

The ground system demonstration and validation accomplishments of the S<sup>4</sup> SGD program were planned to systematically reduce the risk of flight implementation through building increasingly more complex solar sail systems together with testing of the highest fidelity possible in the terrestrial environment. The progression of major hardware builds over the program is depicted in Figure tbd. Incremental design and demonstration was pursued to minimize

---

Approved for public release; distribution is unlimited. (tbd)

\* This effort was performed under sponsorship of the NASA In-Space Propulsion Program, directed by Marshall Space Flight Center under contract no. NAS8-03043.



cost and risk while methodically elevating the Technology Readiness Level (TRL) of dependant systems prior to full system demonstration.

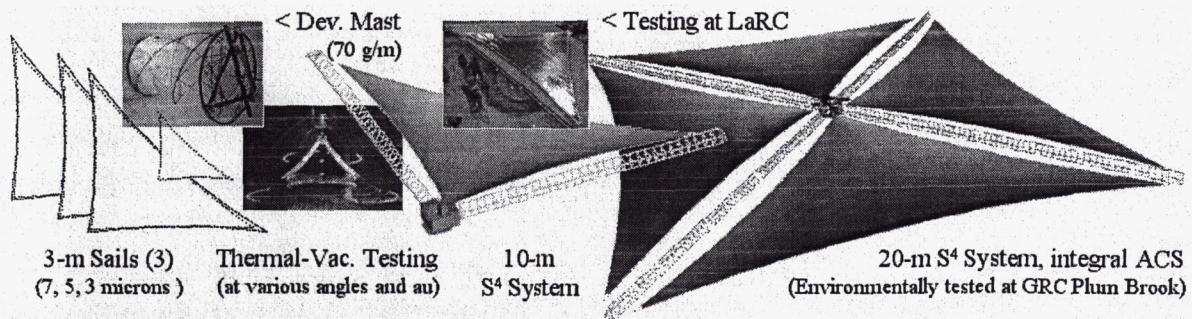


**Figure tbd. ISP Program Milestones: Progressive Growth in Technology Maturation, Size, and Complexity**

Early in the first hardware development cycle (Phase 2 of the 3 phase program), CP1 sails and prototype graphite coilables were assembled and tested. Then to culminate Phase 2 a ¼-symmetry deployable system 10 meters in size was built and tested. The ¼-symmetry of the S<sup>4</sup> system allowed a Quadrant to be built that validated fundamental aspects of the full system while minimizing overall costs. In the 3<sup>rd</sup> phase a complete 20-m S<sup>4</sup> system was built and rigorously tested, validating both the hardware design and scaled analytical and computer models. Testing activities in Phase 3 included sail assembly deployment trials at SRS, subsystem evaluations at ATK—prior to and during system integration and check-out, launch venting at Wyle Laboratory, vibration testing at Environmental Associates, and most importantly: system deployment, functional demonstrations, and shape and dynamics measurements in the 100-ft-diameter thermal-vacuum chamber at the NASA Glenn Research Center (GRC) Plum Brook facility. Extensive membrane evaluations and life testing<sup>ref</sup> at the SEE laboratory took place in parallel during Phase 2 and 3, results of which are summarized herein.

## SUBSYSTEM DEVELOPMENT AND DEMONSTRATION

As mentioned earlier, various S<sup>4</sup> hardware subsystems were designed and demonstrated incrementally in the 3-phase ISP program. After the studies completed in the 6-month Phase 1 period, key subsystem technologies were build and demonstrated in Phase 2. Namely, two Engineering Development Unit (EDU) masts and a number of sail assemblies. Longer masts and a thinner, refined sail assembly were built next and integrated together into a deployable quadrant of the symmetric sail system, as shown in Figure tbd. The central assembly was a low-fidelity structure of aluminum plates, which served as housing for the stowed masts and sail, and the mechanism necessary for their deployment. It was left to the 3<sup>rd</sup> phase of the program to develop a flight-representative carbon-composite central structure, and to add other mechanisms (e.g. ACS actuators). These advancements, together with larger, lighter sails and longer masts, allowed the S<sup>4</sup> sailcraft systems to be completely demonstrated.

The 10-m system consisted of three major subassemblies: The Sail Assembly, the Mast Assembly (qty. 2), and the Central Assembly. The 7-m carbon composite mast was (as for the 20-m system) a truncated length of structure optimized for an 80-m sail system. The sail was composed of an aluminized 3-micron CP1 membrane with integral shear compliant borders and carbon-fiber edge cords.<sup>11</sup> The subassemblies and the system were put through a complete series of ambient and vacuum testing. The design features and evolution of the mast and sail hardware are discussed next, followed by the results of subsystem and 10-m Quadrant testing.

### THE MAST

The sail masts are an advanced version of the continuous coilable longeron structures ABLE has flown 27 times in space, with 100% success. The *graphite* coilable design incorporates design advances which provide minimum-mass configurations appropriate to the gossamer loading of a sail mission. The coilable is a very mass-efficient elemental structure: A 34 g/m sail mast with a stiffness >10,000 N·m, has been demonstrated.<sup>ref</sup> This mass is less than 1/7<sup>th</sup> the mass of an equivalent diameter heritage coilable.

EDUs of the new mast were developed and tested first, before the units for the Quadrant were fabricated. The first ultra-light carbon coilable was constructed of off-the-shelf composite, as the focus was on new gossamer concepts for the 2DOF structural joints along the longeron at the interface of the battens and diagonals. This “node” design, which was also radically optimized for mass production, proved unsatisfactory in strength and kinematic reliability. A second EDU (also 10 bays in length) was built with fittings derived from flight-heritage masts, but sized much smaller and composed mostly of magnesium. The kinematic function and strength of these new fittings proved robust and lightweight (less than 10% of the mast mass). This mast also successfully demonstrated new custom-pultruded IM9 graphite composite structural members (longerons and battens). The linear mass of this 40-cm diameter mast design was 70 g/m. The functional validation of this new gossamer sail mast design provided the



confidence to proceed with the fabrication of the two 7-m (31-bay) masts needed for the 10-m Quadrant Assembly. The same basic structural design (simply longer in length) was used for the 20-m system as well, so the results of EDU and 7-m mast testing, reviewed in detail in reference tbd, are directly applicable to the Phase 3 14-m masts. In summary, the 7-m masts met the expected linear compaction factor (0.85%) when stowed. Deployments were performed horizontally with an overhead rail car for tip off-loading. The masts, which self-deploy due to strain energy stored when coiled, were measured to provide a push force of nominally 7 lbs, as was predicted by closed form calculations. Stiffness and strength were evaluated using lateral tip deflections imparted by a simple setup consisting of a pulley and various weights. The deflections were measured using a laser tracking system that followed a corner cube mounted on the mast tip ground support equipment (GSE). As the masts are self-supporting at a 7-m length, free vibration could also be documented with the laser tracker. The first bending mode was calculated from averaging the vibrations over the first 10 cycles. The bending stiffness could not be measured directly as one third of the compliance under lateral tip loading is due to mast shear stiffness (GA). A pre-test FEA model of the mast, which captured shear and bending compliance, predicted the dynamic behavior. Post-test correlation showed close agreement between the estimated and measured first mode, demonstrating that the coilable is generally a very predictable, readily-modeled, linear structure. However, longer masts and or substantially lighter designs are susceptible to stiffness—and hence also strength—reduction due to local and global imperfections.<sup>ref</sup> A key feature of the coilable is that the *open-lattice* eliminates the possibility of asymmetric thermal loading, in which hot-side vs. cold-side strains induce bow. A potential for thermal bow arises if the sun angle is such that one structural element shades another. This can be overcome by building a 180° twist into the overall length of the mast, an approach which has flown several times.

### THE SAIL

In efforts in parallel with the EDU masts, SRS Technologies began developing fabrication equipment and processes for assembly of the sails. The first ISP-program sail incorporated 5-micron sail material, adhesiveless seaming processes and new border and cord designs. This sail assembly, named the Workhorse Sail, was critical for the timely development of packaging and deployment methods. Various further developments in design and fabrication methods were incorporated on a second 5-micron sail. In particular, sequencing elements developed using the Workhorse (to provide a managed deployment) were incorporated. This Refined Sail (RS5) and a third sail (RS3) incorporating 3-micron film and further upgrades were both used for system level test and modeling correlation performed at LaRC.

The sail material is a thermally-imidized polyimide material developed by NASA LaRC and produced under exclusive license by SRS Technologies. This material has had significant space environment exposure in both real and simulated environments. More than 10,000 ft<sup>2</sup> of material (< 3 mil) has flown on Boeing GEO spacecraft since 1999. The material has been flight qualified for a 15-yr exposure in a GEO environment. In addition NASA ISP has done extensive testing of sail gauge ( $\leq 3$  micron) CP1 material in simulated UV and radiation environments.<sup>3 by Edwards</sup>

The sails built were all configured as triangular “quadrants” with scalloped edges, with 3-point-attachment to structure. A strong motivation behind the selection of a 3-point-attach configuration is to ensure planarity, regardless of intra-sail optical or mechanical anisotropy, system orientation to the sun, or thermal cycling. The border scallops are trimmed with a high-strength graphite cords that impart robustness for handling and deployment. Inboard of the cords is a “ruffled” border area that allows thermal and mechanical strain decoupling to the main sail. These elements insure uniform stress in the sail, which further assures predictable shape and high propulsive efficiency. When designed with a modest scallop (90% sail-level fill factor), the border controls these various edge effects without significantly increased boom loads. Sequencers (located along the borders in the final design) control the deployment of the sail. As can be seen in the figure below, the delicate sail material (< 2 microns for ST9) is kept away well from the masts and is staged deterministically. Deployment, stowage (in a matter of hours), and re-deployment are reliable and repeatable.

The sails are grounded by halyards to the mast, which is part of the structural path linked to spacecraft ground. Grounding of the joined membrane sections is achieved through the combination of conductive adhesive patches between materials that bridge the conductive aluminum coating and mechanical grommet connections that attach to the 3 halyard corner attachment points. This method was verified on multiple sails made for the ISP program, where only the coated side of the membrane was grounded. The anti-sun side of the sail was left uncoated to maximize thermal emission from the base CP1, which is optically clear. The necessity of rear-side or bulk sail conductivity has been debated by leading electrostatics engineers. SRS has developed methods for enhancing the bulk conductivity of CP1 by addition of carbon nano-tubes to the resin matrix. This provides a surface resistivity in the range of 10<sup>6</sup> ohms/square, which can be utilized to reduce risks from plasma interactions. In addition, this black CP1 has a greatly increased emissivity, which allows closer solar approach mission trajectories.

A solar sail quadrant is necessarily constructed of a disappearingly thin and therefore delicate membrane. The fundamental challenges are to fold for stowage in a manner effective for compact packaging and launch survivability, to utilize a process that is time and manpower efficient, as well as scalable, and to permit effective ground demonstration. When deploying on-orbit the kinematics must insure low mast loading, with reliable and deterministic



staging throughout the deploy sequence. Most critically, the approach must support the key metric for a solar sail: low areal mass density. Our team developed and tested a number of different approaches over the course of the program, that finally supported all of the goals necessary for robust high performance sail systems. The evolution in the stowage and deployment design and functionality from the Workhorse Sail to the final 20-m sail is reviewed in references tbd and tbd. The specific placement and design of the sequencers used on the 20-m sail is depicted in Figure tbd in reference tbd. The solar sail quadrant is folded for stowage first in lines that run parallel to the midline (bisector). Such folding can also apply to the manufacture of the sail, which means the assembly room need only be about half as long as the sail square dimension and as wide as two sections of membranes being joined. The folded sail is rolled onto a lightweight composite drum, which is installed into the central structure. The stowage procedure is time and manpower efficient, and completely scalable. Sequencing elements are distributed on the perimeter of the sail, where the strength is substantial due to the embedded cord. This allows the main sail to be constructed of the thinnest producible materials for lowest areal mass density. When deploying on-orbit the kinematics will insure low mast loading, with reliable and deterministic staging throughout the deploy sequence.

## 10-m QUADRANT DEMONSTRATION AND VALIDATION

After completion of the mast and sail subassembly validations in Phase 2, the integrated 10-m Quadrant was prepared for test. In order to validate deployment characteristics as well as sail shape and system dynamics, a series of tests were planned utilizing a LaRC vacuum chamber facility. Testing in vacuum is necessary because both the deploying and deployed dynamics of a sail would otherwise be greatly affected by the surrounding air mass. As an illustration, the air within 2 mm of either side of the sail surface is alone equal in mass to a 3-micron sail film. All sail dynamics testing at LaRC took place at pressures near 1 torr. The priorities for testing were first to validate deployment, second to measure deployed shape of the (horizontal) sail billowed under gravity loading, and third, to validate models for system dynamics. The ABLE/LaRC test team planned an extensive series of tests to capture the data needed to support these priorities, as well as to meet goals for developing test methods applicable to 20-m testing and to in-flight investigations.

The testing sequence and findings were reviewed in detail in references tbd and tbd. In summary, formal testing at LaRC with the 10-m Quadrant began on March 30<sup>th</sup>, 2004 with an ambient deployment of the system to verify the GSE setup after shipment and installation in the vacuum chamber. A large tear was experienced, which led to further evolution in the sequencer design. With the system deployed in a horizontal condition measurement of sail shape was undertaken. Knowledge of shape is critical for two reasons. Firstly, global shape affects cp-cg offset torques (in-flight) and the modal response of the GSD sail. In general, the ability to confidently predict approximate frequencies of the first few system modes is essential for control system design for flight. Secondly, fine scale topology is critical the thrust performance. LaRC employed a laser radar scanner system to allow measurement of the entire sail surface with high accuracy. Shape data was obtained on both the RS5 and RS3 sails, and comparing the global billow to the predicted shapes gave reasonable agreement, typically within 3 cm across the 10-m sail. A second ambient deployment was conducted April 6<sup>th</sup>, where again, data on mast and sail deploy speed, motor current (convertible to lanyard and halyard loads), and tack line tension were recorded, as well as imagery from two fixed position digital cameras and three pan-zoom video cameras. An image from one of the digital cameras is shown in Figure tbd. The repaired tear is evident at the right. The gossamer masts are hardly visible, but the distribution of photogrammetry targets and the sail compliant borders are brightly lit.

Mast dynamic testing was performed with excitations magnetically coupled in at the 6<sup>th</sup> bay. Using laser vibrometer targets at the mast tip, the in-plane and out-of-plane first bending mode and the first torsional vibration mode were captured. Greater mass distributed along the mast (harnessing and vibrometry targets) and at the tip, in combination with the central structure and GSE flexibility, resulted in lower mast modes (4.4 vs. 5.7 Hz) than were recorded during earlier component level testing at ABLE, and slightly lower than (pre-test) predicted (4.7 Hz) for the integrated masts. The first 4 modes of the system were captured

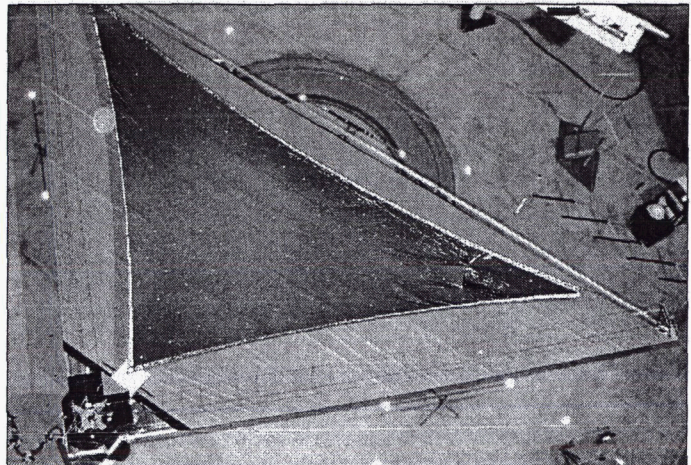


Figure tbd. 10-m Quadrant Test at 16-m LaRC Vacuum Facility

in test, and overall the agreement to the predicted shapes was reasonable. The first FEA mode frequency was lower (by 10%) than found in test, which could be expected given the FEA shape result over-predicted the billow depth



(likely due to halyard tension uncertainty and load angle variation) which leads to an under-prediction of the first mode frequency. The higher frequency modes were also found to be shaped as predicted. The FEA frequencies were generally higher, as they are more dependant on mesh density, effective extensional modulus, and stress distribution, which are interrelated in the prediction of local shape and stiffness.

## SCALABLE FULL SYSTEM DEMONSTRATION

### DESIGN EVOLUTION

The soundness of the fundamental elements of a deployable integrated sail and structure were validated with the tests performed on the 10-m quadrant. But the low fidelity of the central structure and the lack of representation of a full compliment of sails and other hardware necessary to complete the  $S^4$  architecture left a significant level of risk in the 20-m system design definition, which began shortly after analytical correlation and reporting on the Quadrant test series. Major elements added to the design consisted mainly of attitude control mechanisms. But the best implementation forced complete redesigns for the tip and central structure mechanisms, as well as the incorporation of associated actuators and electronics. Demonstration of a flight-fidelity central structure and the pursuit of an integrated sailcraft philosophy (rather than a propulsion "backpack") were also major objectives achieved. A discussion of the major changes and challenges between the 10 and 20-m systems is tabulated below.

**Table 1. Design Changes and Challenges: 20-m vs. 10-m Demonstrator**

$S^4$ System	Quadrant took advantage of the 1/4-symmetry of a square sail. The 20-m is a complete system, structured to act as a sailcraft bus chassis: with integral solar panels, ACS, and PAF interface.
Mast Assy	Added elements added inside each batten to guide the traveling ballast bars (ACS pitch and yaw control) down the centerline.
Sail Subassembly	4x larger. Thinner material, shallower scallops, thinner cords, and ripstop elements. Folded first in a direction opposite to 10-m sail design. Deploy sequencers moved to edge cords, and redesigned.
Central Structure	The 10-m central assy was a low fidelity aluminum structure, which served as a volumetric housing for the masts and sail (and the 1 <sup>st</sup> generation deployment mechanisms). The structural approach was upgraded to a flight-worthy light-weight construction.
Central Mechanism	With the addition of ACS, a complete overhaul of the central mechanisms was needed to minimize overall mass and complexity. ACS controls combined with mast & offset boom deploy functions.
Mast Tip Mechanisms	With addition of movable spreader bars for roll ACS at mast tips, necessary mechanism complexity at tips increased significantly.
Electrical Sensors & Drivers	Added to central assy and tip plates: Motors/driver boards for reeling up the sails at the mast tips and for running the ballast masses, limit switches and optical sensors to provide end of travel indications, load cells for added sail deploy diagnostics, and $\mu$ PPT controls.

Another element "added" to the system was an instrument offset boom. In the original  $S^4$  concept,<sup>ref</sup> such an appendage was configured to extend the spacecraft host bus away from the sail so that it could be gimballed to provide propellantless attitude control (in pitch and yaw). In Phase 2, when a detailed trade of ACS options was undertaken,<sup>ref</sup> an alternate approach was adopted. But an offset boom demonstration was retained due to its general utility as an instrument platform. The  $S^4$  design offers the option for an offset boom(s) to deploy instruments fore and/or aft of the sail. The maximum length of offset boom (that stows fully within the central structure, which is not a requirement, but was demonstrated) is approximately 25% of the sail size. The 20-m system was configured for instrument deployment 2.3-m to the anti-sun side, as this direction is preferred for an earth-orbiting validation mission. The mass of bus components on the sun-side deck of the central structure could be balanced by the instrument mass (e.g. cameras), given the proper boom length, to create an attitude-neutral sailcraft (preferred to a cp-behind-the-cg stability approach for the reasons given in reference tbd).

In a solar sailing demonstration mission of  $S^4$  technology, the need for photogrammetry is weak to non-existent because the sails will be flat (1 cm depth at 1 psi, 5 cm at 0.1 psi), unless a deployment anomaly occurs. However, cameras are ideal to best document a nominal deployment (particularly membrane management), and would be invaluable to investigate anomalies if they occur.

### 20-m SYSTEM DESCRIPTION



The evolved  $S^4$  system integrates gossamer coilable mast and sail membrane technology, solar arrays, launch tie-down and release mechanisms, and attitude control actuators, efficiently packaged within structure shared by other bus components and mission payloads. These subsystems together form a generic scalable sailcraft possessing reliable deployment, structural robustness and determinate sail shape with—most critically—minimized overall mass and volume. CAD representations of the 20-m  $S^4$  sailcraft system built in Phase 3 are shown in Figure tbd. The mast structures used here were “truncated” in length, meaning the diameter (40 cm) was sized for the needs of an 80-m system. As the system “size” is 20 m from mast tip to mast tip, approximately 14 m-long masts were required. The central assembly, approximately 1-m across, was sized to hold enough mast structure for a 40-m sail system. The sizing choices made for the central assembly and masts were to allow the maximum benefit from design, fabrication, and validation activities in the ground demonstration toward a flight validation of a 40-m class  $S^4$  sailcraft.

The packaged sails and masts are arranged symmetrically around a central bay which houses the stowed offset boom and mechanisms used for tiedown release of coilables and sail bay panels (solar arrays), deployment of the coilables, and ACS mechanism control. The remaining volume is used to store the sails, which are packaged on drums which possess rate-limiting constant torque devices and load sensors. Only a single motor is needed for deployment of each structural axis and later, to control ballast bar position for attitude control. During deployment, the tiedowns and instrument boom are released first. Next come the sail masts pairs, deployed sequentially under rate-limiting control of a common lanyard tape spool (part of the central mechanisms). The coilable self-deploys by the strain energy of its stowed longerons. To assure kinematic determinacy the base end is biased to erect first and the transition zone progresses outward with the tip as the lanyard is payed out by a rate-controlled stepper motor. With masts fully erected, the sails are deployed next, in unison, by motors at the mast tips. Later these same motors are used for spreader bar rotation (roll ACS). Sequential operation simplifies mechanization, increases ground testing fidelity, and improves reliability.

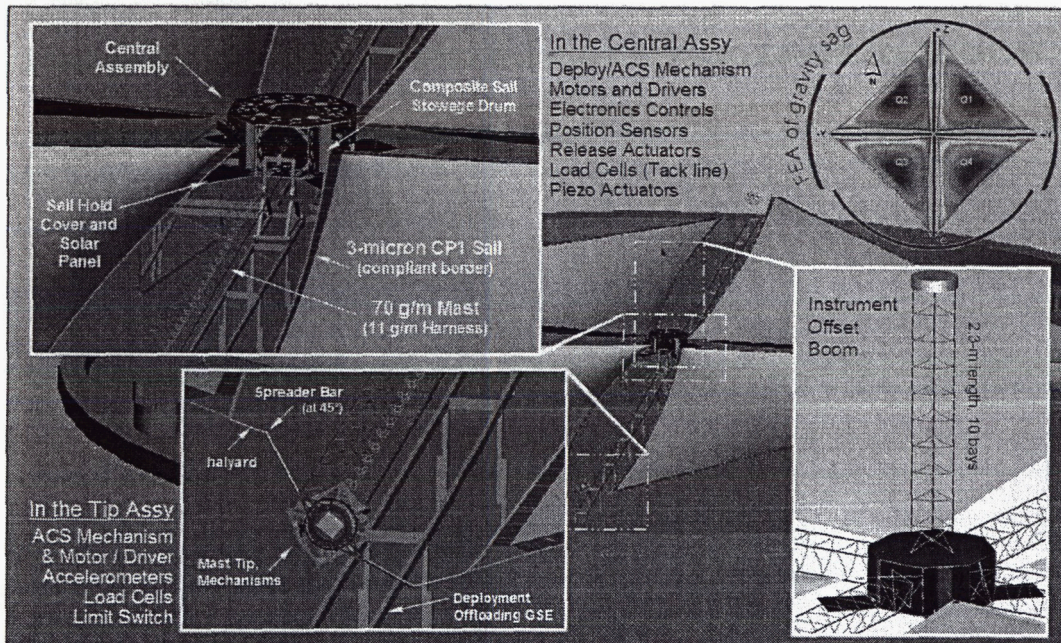


**Figure tbd. Depiction of a 20-m  $S^4$  System in Plum Brook Chamber with Details of Major Subassemblies**

As can be recognized in the figure above (TBD), the sails are connected to structure at three points, which provides for a deterministic structural loading condition and assures a planar sail shape. At the tips of the masts adjacent sails are tied to a spreader bar with near-constant-force (Negator) springs to assure steady tension regardless of sail temperature, which varies with solar orientation. If all spreader bars are rotated off flat in unison, the quadrants form a slight “windmill” shape. Solar forces then create moment that is used to effect roll control. Pitch and yaw control are integrated to the sail system in a method that dual-purposes the mechanisms: Each mast axis is deployed with a motor-controlled lanyard, then this motor and lanyard is used to move a ballast bar that adjusts the center of mass (cm) relative to the center of pressure (cp) of the sail.

The 20-m  $S^4$  system demonstrated a significant number of flight-applicable embedded control systems and sensors. The utility of each in a flight application, chronologically arranged following deployment initiation, is detailed here:



- Separation nut firings indicate tip plate release (1 per mast). Their current is monitored to insure heating is occurring. This activity can be validated with co-located thermal sensors. The initial motion of each mast when the tiedown is released can be validated by the accels on each mast tip. Each sail bay door (which also functions as a solar panel) opens when the adjacent mast kicks over at the base (when about 8 bays are deployed). This will also be evident in the accelerometer traces (and to the spacecraft as a power production change).
- Current monitoring of the deploy motors (one per axis) will be evidence of the mast pairs deploying nominally (they are retarded by the motor and lanyard system).
- The sails are hoisted using halyards that are reeled up onto spools at the mast tips. Current monitoring of these deploy motors (one per tip) will be evidence of the sails deploying nominally (a profile for motor current would be predeveloped).
- The halyards run over pulleys at the ends of the spreader bars. As the halyards are tensioned the bending load in a spreader arm is reacted by a load cell in the "armpit". This sensor monitors the deployment loads, and the deployed forces applied to the sail over time, such as the small changes in load with spreader bar angle adjustments.
- The sail drum is mounted with a load sensor at one end. This allows the load into the sail at the tack corner to be monitored while the sail is deploying, and also provides the deployed load over the mission (redundancy in 3-point deployed system state knowledge). The load profile during deployment experiences peaks as each sequencer loads and then breaks, and in between...the load is a function of the retarding torque provided by the ratchet on the other end of the drum.
- The accelerometers on the mast tips are useful for motions during deployment (as mentioned above) *and* after. The accels will provide a second record of the timing of the sequencer releases as the sails deploy. And after the system is fully deployed, they will allow interrogation of the modes of the system.
- Once the final kick-over of each deployed mast has been observed (accelerometers again), drive-able piezos located in-line with the mast longerons (at the root) can be used (in conjunction with the accels) to interrogate the bending modes of the masts (prior to sail deployment).
- The accelerometers are also useful to monitor loading from spin rate (steady state g's are readable) if used to assist deployment, and reactions from any later attitude control maneuvering.
- The embedded ACS system (ballast bars and spreader bars) telemetry will involve motor current and position sensing. Bar positions are calculated from motor step count and home switches are included to insure that knowledge of the absolute position can be obtained if step count is lost.
- The controls for the stepper motors, located on the mast tips, are kept warm by an auto-regulating heater circuit. And temperature is monitored there, at the tie-down actuators, the central motors, and at other key locations by numerous RTDs.

All these embedded elements were present and validated on the 20-m system at Plum Brook. The information that can be captured by clever employment of these devices will form an invaluable companion to the critical deployment imagery acquired by cameras on the offset boom. Tracking of localized areas of interest (boom unfurling, lanyard advancement, tip kickover, ballast movement, spreader bar motion, halyard mechanization, sail synchronization, etc.) during deployment and close inspection of deployed sail surface morphology would be best enabled by a pan-tilt camera. Documentation of deployment is of primary interest, followed by identification of shape and fundamental system modes. Since the sail is nominally flat, and the targets will have been applied in known locations, the verification of nominal shape (global and local) in any area can be accomplished with study of imagery from a single camera with changing lighting conditions. Fundamental system modes can also be captured with imagery, but would require significant frame rates. Due to the small displacements involved, a better instrumentation option is an accelerometer. As described above, 20-m system demonstrated the inclusion and operation of a suite of accelerometers and a host of other embedded systems for full interrogation and nominal/fault behavior identification.

Attitude control after tip-off, during deployment, while sailing, and after sail jettison, must all be accomplished with reliable and low-mass solutions. The  $S^4$  system utilizes a propellantless method of 3-axis control (described above) that relies on solar pressure on the extended sails. For a mission where the sail is jettisoned at some point, a traditional bus ACS may be employed, and may also be used during deployment. Thrusters may be a more cost-effective method for control given the short term of a validation mission. The propellant tank can be sized to also provide for the required de-orbit. Recommendations for primary, secondary, and backup ACS types and control during deployment and other mission scenarios, are discussed in detail in reference tbd. The primary (sail) ACS together with a reaction gas system on a host spacecraft is a robust pairing for a flight validation. For typical science missions, backup control of a large sailcraft could potentially expend all gas reserves and would require outlandishly large wheels. A secondary ACS utilizing mast-tip-mounted pulsed plasma thrusters (PPT) was presented as a new lighter weight, lower cost, more robust alternative in reference tbd. PPT-based ACS provides more reliable capability for recovery of attitude given any off-nominal conditions, including tumbling, that cannot be handled by either the



propellantless primary ACS or by conventional ACS within at the center of the system. PPT attitude control would be particularly useful for 3-axis stabilization of a sailcraft after release from the launch vehicle, during deployment, and for pre-flight sail checkout operations on a science mission where total mass is at a premium, secondary control is warranted, and the sail is not jettisoned prior to the completion of the mission. Discussion of the state-of-the-art in  $\mu$ PPT technology, performance requirements for solar sails, and pulse-modulated control design and simulation results were presented in reference tbd. Development and test of a demonstration system are reviewed in references tbd and tbd.

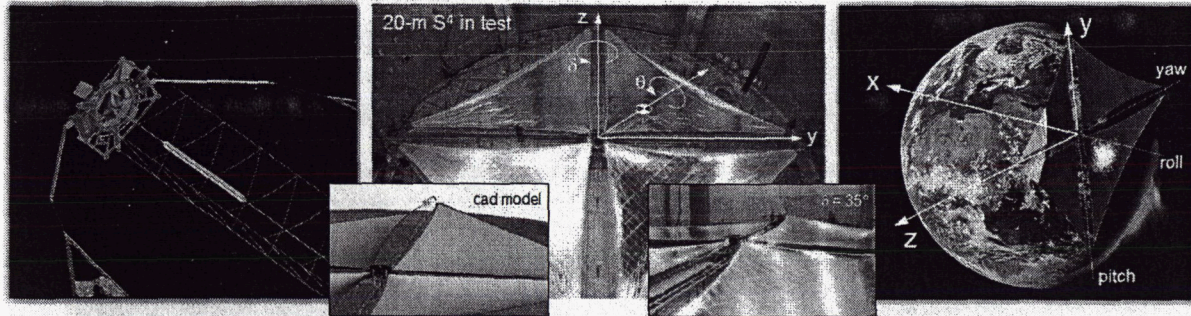


**Figure tbd. ACS Coordinate Definition and Depictions of Systems in Use**

The 20-m hardware demonstrated the rate and range performance of the mechanisms which provide for primary roll, pitch, and yaw, and the interfaces necessary for  $\mu$ PPT thrusters, with associated wiring and control, at the tips of the masts. In Figure tbd is shown (from right to left) the coordinate definition, the 20-m system with spreader bars (roll control) positioned from  $0^\circ$  to  $45^\circ$  degrees, and a ballast bar (pitch and yaw control) approaching the mast tip. This lightweight, robust, propellantless ACS can be appropriately sized and designed to meet the requirements of a wide range of missions.<sup>ref</sup> For example, a 40-m class sailcraft has the following performance and stability characteristics:<sup>ref</sup>

- 35-degree attitude maneuver within 2 hours
- Thrust vector pointing range of 60 degree
- TVC pointing error of less than 1 degree
- TVC pointing stability/jitter less than 0.01 degree

The standard robust PID control logic (with saturation control loop) investigated by ASU provides zero steady-state pointing errors of the bus-fixed reference frame in the presence of constant solar disturbance torques. However, in practice, there are always unavoidable (but small, acceptable) control loop hardware errors caused by attitude sensors and actuators (misalignments, resolution, noise, etc). Additionally, the thrust vector control pointing error analysis does not include SRP modeling uncertainty errors (reflectivity, billow, creases, etc), which must be included for predicting the actual magnitude and direction of the thrust vector. SRS has developed a Solar Sail Propulsion Modeling Toolkit (SSPMT) to investigate the nuances of attitude control system design given non-nominal cp-cg conditions and bounding cases of mission maneuvering requirements. The tool kit interfaces with high fidelity finite element models to determine the shape of the solar sail under combined thermal, solar pressure, boom and inertial loads. The figure below (tbd) illustrates the importance of accurately modeling sail shape. This analysis shows that the sail billow for an 80-m  $S^4$  system will be approximately 35 mm for a 1-psi sail design. This deformation has negligible effect on the magnitude of thrust generated. However, SSPMT illustrates that the center of pressure shifts significantly as angle to the sun increases. The toolkit is also useful for evaluation of the effects of optical properties variation, sail deployment tolerance requirements, and sail damage effects on vehicle thrust and moments. SSPMT usage insures proper design margin is included in the development of the vehicle control system.

Although, control modeling with flexible body dynamics has only been initially investigated at this time,<sup>ref</sup> it is within the capabilities of the system modeling tools developed by PSS. With structural inputs from ATK, ACS margin evaluation from SSPMT, controls guidance from ASU, and mission definition from NASA, the Solar Sail Control Toolbox (SSCT)<sup>ref</sup> can be utilized to interrogate performance for a multitude of parameters in a propagating orbital analysis.



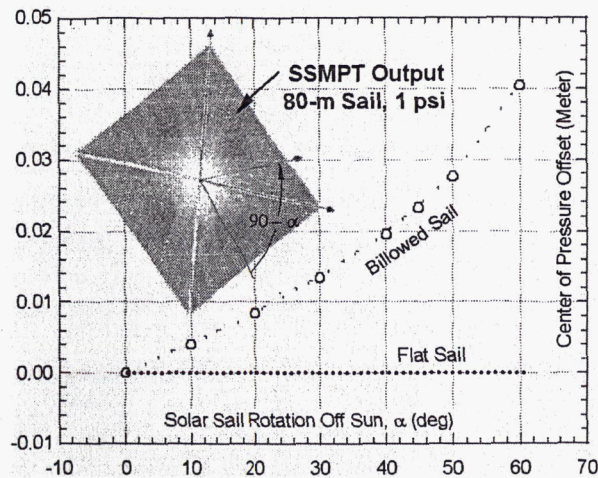


Figure tbd. Example of the Evaluation of Center of Pressure Offset Effects from FEA Shape Models

#### 20-m TESTING ACTIVITIES OVERVIEW

During the assembly of the 20-m system component evaluation was completed by form, fit, and function and some sub-assembly testing was undertaken for risk reduction. The accelerated schedule included significant design modifications to test bed hardware made in parallel with system assembly. The completed assembly passed general electrical and physical inspections, but there was only time for a few single-sail, and 1 dual-sail, functional system deployment trials before it was necessary to prepare the 20-m system was for shipment to Ohio for testing in the 100-ft vacuum chamber at NASA Glenn Research Center's Plum Brook Station. The primary formal tests for S<sup>4</sup> demonstration and validation occurred at Plum Brook. The priorities for this activity were to demonstrate deployment robustness, and to capture sufficient shape and dynamics data to allow model validation. The ATK/LaRC test team planned an extensive series of tests to capture the data needed to support these priorities, as well as to meet goals for developing test methods applicable to larger scale testing and to in-flight investigation.

Three full system validation deployments were completed: The first in ambient, the second in vacuum, and the third (also at  $10^{-5}$  torr) with a thermal gradient imposed across the stowed system. During the third deployment an intervention was required to correct an assembly error. Otherwise the deployments were successful. The key analytical validations for the 20-m system paralleled activities performed on the 10-m quadrant in Phase 2, namely shape and dynamic characterization. To capture shape data on the effects of gravity on mast droop and sail sag, LaRC employed five photogrammetry cameras to measure the system at three spreader bar positions (nominal and the two extremes). To capture dynamics data, LaRC used both external inputs and response sensors, to measure the first modes and modal frequencies of the system as well as embedded actuators and sensors that are applicable to a flight program. Shape and dynamics data compared well with pre-test analyses. A review of the testing and analytical correlation findings for each is given below.

#### SHAPE TESTING AND MODEL VALIDATION

Measurements of sag induced by gravity are predominately related to the sail, which were supported only at their three corners to the S<sup>4</sup> structure. The masts were offloaded at the tips, leaving the system grounded only at the central structure. The offload negators were balanced to place the mast tips in the same plane as the mast roots when the sails were raised. Each of the sails was delivered outfitted with a series of 41 1-inch retro-reflective targets in the field, plus 3 at the sail corners. Photogrammetry targets were placed on the mast tips to capture tip motion in plane (due to quadrant mass differences) and on the spreader bar ends to allow the rotation to be tracked as they were actuated  $\pm 45^\circ$ . The tip positions and sail sag and reference targets were then measured by photogrammetry cameras under low and high intensity lighting. Shape testing with the spreader bars at  $0^\circ$ ,  $22.5^\circ$ , and  $45^\circ$  was completed. Typical measurement precision out of plan was 0.5 mm.

The shape imparted to the 20-m sail is somewhat similar to the billow induced by solar pressure in space, but 200x greater. The stress in the sail is also significantly influenced by gravity. The nominal stress is nearly 20x higher and isotropic stress conditions are no longer possible. About half the load that would normally be carried uniformly across the compliant borders and into the scallop cords is carried instead by jumper straps at the sail corners. Consequently, the load sensors in-line with the halyards and tack line do not relate the cord load precisely, only the total load shared by the cords and jumper strap. This complicates the prediction of sail sag greatly, compared to zero-g modeling.



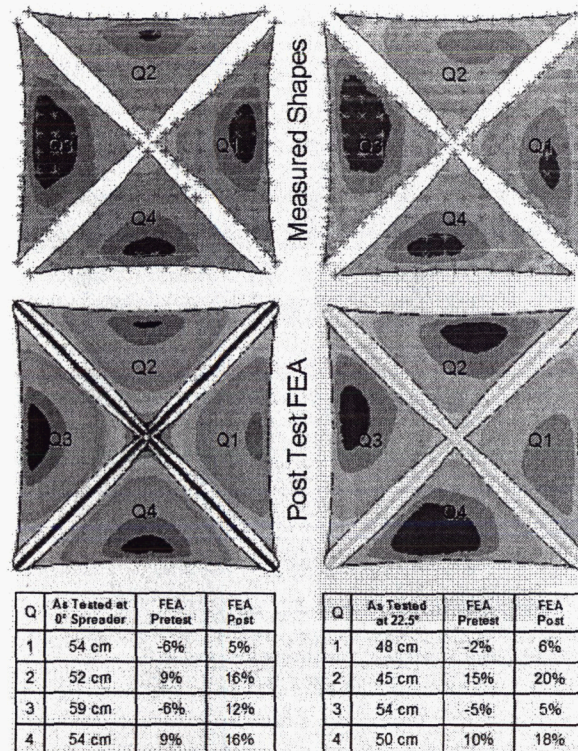


**Figure tbd. 20-m Shape Correlation Findings**

As can be seen in the tables above, the nominal error for the maximum sag deflection point is 10%. The finite element analysis (FEA) correlation did not improve when the model was updated to include measured test conditions for halyard loading and to capture the fact that the tack strap on Q4 was broken. The halyard load assumption was 6 pounds each for pre-test analysis. The loads were actually 4.1 to 6.7 lbs in test, but due to the difficulties in obtaining (1-g) sail model convergence, the loads were updated to the *average* for each sail's halyard load. This was judged a reasonable expediency as the loads themselves had a  $\pm 20\%$  uncertainty due to friction in the halyard negator mechanism. The predictive accuracy of the FEA model was improved relative to the 10-m results, even though the modeling was complicated by the sail being twice as large, the jumper straps carrying load, and the mass differences between the co-suspended sails. The latter effect caused the mast tips to move in-plane, leading to uncertainty in the halyard angles. Additional testing was performed with the goal being to measure the shape of a sail without the influences of other sails or halyard hysteresis. Testing was performed at SRS under three specified load conditions on quadrant 4. Photogrammetry was used to identify the membrane surface target locations in 3D space, and the location of the support line terminations. Simple low friction pulleys and dead weight were used to load the outboard sail corners precisely to 6 lbs. Given known boundary conditions (line angles and loads), the same sail model correlated to the measured shape with an accuracy less than 1%.

#### DYNAMICS TESTING AND MODEL VALIDATION

The 20-m  $S^4$  system is shown in Figure tbd, as oriented inside the Plum Brook vacuum chamber in the deployed test configuration. The coordinate reference frame, quadrant numbering, and excitation locations are indicated. Retro-reflective targets on the sails, mast tips, spreader bars, and various scale bars (used for photogrammetry) are visible. Baseline sail dynamics testing at Plum Brook took place at pressures from 1–2 torr.



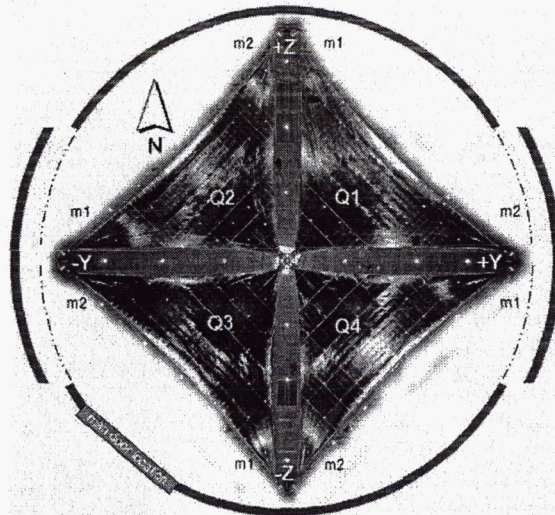


Figure tbd. 20-m System in 30-m Vacuum Chamber

Measurements of dynamic response were made primarily at the 44 retro-reflective targets on the sails, using a laser vibrometer. Baseline testing used dynamic excitation by magnetic forces (non-contact) at the quadrant corners. Other excitation methods were evaluated for their suitability to on-orbit modal investigations, such as piezoelectric stack actuation from the mast roots, spreader bar rotation (at the mast tips), and bi-morph piezoelectric patch actuation on the sail cords. The masts were tested separately, using the piezos (in ambient atmospheric conditions) to provide a baseline for the response of these primary structural members. This approach could be followed in flight as well, given sufficient time is arranged before the deployment of the sails.

The first two modes were found to agree within 1% on all four masts. The frequency responses for the Z-axis mast are shown in Figure tbd, at the left. The first mode, at 0.81 Hz, represents cantilever bending where the tip moves in plane, with slight pendulum-effect stiffening from the 1.8-m overhead support cable. The second mode is driven by mast torsional compliance and the tip mass rotational inertia. The third peak is attributed to the tip mass bouncing vertically on the support cable. The fourth peak is the second in-plane bending mode. At the right in Figure tbd is shown the response of all four masts during *system* testing. The modes are lower because the masts are supporting the weight of the sails. For system testing, the changes in tip-offloading consist of the addition of a negator spring in-line with the support cable (at the top), and a 2.3-kg counterweight mass added to the tip plate. The negator spring system provides a low frequency suspension to free-up system modes which are out-of-plane. The counterweight mass is cantilevered 1/2-m above the tip plate, to counteract the torsion imparted by the sail halyards when the spreader bar is rotated away from the 0° (balanced) position. Increases to the effective rotational inertia at the tip cause the first twist mode to drop to 0.50 Hz. The second clearly visible peak is a combined twisting and bending response at 1.06 Hz. The in-plane mode was not captured because the reflector aligned to register mast lateral motion was not captured in system testing. The observed modes agreed within 2% relative to the pre-test predictions. Piezo actuations were well behaved, resulting in exceptionally clean response peaks (note that the data in Figure tbd is plotted in semi-log format). This mode of excitation is now planned for use on the SAILMAST flight experiment.<sup>ref</sup>

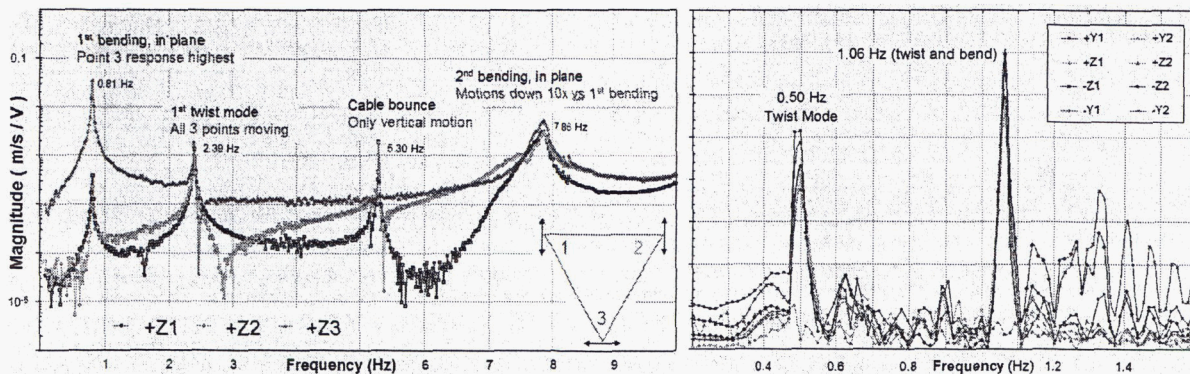


Figure tbd. Mast Tip Responses, in Ambient (L), with Sails and Counterweight in Vacuum (R)



Measurements of system dynamics were made for various magnet excitation combinations and input parameters, at both the quadrant level and system level. The lowest modes of interest on the 20-m system are dominated by the mast motions in bending and torsion. This is due mostly to the presence of the counterweight. This mass had to be used when the spreader bar is at 0°, because the off-loading negator provides tip support to only the nominal weight.

For the baseline test configuration, the sail spreader bars were horizontal, and then they were rotated 22.5 degrees for another sequence of tests. Similar modal responses were seen in the four sails at each position. The expected modes for the baseline sail and position (Q4 at 0°) are shown to the left in Figure tbd. The responses of the targets are graphed with the data points which fell below the response of the target beside the input (red line) trimmed out for clarity. Where the first peaks occur are fundamental modes in the range of 0.50 and 0.62 Hz. Each of the sails has a slightly different mass, so this creates sets of four spread modal responses for each fundamental mode. The FEA mode corresponding to Q4 motion (0.483 Hz) is shown in Figure TBD, above the operational deflection shape (ODS) mode found in the testing. The same response (0.050 Hz) was found for various inputs, i.e. at magnet 1 (M1), at magnet 2 (M2), and for out-of-phase excitation of M1 and M2. The second mode shown in Figure TBD corresponds to mast bending. Again, there were 4 related modes predicted (from 0.62–0.64 Hz) for various combinations of mast motion phasing. The modal responses found in test peaked at 0.625 Hz for the three various inputs, but the ODS shape for each varied slightly, as shown in the figure. The nodal line shifted toward the input, as may be expected in a very flexible non-linear system.

The best location for modal excitation is ideally at the anti-nodes of the system response. Magnets were positioned at the 3 corners of the sail, and at the middle of the hypotenuse cord. The latter was unusable due to variations in the sail position after pump down. Condensation forms on the membrane as the chamber is initially evacuated. This increases the effective mass of the sail and the negator-spring-mounted halyards are extended. When the chamber reached a substantial vacuum, the water evaporated, returning the supported load to nominal. A small amount of positional variation (due to hysteresis) in the negator mechanism was amplified to result in a positional variation at the middle point of the hypotenuse of 5-15 cm. The variation was greater than the stroke of the magnet position adjustment actuators, and the testing schedule did not allow time for diagnosis, mitigation testing, and added pump-down days.

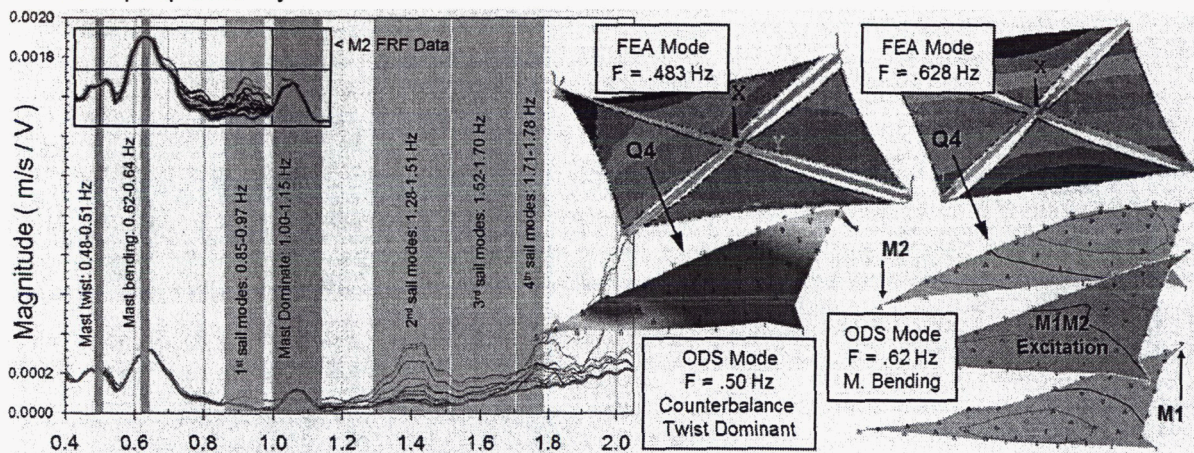


Figure tbd. System Dynamic Responses to M1 Input, Lowest Modes Due to Mast Tip Counterweight

TBR: Discussion of random vibration and ascent venting to be added here.



## SAIL MEMBRANE LIFE TESTING

Samples of sail material (2.5 and 5  $\mu\text{m}$  aluminized CP1) were exposed to various space environmental effects (SEE). Testing at the MSFC SEE laboratory included electron, proton, UV, and micrometeoroid exposure. Optical (reflection, transmission, and specularity) and mechanical (modulus, stress and strain to failure, and cyclic stress fatigue limit) properties were measured before and after exposure. The solar-averaged reflectivity of the aluminized sail material was baselined at 91.8% (+0.3% over 30 samples). Transmission through the 800-angstrom VDA coating was undetectable. Exposure to 250–400 nm near ultraviolet (NUV) radiation was at an intensity of 2 suns. Increased curling of the samples was observed during the first 250 hours of exposure, but optical properties were unaffected by the 1000-hr (80-day equivalent) test.

The radiation fluence for the 3-year Solar Polar Imager (SPI) mission was estimated, and the material was exposed to various flat-dose levels with 50 keV and 700 keV protons. As shown in the figure below shows, a 5 Grad flat-dose electron exposure is well in excess of the average dose at depth for the SPI mission. A 5 Grad flat-dose proton exposure is more than 2x the expected dose at every depth. The L1 mission environment is much less severe, per year, than the SPI mission (at 0.48 AU).

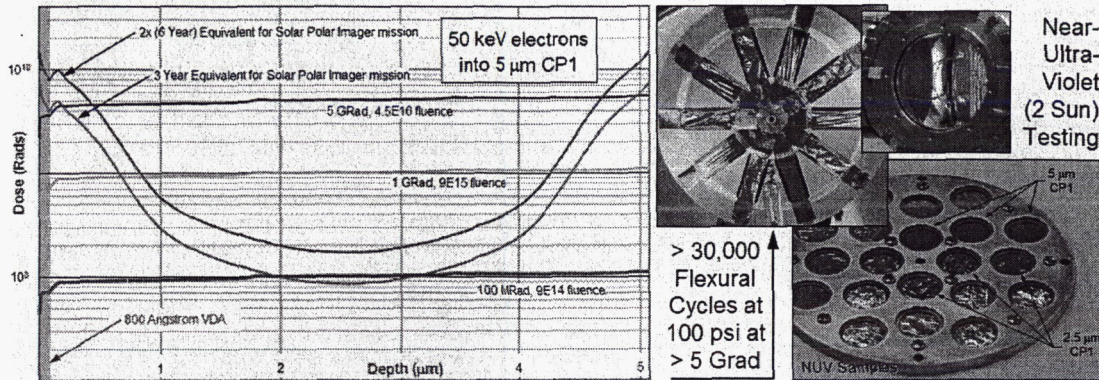


**Figure tbd. Sail Material Life Testing; Flat dose e and p radiation, flexural cycling, UV exposure**

Five or more 5  $\mu\text{m}$  samples were subjected to various exposures (bounded by a combined 5 gigarad electron, 5 gigarad proton, 1000 NUV sun hours case), then removed from the chamber and tensile tested. There was little change in modulus or strength (nominally 430 ksi and 14.4 ksi), and the material maintained more than 50% of the control sample ductility (strain to failure). The property variations for all exposures are shown below.

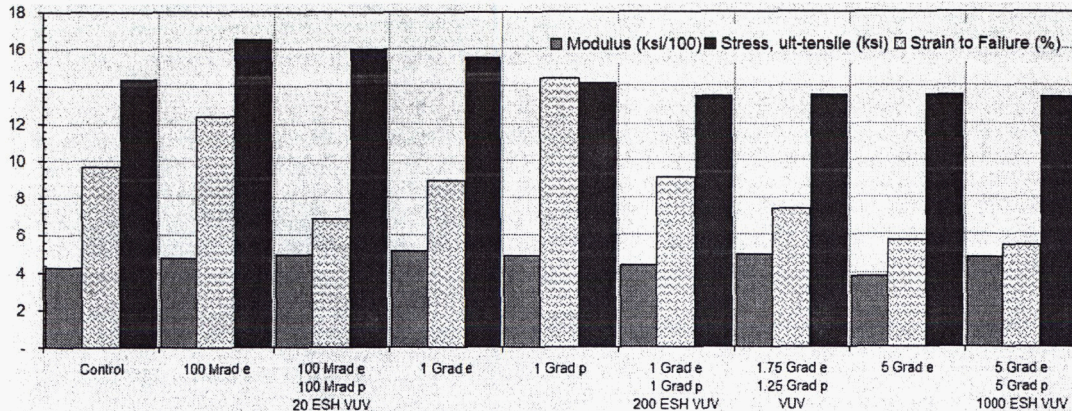


**Figure tbd. CP1 Properties Variation as a Function of Dose**

Samples of 2.5 and 5  $\mu\text{m}$  CP1 were also tested under cyclic loading conditions (0–100 psi) while being exposed to 50 keV electrons. Three 5  $\mu\text{m}$  CP1 samples survived 14 Grad and 70,000 cycles and demonstrated an average ultimate stress of 7.2 ksi at the conclusion of testing. Two 2.5  $\mu\text{m}$  CP1 samples failed during testing, at 7 Grad and 30,000 cycles, and 12 Grad and 50,000 cycles. When tested without cycling, the 5-sample average failure stress after 14 Grad electron fluence was 10.5 ksi for 5  $\mu\text{m}$  samples and 7.8 ksi for 2.5  $\mu\text{m}$  samples. These tests demonstrate the robustness of CP1 as a sail material: The nominal operation stress of a sail is 1 psi.



CP1 performed well in all aspects of simulated space environment testing, demonstrating the sail membrane can withstand space environmental influences beyond the level identified for near-term sailing missions. More detailed reporting of the testing performed can be found in references tbd.

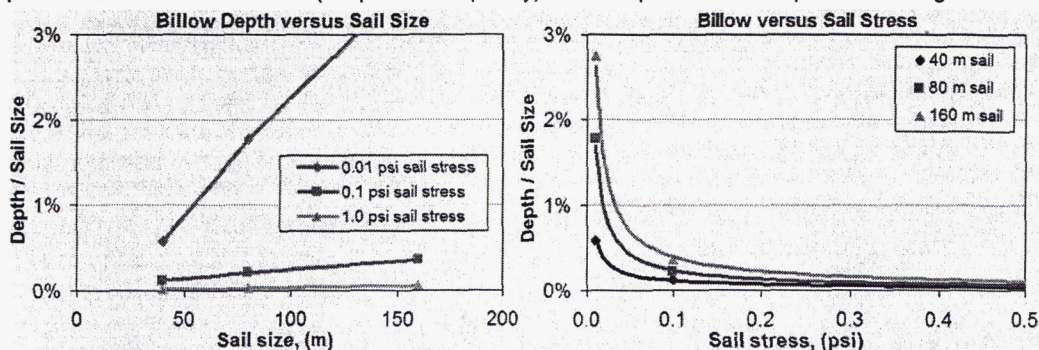
## SCALED PERFORMANCE

The ISP program set requirements for the performance of the demonstrated system scaled to a 100-m class (10,000 m<sup>2</sup> reflective area required). The evolution of the original design changed the mass estimate very little, but the design baselines a stronger coilable, which resulted in a less compactly stowed final scaled design estimate, and a slightly higher first mode frequency.

Sail System Parameters	Program Req'ts	Ph.1 Design	Final Point Design
Sail Area	10,000 m <sup>2</sup>	10,000 m <sup>2</sup>	10,000 m <sup>2</sup>
Areal Density	<12 g/m <sup>2</sup>	10.8 g/m <sup>2</sup>	11.3 g/m <sup>2</sup>
S <sup>4</sup> Volume	<1.5 m <sup>3</sup>	0.9 m <sup>3</sup>	1.5 m <sup>3</sup>
1 <sup>st</sup> System Mode Estimate		0.02 Hz	0.03 Hz
Volume Description (Goal: Fit within a 2.5 m fairing)		1.5 m dia. by 0.53 m	1.9 m dia. by 0.54 m
Mass of Scaled S <sup>4</sup> System		108 kg	113 kg
Characteristic Acceleration (a <sub>c</sub> ) (exp. w/ 130 kg bus+payload)		0.76 mm/s <sup>2</sup> (0.34 mm/s <sup>2</sup> )	0.73 mm/s <sup>2</sup> (0.35 mm/s <sup>2</sup> )

**Table 2. ISP Program Requirements and Other Metrics of Interest**

The coilable sizing is directly related to the sail stress assumed. Investigations into the propulsive performance of a post-packaged membrane (crinkled surface topology) indicated the nominal sail stress (1 psi) can be reduced towards 0.1 psi. A number of other planned for future systems, which would be best implemented in a spiral development approach, include thinner membranes, jettison of extraneous central structure, strategies for reduced complexity in attitude control, and stayed masts. None of these options is required for near-term mission such as HelioStorm (at L1) and Solar Polar Imager (SPI), as the current performance supports these missions with adequate margin. But future efforts will undoubtedly incorporate at least some of these methods for improving the key performance metrics of solar sails: Characteristic acceleration (a<sub>c</sub>, mm/s<sup>2</sup>), and areal mass density (ρ<sub>a</sub>, g/m<sup>2</sup>). The options listed, in combination, have been shown to reduce the areal density of a 160-m sail subsystem to 3 g/m<sup>2</sup>. Scaled performance for other metrics (shape and frequency) of sails up to 200-m are provided in Figure tbd.



Graphs for Frequency vs. Size and Stress TBD



### Figure tbd. Scaled Performance of the S<sup>4</sup> System: Billow and Frequency vs. Size and Stress

Another important parameter for solar sail propulsion is the maximum solar loading permissible. Missions such as PASO (0.19 au) require, and outer planet explorers are enhanced (travel time is reduced) by, a closer solar approach. The temperature of a 2-micron CP1 sail at L1 is 31°C (and as low as 9°C if off-sun 35°). This same sail can be used for the SPI mission, which will operate at 156°C at 0.48 au. The max temperature capability of CP1 is 250°C. By utilizing a carbon-load CP1 ( $\epsilon = 0.8$ ), a temperature of 220°C will be reached at 0.2 au. This allows the PASO mission, is of benefit to outer planet explorers, and improves the mission timeline for an interstellar probe.

## SUMMARY AND CONCLUSIONS

ISP program activities have systematically reduced the risk of flight implementation with substantial technology development, through a series of demonstrations of increasingly more complex solar sail systems, and by testing of the highest fidelity possible in the terrestrial environment. The progressive demonstrations of S<sup>4</sup> technology at the component, 10-m, and 20-m levels has elevated the TRL of solar sailing technology in all critical areas to prepare for a low-risk flight validation mission in earth orbit. The soundness of the design for deployment and control of a fully-integrated sail and structure system has been validated with an extensive series of tests. Analytical correlation activities showed sound agreement with test results. The continuum of system design and analytical development activities together ensure a functionally scalable design and mathematically predictable result for larger sail systems, such as a flight demonstration system (40-m scale), and mission systems of up to 200 meters on a side.

## FUTURE WORK

Man has dreamed of sailing on starlight for more than a century. Jules Verne's 1865 novel *From the Earth to the Moon* mentioned light as a "mechanical agent", a direct application of the discovery at that time, by James Clerk Maxwell, that *light* exerts a pressure on surfaces. Over the past 50 years many prominent hardcore science fiction writers have employed descriptions of solar sailing to astound readers. From early master SF writers came stories such as *Clipper Ships of Space*<sup>ref</sup> and *The Wind from the Sun*.<sup>ref</sup> Solar sailing is an inspiration for poets as well:

*"I cannot cause light; the most I can do is try to put myself in the path of its beam. It is possible, in deep space, to sail on solar wind. Light, be it particle or wave, has force: you rig a giant sail and go. The secret of seeing is to sail on solar wind. Hone and spread your spirit till you yourself are a sail, whetted, translucent, broadside to the merest puff."*

From "Pilgrim at Tinker Creek" by Annie Dillard



Imagination has become reality. The ground demonstrations and validations of S<sup>4</sup> system technology has elevated the TRL of solar sailing in all critical areas necessary to support a low-risk light validation mission in earth orbit. It is time to set sail.

## ACKNOWLEDGMENTS

The work described in this paper was funded by the In-Space Propulsion Technology Program, which is managed by NASA's Science Mission Directorate in Washington, D.C., and implemented by the ISP Technology Office at Marshall Space Flight Center in Huntsville, Alabama. The program objective is to develop in-space propulsion technologies that can enable or benefit near and mid-term NASA space science missions by significantly reducing cost, mass or travel times. This paper was written to maximize dissemination of information, derived from the efforts of many within the ISP S<sup>4</sup> ground demonstration system activity, to the benefit of the national space program. The author wishes to thank Sandy Montgomery and the ISP projects staff for their leadership and support, to acknowledge SRS Technologies for their fine accomplishments in sail design and fabrication, LaRC for their close partnership in testing and modeling, the MSFC SEE lab for their extensive testing of CP1, and to enumerate the engineering staff at ATK Space Systems, Goleta, for the dedicated efforts provided by Peter Barker, Richard Cope, Mark Douglas, Brian Macy, Mike McEachen, Ariel Pavlick, Peter Sorenson, Ron Takeda, and Tom Trautt.

## REFERENCES

1. Garbe, G., Montgomery, E., Heaton, A., Van Sant, J., and Campbell, B., "NASA's Integrated Development of Solar Sail Propulsion," AAS 04-103, 14<sup>th</sup> AAS/AIAA Space Flight Mechanics Meeting, 2004.
2. Murphy, D., Murphey, T., and Gierow, P., "Scalable Solar-Sail Subsystem Design Concept", AIAA Journal of Spacecraft and Rockets, Volume 40, No. 4, pp. 539-547, July-August 2003.
3. Murphy, D., Trautt, T., McEachen, M., Messner, D., Laue, G., and Gierow, P., "Progress and Plans for System Demonstration of a Scalable Square Solar Sail," AAS 04-105, 14<sup>th</sup> AAS/AIAA Space Flight Mechanics Meeting, 2004.
4. Murphy, D., Macy, B., and Gaspar, J., "Demonstration of a 10-m Solar Sail System", AIAA Structures, Structural Dynamics, & Materials Conference, 5<sup>th</sup> Gossamer Spacecraft Forum, Palm Springs, CA, April 19-22, 2004.
5. Taleghani, B., Lively, P., Gaspar, J., Murphy, D., and Trautt, T., "Dynamic & Static Shape Test/Analysis Correlation of a 10-m Solar Sail Quadrant", AIAA 2005-2123, 46<sup>th</sup> AIAA Structures, Structural Dynamics, & Materials Conference, 6<sup>th</sup> Gossamer Spacecraft Forum, Austin, TX, April 18-21, 2005.



6. Murphy, D., Macy, B., and Gaspar, J., "Demonstration of a 20-m Solar Sail System", 46<sup>th</sup> AIAA Structures, Structural Dynamics, & Materials Conference, 6<sup>th</sup> Gossamer Spacecraft Forum, Austin, TX, April 18-21, 2005.
7. Montgomery, E., and Johnson, L., "The Development of Solar Sail Propulsion for NASA Science Missions to the Inner Solar System", AIAA Structures, Structural Dynamics, & Materials Conference, 5<sup>th</sup> Gossamer Spacecraft Forum, Palm Springs, CA, April 19-22, 2004.
8. The Sun-Earth Connection Roadmap 2003-2028, Understanding the Sun, Heliosphere, and Planetary Environments as a Single Connected System, NP-2002-8-500-GSFC. Available at <http://sec.gsfc.nasa.gov>
9. Crawford, R., and Benton, M., "Strength of Initially Wavy Lattice Columns", AIAA Journal, Vol. 18, No. 5, pp. 581-584, May 1980, Presented as Paper 79-0753 at the AIAA Structures Dynamics and Materials Conference, 1979.
10. McEachen, M., Trautt, T., and Murphy, D., "The SAILMAST Flight Validation Experiment", AIAA-2005-1884, 46<sup>th</sup> AIAA Structures, Structural Dynamics, & Materials Conference, 6<sup>th</sup> Gossamer Spacecraft Forum, Austin, TX, April 18-21, 2005.
11. Gaspar, J., et al, "Development of Modal Test Techniques for Validation of a Solar Sail Design," AIAA 2004-1665, 45<sup>th</sup> AIAA Structures, Structural Dynamics, & Materials Conference, 5<sup>th</sup> Gossamer Spacecraft Forum, Palm Springs, CA, April 19-22, 2004.
12. <http://facilities.grc.nasa.gov/spf/index.html>
13. Murphy, D., and Wie, B., "Robust Thrust Control Authority for a Scalable Sailcraft", AAS 04-285, 14<sup>th</sup> AAS/AIAA Space Flight Mechanics Meeting, Maui, HA, February 8-12, 2004.
14. Wie, B., Murphy, D., Thomas, S., and Paluszczek, M., "Robust Attitude Control Systems Design for Solar Sails (Part 1): Propellantless ACS", AIAA 2004-5010, AIAA/AAS Astrodynamics Specialist Conference, Providence, RI, August 16-19, 2004.
15. Pryor, K., Wie, B., and Mikellides, P., "Development of a Lightweight Pulsed Plasma Thruster Module for Solar Sail Attitude Control", Paper SSC04-XI-4, 18<sup>th</sup> Annual AIAA/USU Conference on Small Satellites, Logan, Utah, August 9-12, 2004.
16. Wie, B., Murphy, D., Thomas, S., and Paluszczek, M., "Robust Attitude Control Systems Design for Solar Sails (Part 2): MicroPPT-based Secondary ACS", AIAA-2004-5011, AIAA Guidance, Navigation, and Control Conference, Providence, RI, August 16-19, 2004.
17. Edwards, D., Semmel, C., Hovater, M., Nehls, M., Gray, P., Hubbs, W., and Wertz, G., "Status of Solar Sail Material Characterization at NASA's Marshall Space Flight Center", 7<sup>th</sup> International Conference on Protection of Materials and Structures from Space Environment, Toronto, May 10-13, 2004.
18. Laue, G., et al, "Innovative Structural Design Features for a 10-m Solar Sail Demonstrator", AIAA 2004-1508, 45<sup>th</sup> AIAA Structures, Structural Dynamics, & Materials Conference, 5<sup>th</sup> Gossamer Spacecraft Forum, Palm Springs, CA, April 19-22, 2004.
19. Laue, G., Case, D., and Moore, J., "Fabrication and Deployment Testing of 20-Meter Solar Sail Quadrants for a Scaleable Square Solar Sail Ground Test", AIAA 2005-2125, 46<sup>th</sup> AIAA Structures, Structural Dynamics, & Materials Conference, 6<sup>th</sup> Gossamer Spacecraft Forum, Austin, TX, April 18-21, 2005.
20. Moore, J., et al, "High Fidelity Finite Element Based Modeling for Solar Sail Thrust Vector Prediction from Flexible Sail Models", 52<sup>nd</sup> Joint Army-Navy-NASA-Air Force (JANNAF) Propulsion Meeting, Las Vegas, Nevada, May 10-13, 2004.
21. Thomas, S., et al, "Design and Simulation of Sailcraft Attitude Control Systems Using the Solar Sail Control Toolbox", AIAA 2004-4890, AIAA/AAS Astrodynamics Specialist Conference, Providence, RI, August 16-19, 2004.
22. The Status of Solar Sail Material Characterization at NASA's Marshall Space Flight Center, 7<sup>th</sup> International Conference on Protection of Materials and Structures from the Space Environment, Toronto, May 10-13, 2004
23. Solar Sail Material Performance Property Response to Space Environmental Effects, SPIE 49th Annual Meeting, Optical Science and Technology Symposium, Photonics for Space Environments IX Conference, Denver, August 2-6, 2004
24. Wiley, Carl, "Clipper Ships of Space", Astounding magazine, edited by John W. Campbell, 1951.
25. "The Wind from the Sun" [Sunjammer], Arthur C. Clarke, Boys' Life March, 1964.
26. Edwards, D., et al, Characterization of Space Environmental Effects on Candidate Solar Sail Material, Proceedings of SPIE Photonics for Space Environments VIII, vol. 4823, 2002.
27. Albarado, T., et al, Electron Exposure Measurements of Candidate Solar Sail Materials, Proceedings of ISEC 2003 International Solar Energy Conference, Hawaii, 15-18 March, 2003.
28. Edwards, D., et al, Characterization of Candidate Solar Sail Materials Subjected to Electron Radiation, Proceedings of the 9th International Symposium on Material in a Space Environment, Noordwijk, The Netherlands, 16-20 June 2003.

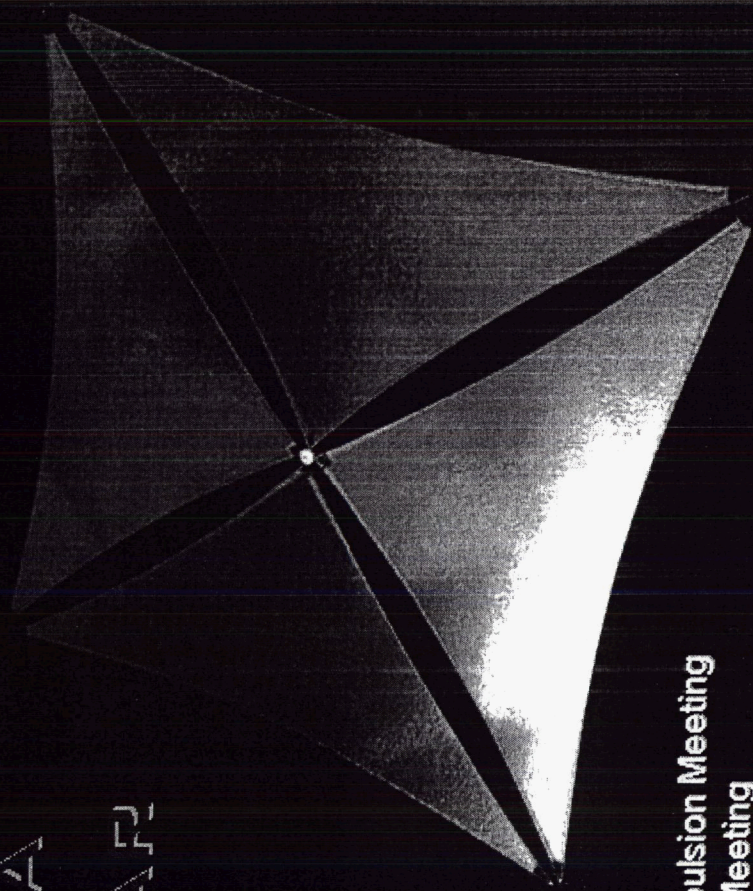




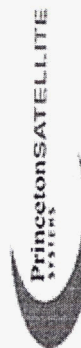
An advanced weapon and space systems company

# VALIDATION OF A SCALABLE SOLAR SAILCRAFT

D. MURPHY  
ATK SPACE SYSTEMS



53<sup>rd</sup> Joint Army-Navy-NASA-Air Force (JANNAF) Propulsion Meeting  
1<sup>st</sup> Spacecraft Propulsion Joint Subcommittee (SPS) Meeting  
Monterey, CA December 5-8, 2005



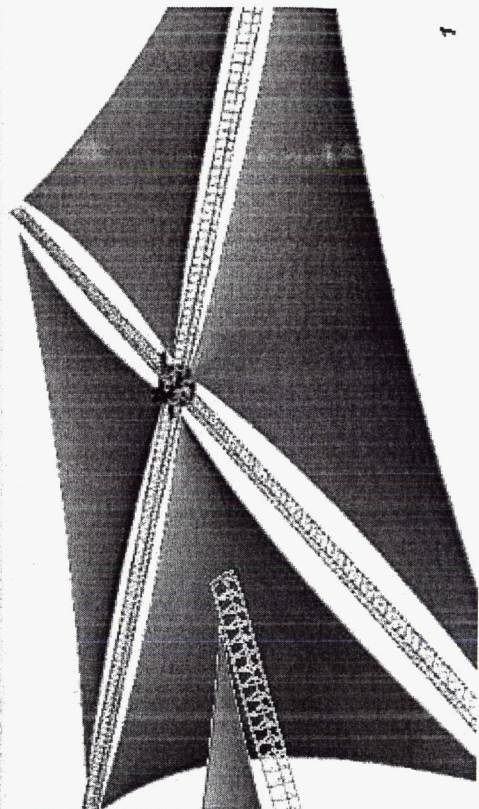
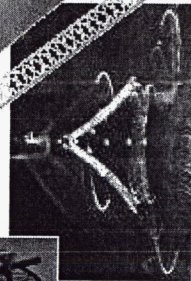
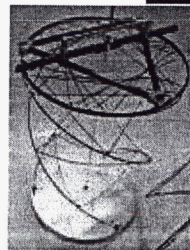
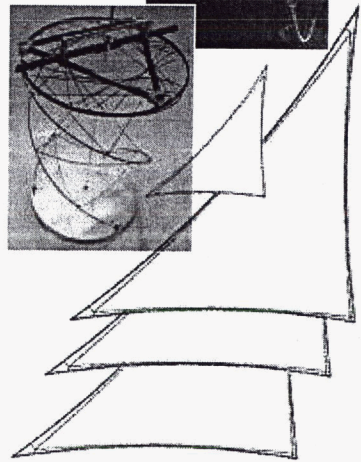


# ISP Roadmap for ATK

Validate, Scale Up, Repeat  
Refine Design, Build, Test

Sails... Masts... 10-m Quadrant System

20-m Full S<sup>4</sup> System





# SOLAR SAILING

## Concept:

- ◆ Utilize solar rays ( $\gamma$  momentum) to accelerate a spacecraft

## Feasibility:

- ◆ The amount of force generated is  $< 1\%$  of a pound per acre, but sunlight has the potential to gradually accelerate a sailcraft to speeds exceeding 100,000 mph within 3 years ... fast enough to reach Pluto in 5 years

## Unique Attribute:

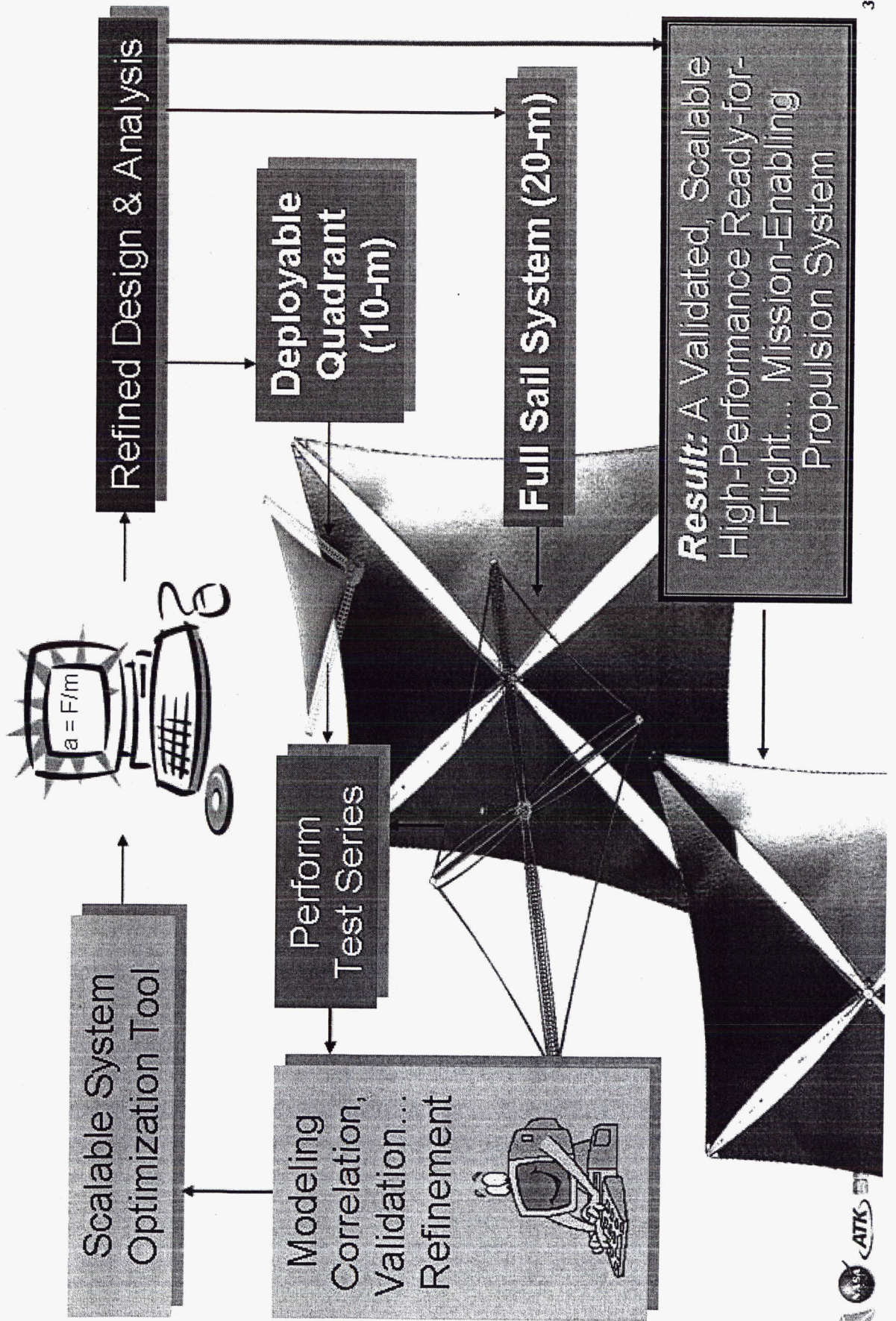
- ◆ Unlike the chemical-fueled rockets currently used to power spacecraft, solar power is constant, giving the spacecraft an endless supply of propulsion

## Uses:

- ◆ Any  $\Delta V$  mission currently not feasible, or too expensive
  - e.g. Sentinel satellites that provide early warning for solar flares, unique vantage points over Earth, Mars, or the Sun, Continuous Communication links for Exploration, ...

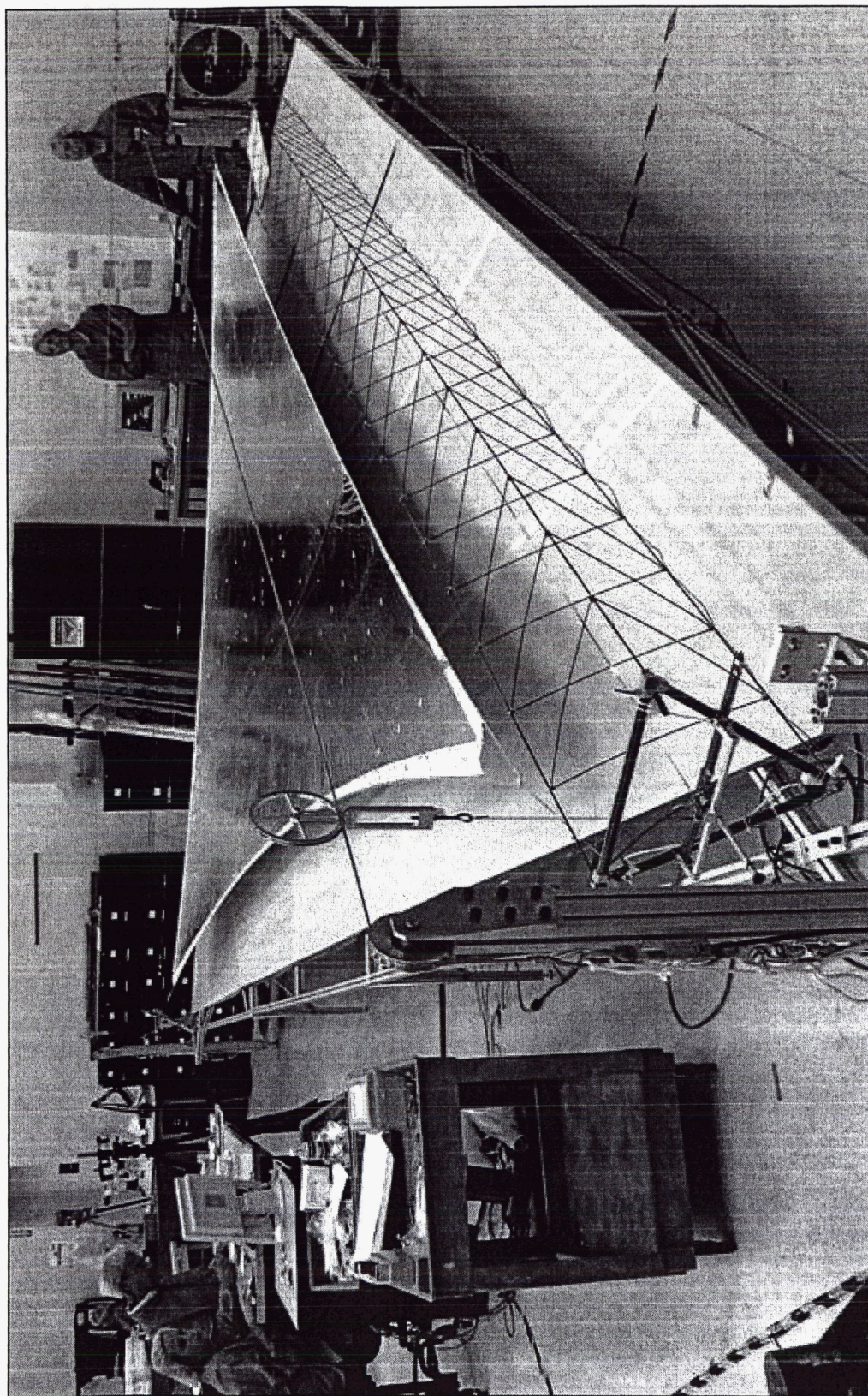


# S<sup>4</sup> PROGRAM SYNOPSIS: TRL ADVANCEMENT THROUGH HARDWARE DEMONSTRATION & VALIDATION



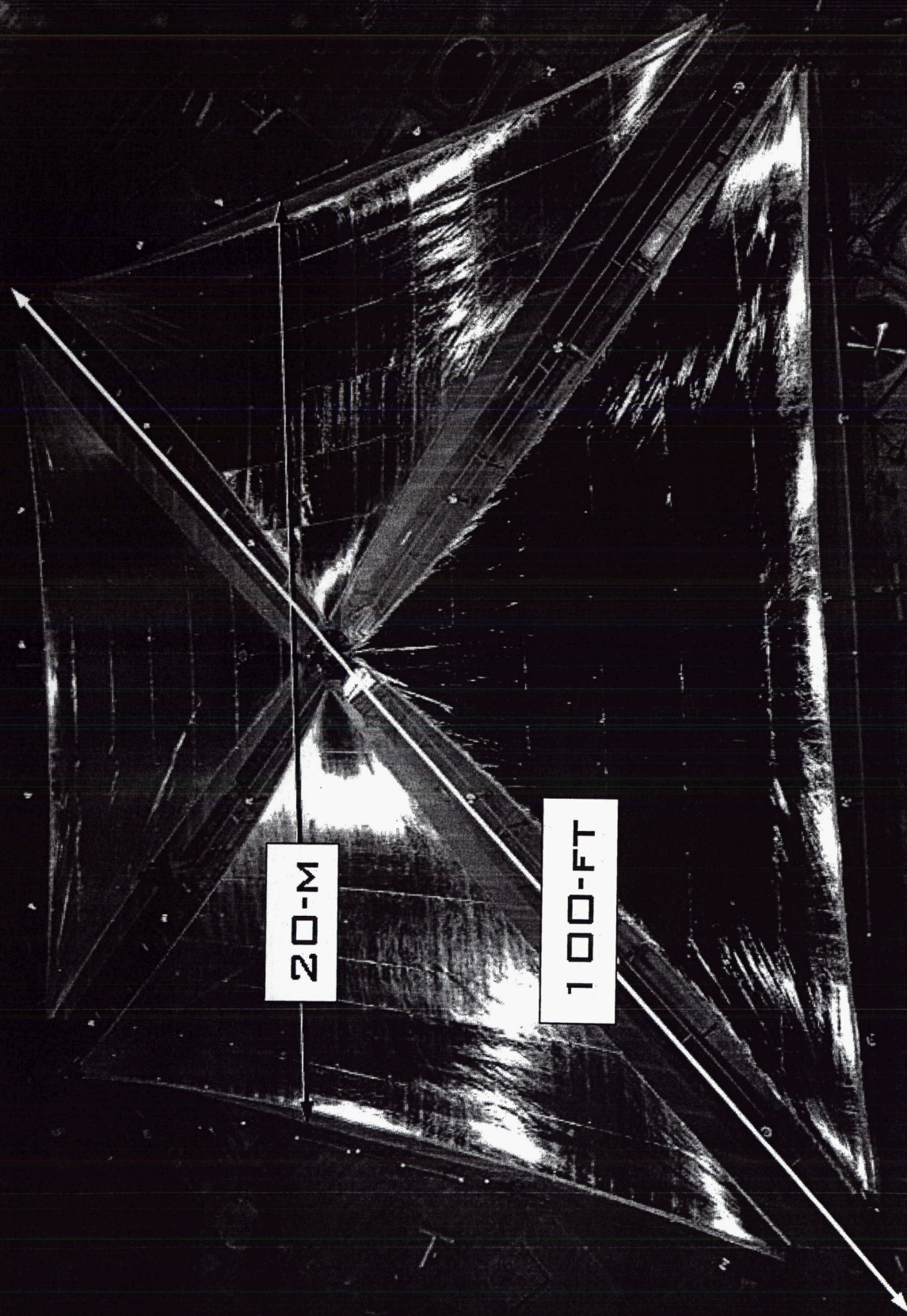


# 10-M QUADRANT SYSTEM





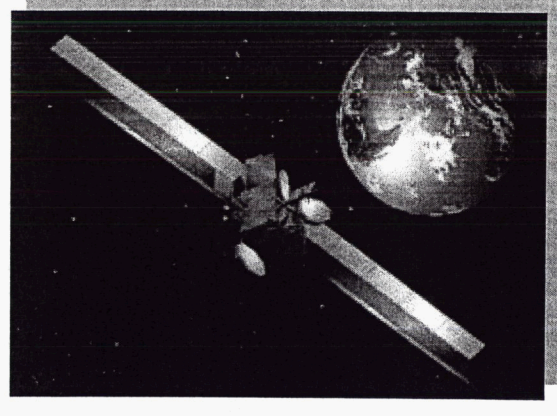
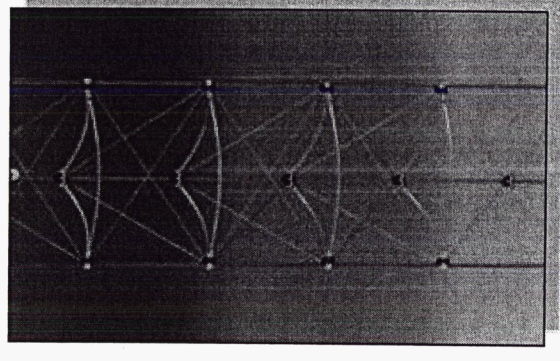
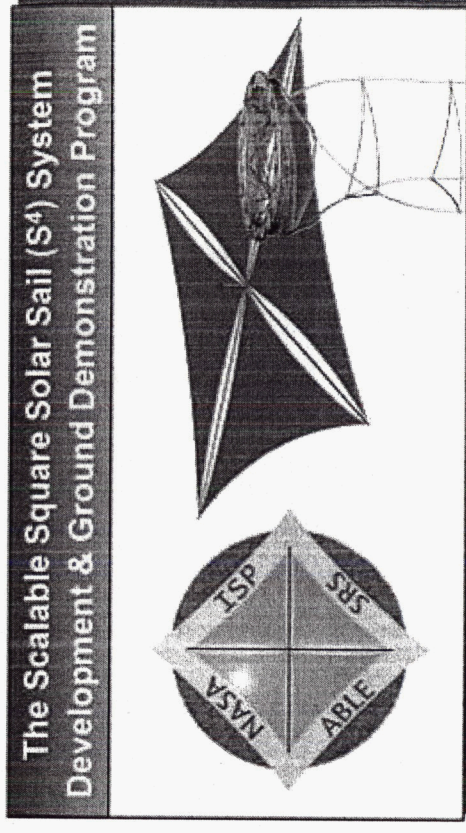
# S<sup>4</sup> SYSTEM AT PLUM BROOK





# BASIC S<sup>4</sup> DESIGN ELEMENTS

- Sail configuration:
  - 4-quadrant planar sail
  - Offset SC as control mass
- Mast - an advanced version of flight-proven deployment technology:
  - Coilable boom... with graphite structural elements plus minimal fittings and mechanization
- Sail material -
  - CP1: A gossamer metalized film construction similar to gusseted, reflective blankets flying on numerous GEOCOM satellites





# S<sup>4</sup> PHASE 1 PROGRAM SUMMARY

## Key effort: Refined S<sup>4</sup> System Concept

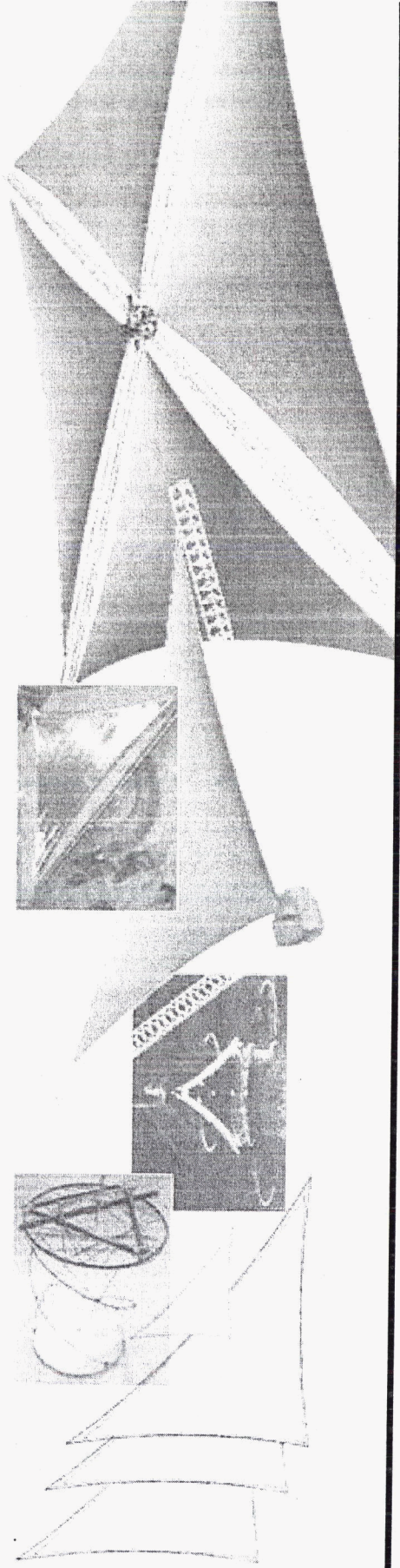
- ◆ Found and justified optimum design
  - Built Scalable Square Solar Sail Mathematical Optimization Tool for system level trades
- ◆ Completed first-level system layout
- ◆ Updated performance predictions

## S<sup>4</sup> Performance Against Primary Requirements

- ◆ Areal Density: 10.8 g/m vs 12 g/m requirement
- ◆ Stowed Volume: 1.0 m<sup>3</sup> vs 1.5 m<sup>3</sup> requirement
- ◆ Size: 100-m System (10,000 m<sup>2</sup> reflective area)

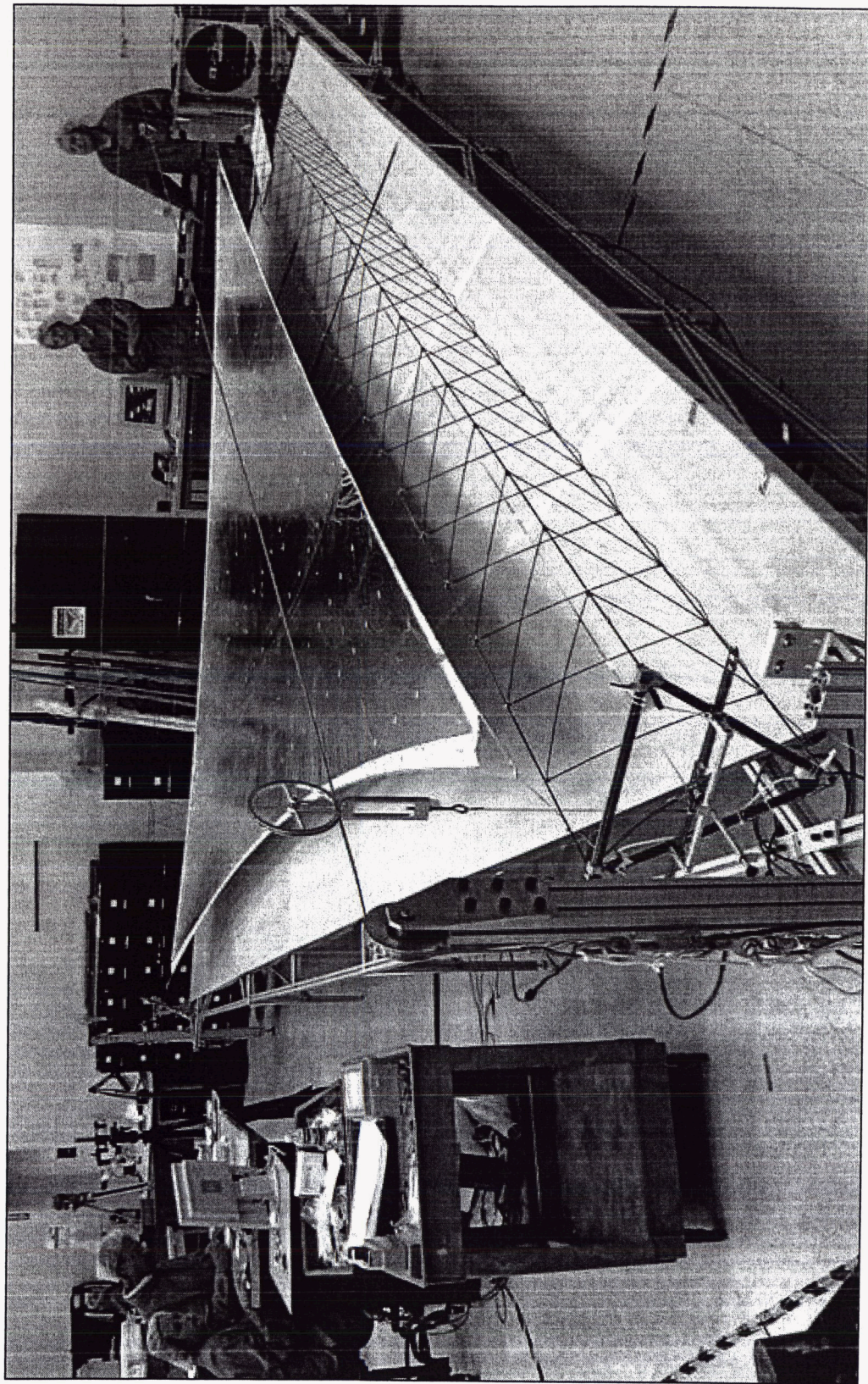


# PHASE 2 - 10-M QUADRANT





# 10-M QUADRANT SYSTEM

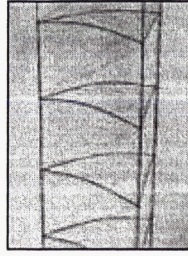




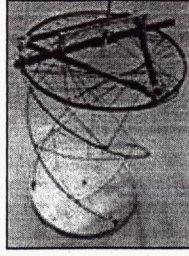
# PHASE 2 DEV & DEMO MILESTONES

## Mast Development

- ◆ EDU1, EDU2, 7-m masts (2)
- ◆ Functional, stiffness, strength, alignment



Mast EDU1



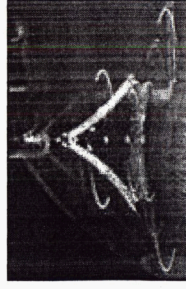
Mast EDU2

## Sail Development

- ◆ Workhorse, Refined Sails (RS5 and RS3), Performance Sail
- ◆ Process Development
- ◆ Material Testing



10-m Sails (3)



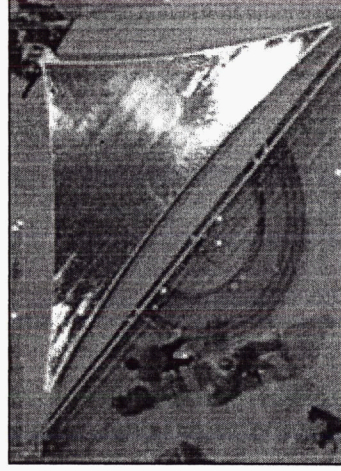
1.5-m Sail  
at GRC

## System Demonstration

- ◆ Packaging, Deployment Control, Ascent
- ◆ Venting, Quadrant Functional (ambient & vacuum), Shape & Dynamics Measurement

## Modeling

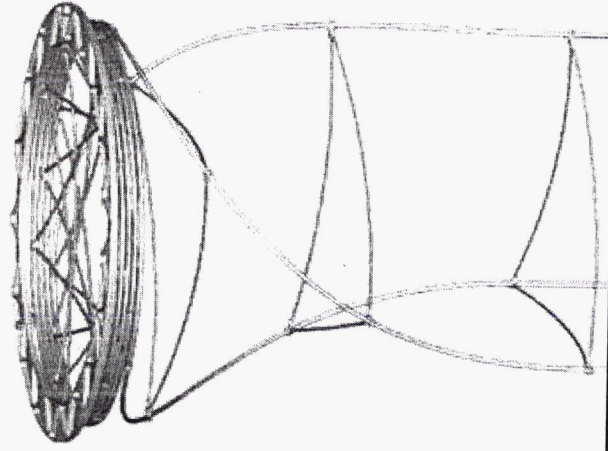
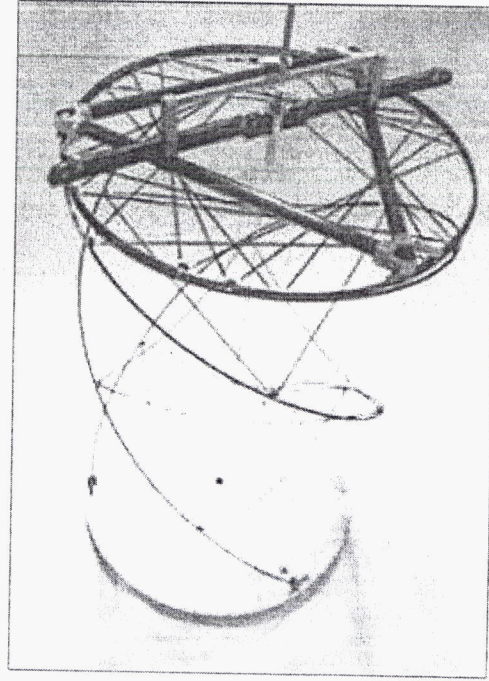
- ◆ Correlations with mast and system testing



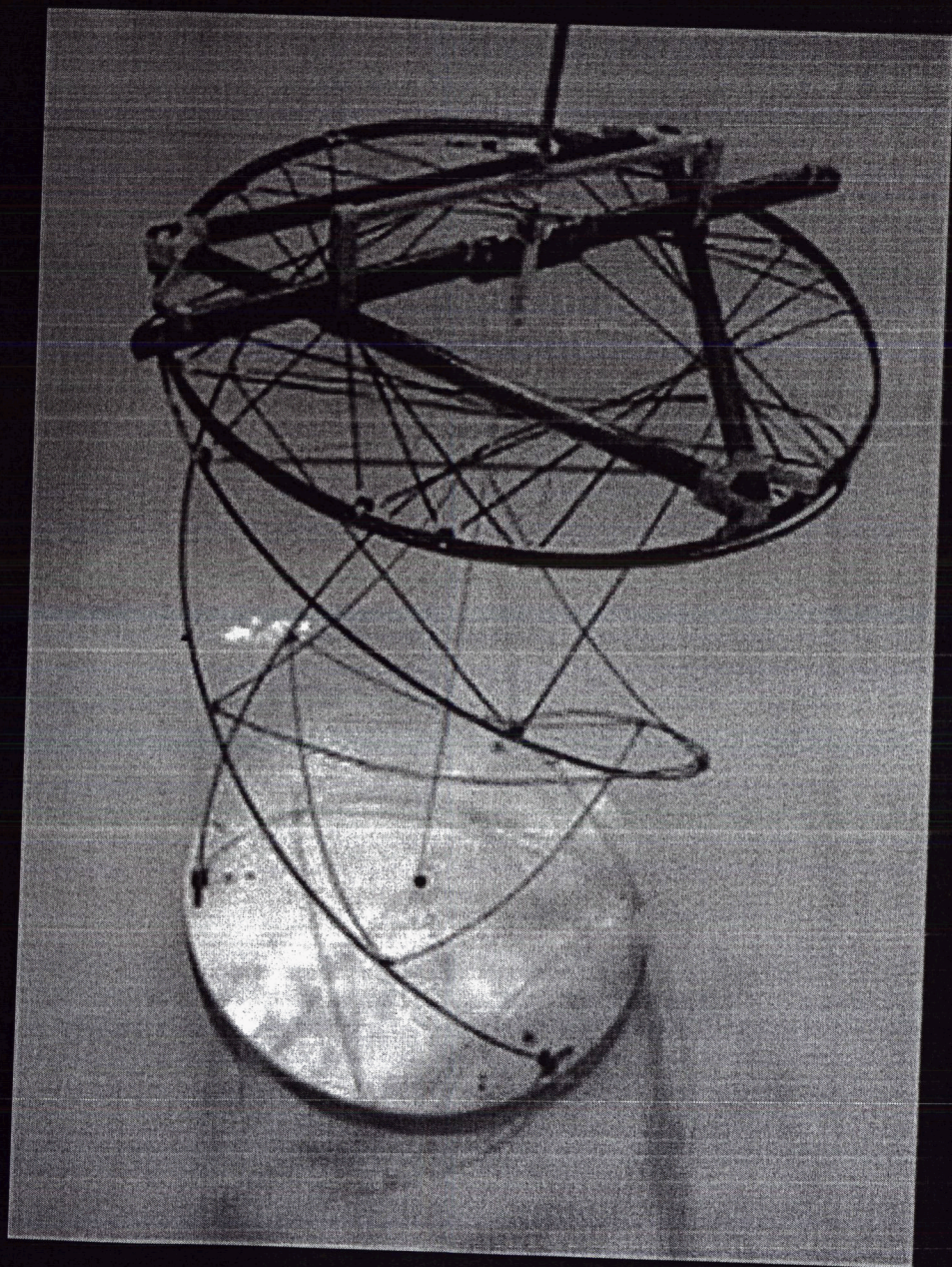
10-m S<sup>4</sup> Sail System  
at NASA LaRC



# MAST TECHNOLOGY MATURATION







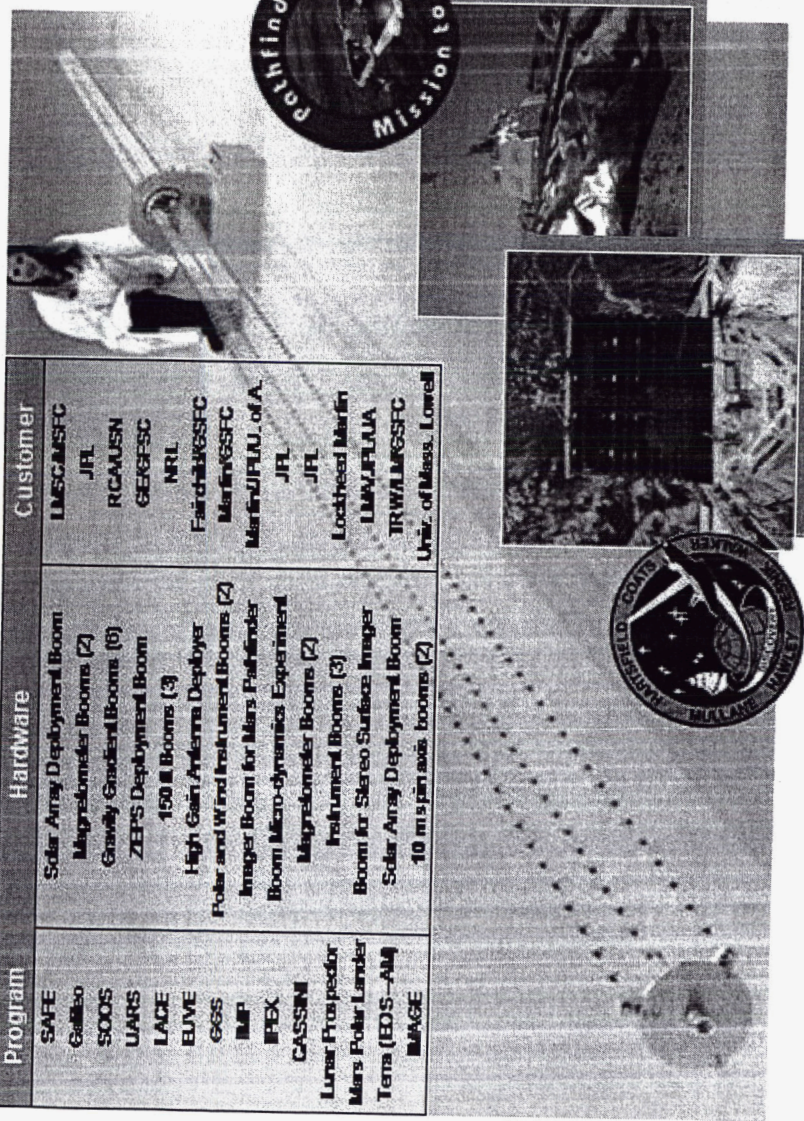
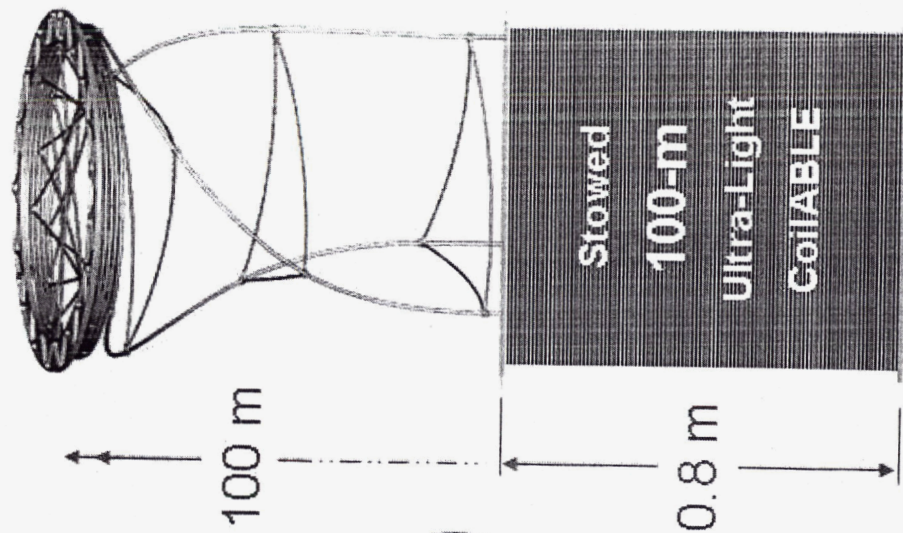


# COILABLE MAST HERITAGE

## 30 Coilable systems have been flown to date

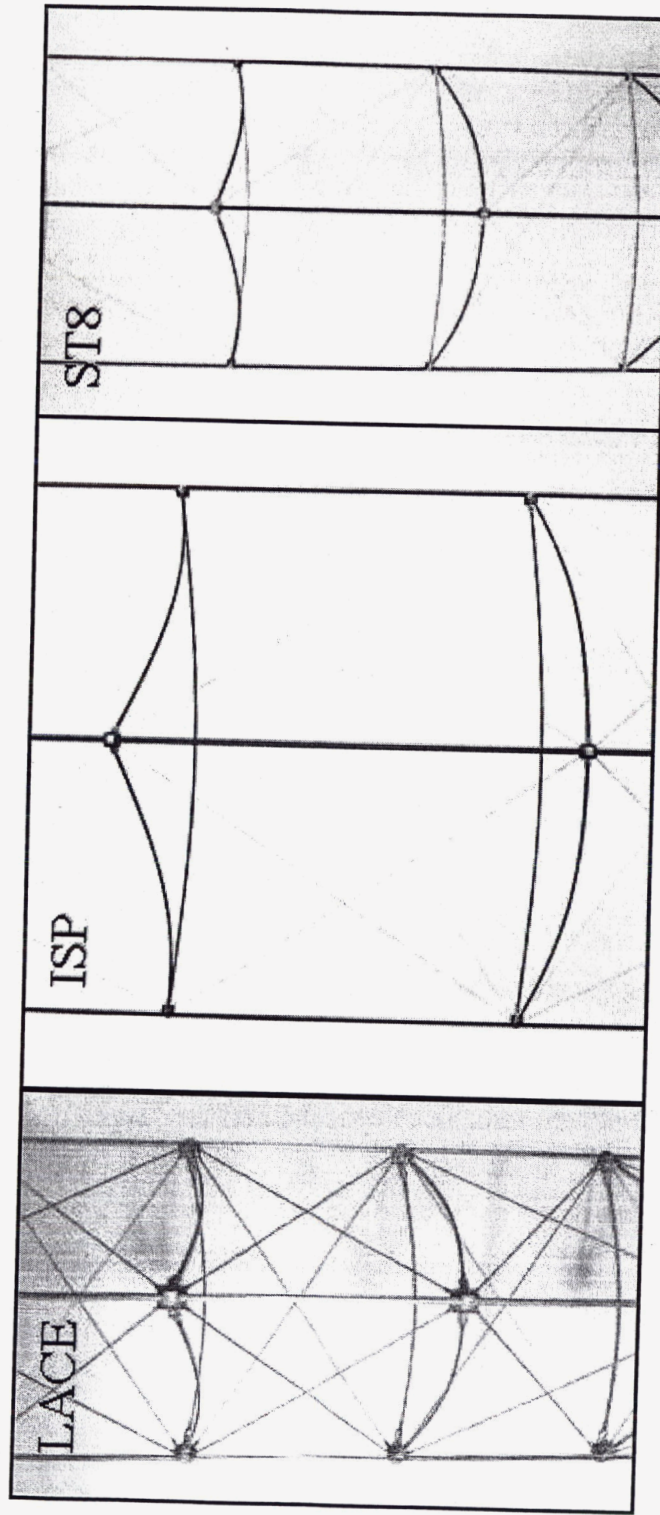
- ◆ A phenomenal Stiffness to Weight ratio, High Dimensional Stability, Robust deployment, and Compact Stowage

Program	Hardware	Customer
SAFE	Solar Array Deployment Boom	USC/MSC
Galileo	Magnetometer Booms (2)	JPL
SOOS	Gravity Gradient Booms (8)	RCA/USN
UARS	ZEPUS Deployment Boom	GE/USC
LAGE	150 m Booms (3)	NRL
ELVE	High Gain Antenna Deployer	Fairchild/USC
GGS	Polar and Wind Instrument Booms (2)	Martin/USC
MAP	Ingras Boom for Mars Pathfinder	Martin/JPL/UA of A.
IFEX	Boom Micro-dynamics Experiment	JPL
CASSINI	Magnetometer Booms (2)	JPL
Lunar Prospector	Instrument Booms (3)	Lockheed Martin
Mars Polar Lander	Boom for Stereo Surface Imager	LMV/FLUA
Terra (EOS-AM)	Solar Array Deployment Boom	TRW/USC
IMAGE	10 m span axis booms (2)	Univ. of Mass., Lowell





# COMPARATIVE MAST PROPERTIES



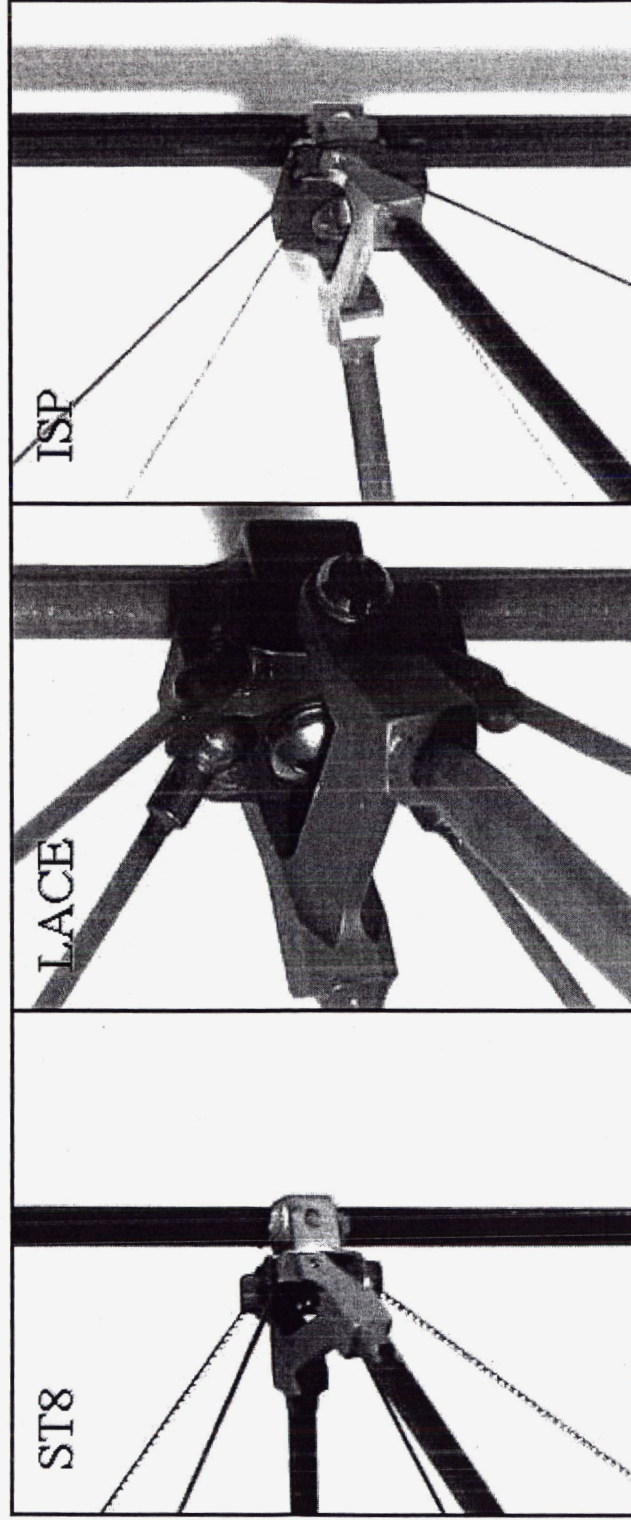
$$\begin{aligned}\phi_M &= 25.5 \text{ cm} \\ L_S/L_D &= 2.0\% \\ \rho_L &= 240 \text{ g/m}\end{aligned}$$

$$\begin{aligned}\phi_M &= 39.5 \text{ cm} \\ L_S/L_D &= 0.85\% \\ \rho_L &= 70 \text{ g/m}\end{aligned}$$

$$\begin{aligned}\phi_M &= 24.0 \text{ cm} \\ L_S/L_D &= 0.88\% \\ \rho_L &= 34 \text{ g/m}\end{aligned}$$



# COMPARATIVE FITTING SIZES



$\varnothing_L = 2.0 \text{ mm}$

$\varnothing_L = 3.8 \text{ mm}$

$\varnothing_L = 2.8 \text{ mm}$



# SOLAR SAIL MAST TECHNOLOGY

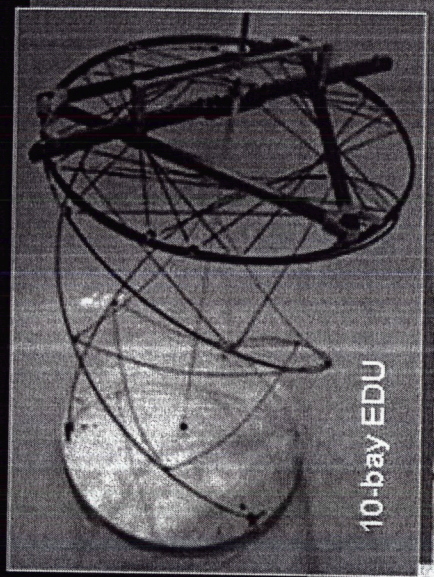
70 g/m at  $D = 40$  cm

◆  $EI = 81 \text{ kN-m}^2$

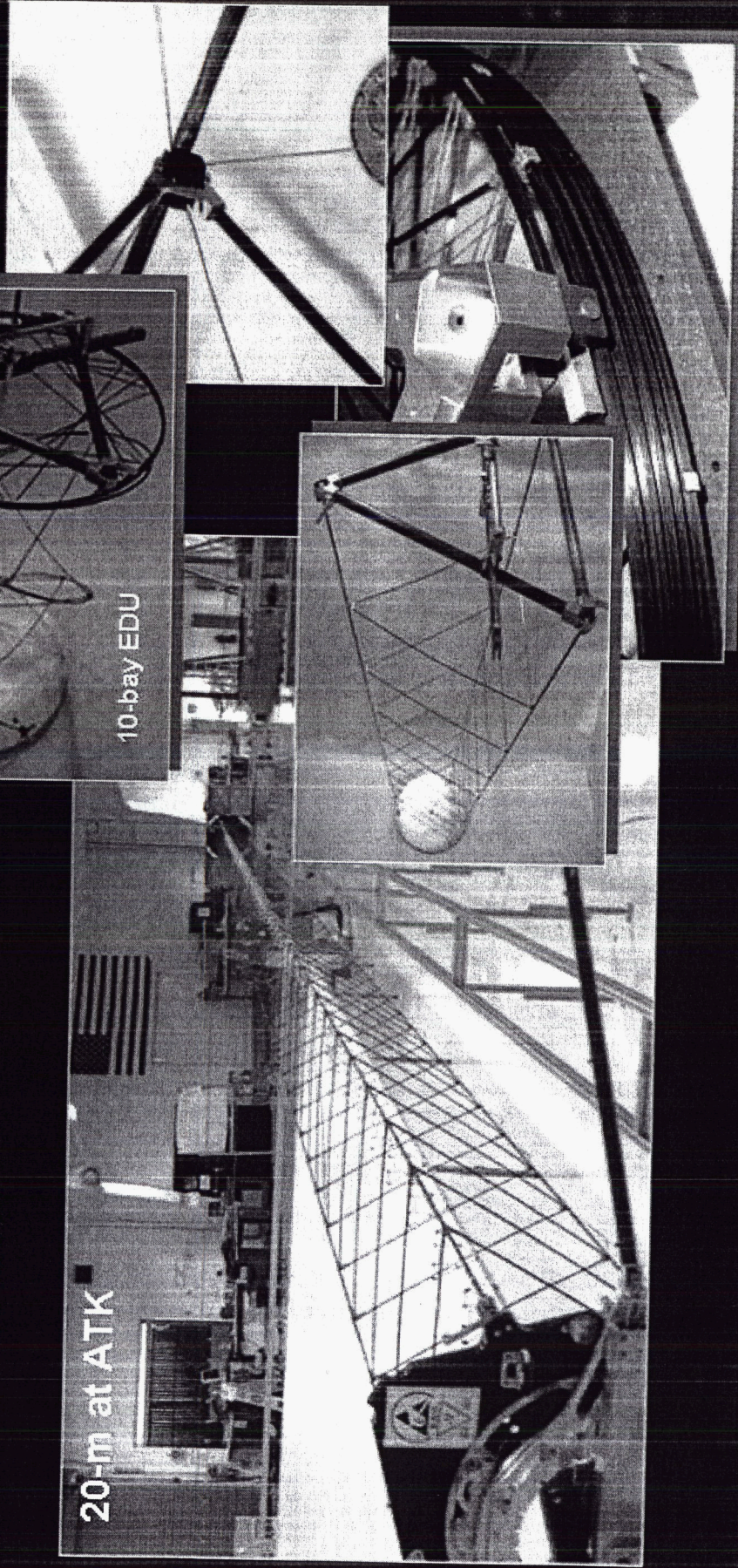
31 g/m at  $D = 24$  cm

◆  $EI = 11 \text{ kN-m}^2$

20-m at ATK

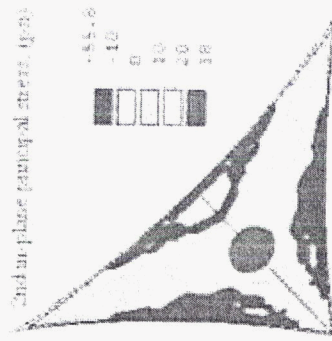
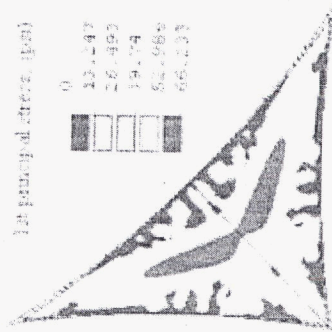


10-bay EDU





# SAIL TECHNOLOGY MATURATION

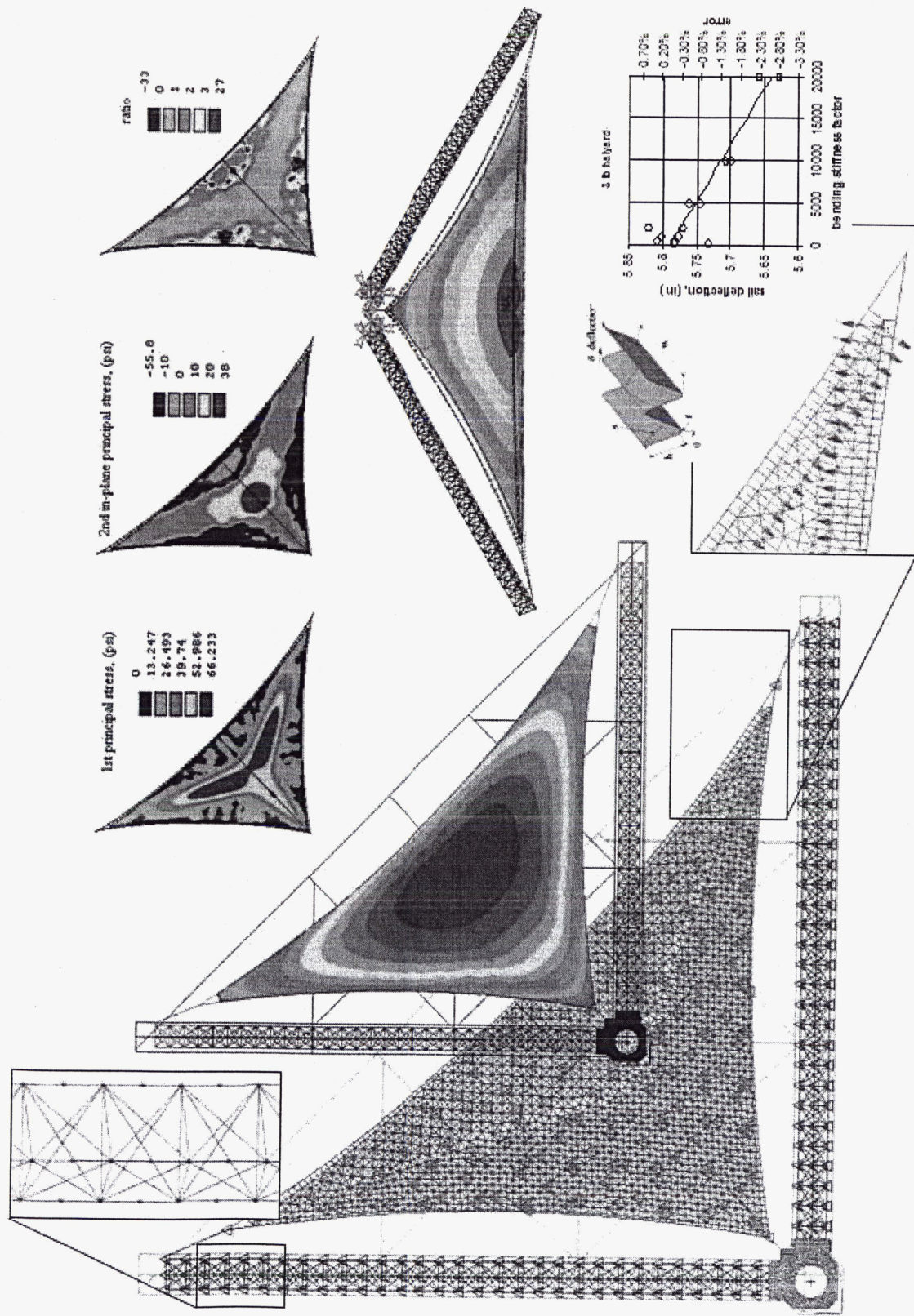






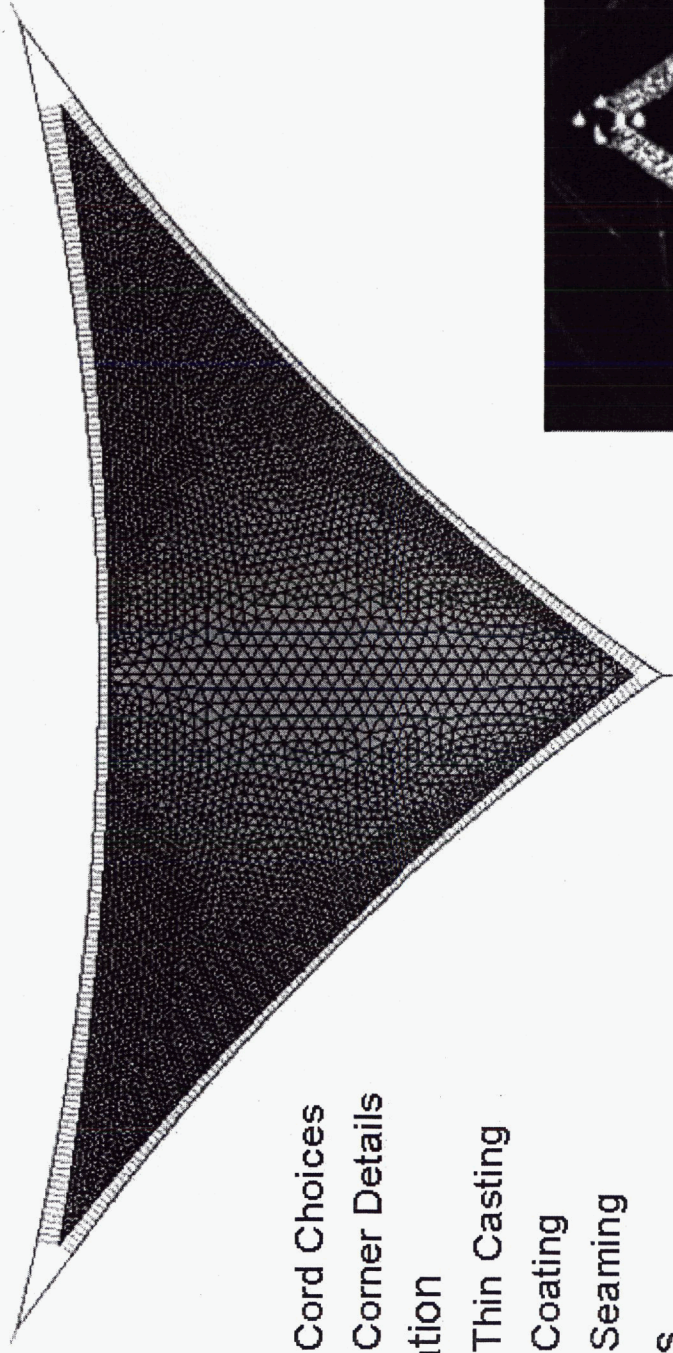


# 10-M ANALYSIS: SHAPE AND DYNAMICS





# CHALLENGES OVERCOME



## Design

- ◆ Cord Choices
- ◆ Corner Details

## Fabrication

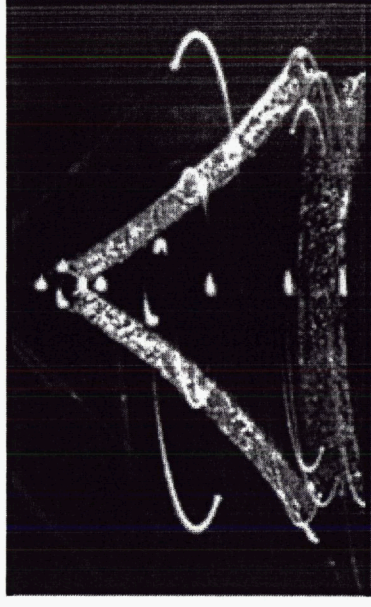
- ◆ Thin Casting
- ◆ Coating
- ◆ Seaming

## Analysis

- ◆ Mechanics of shear in compliant border
- ◆ Efficient 3D nonlinear models, with gravity

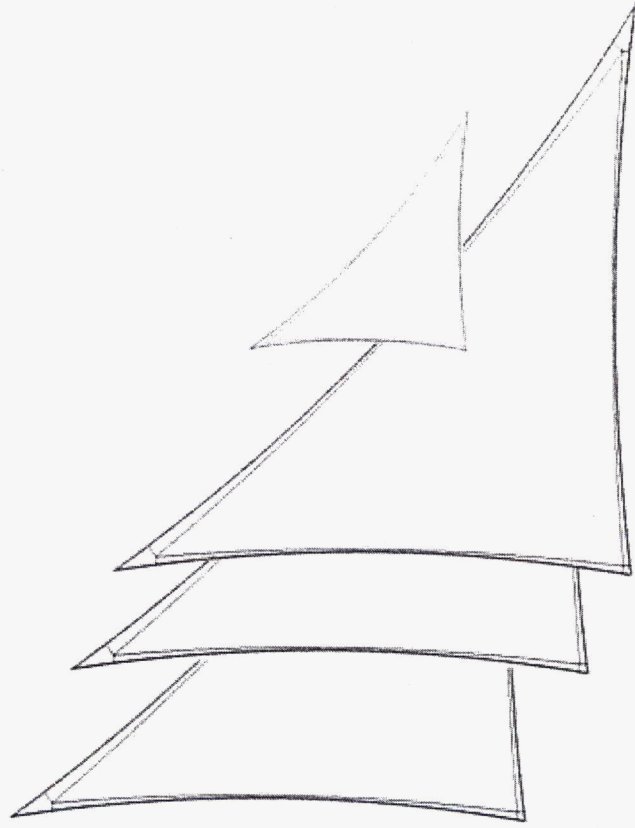
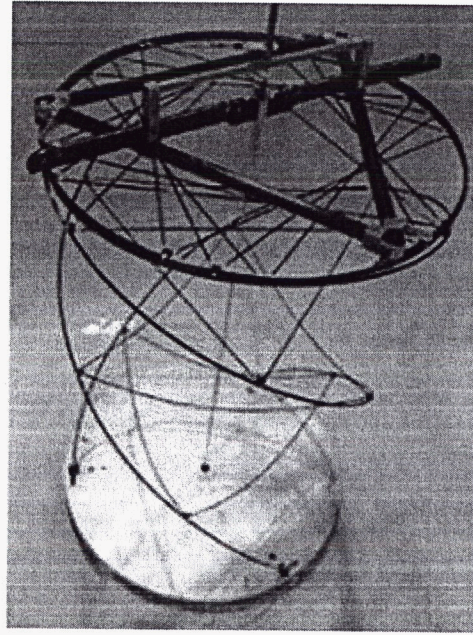
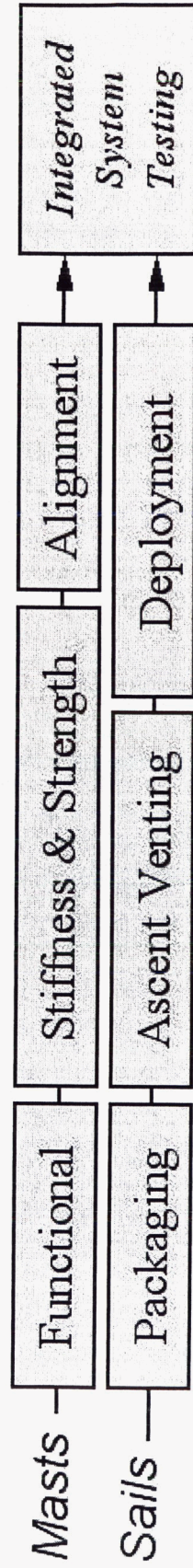
## Functionality

- ◆ Packaging, Folding
- ◆ Deployment Sequencers



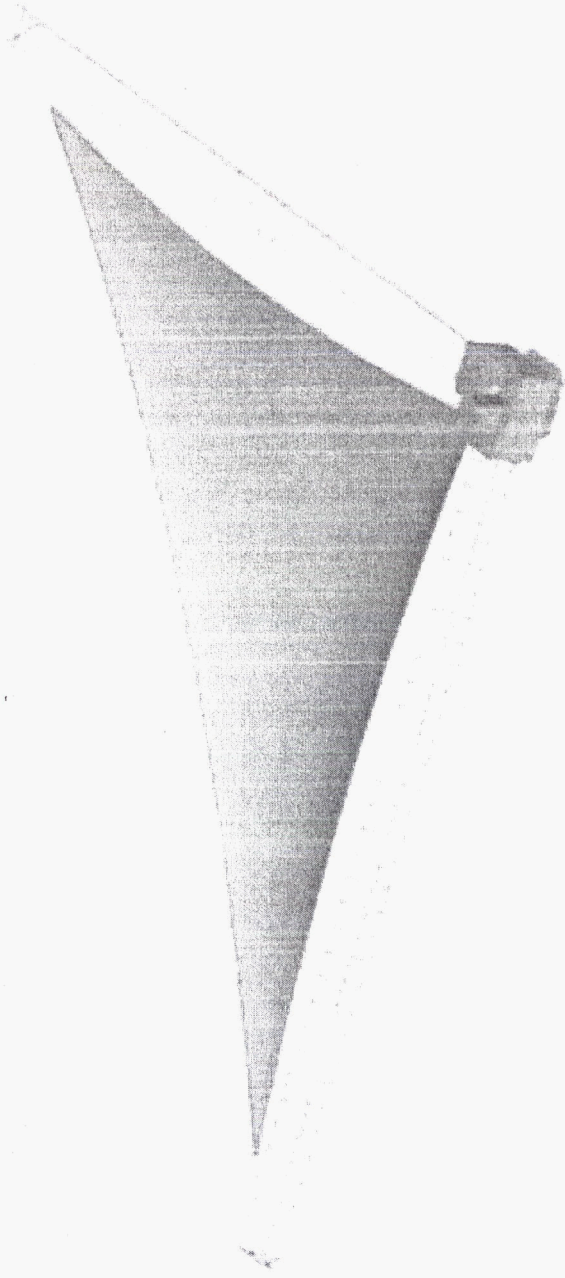


# FLOW DIAGRAM FOR MAST & SAIL TESTING



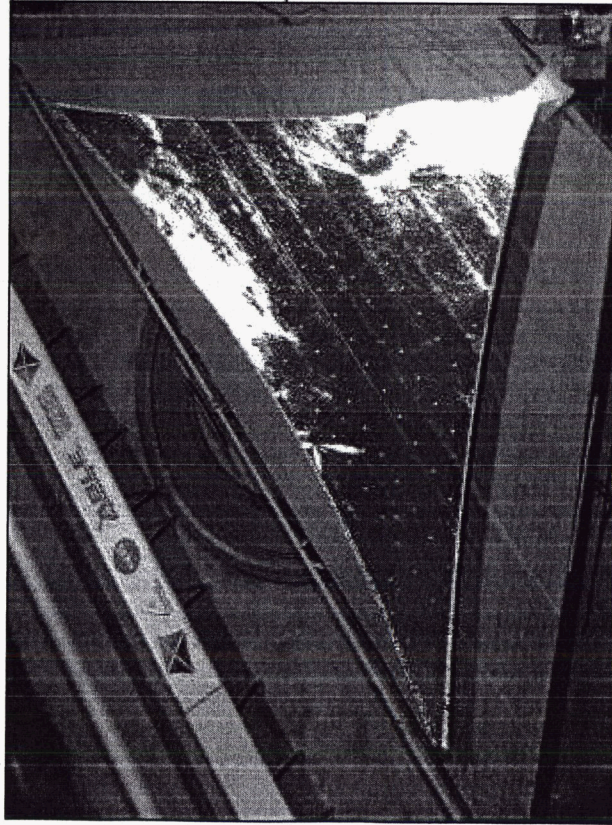


# QUADRANT INTEGRATION

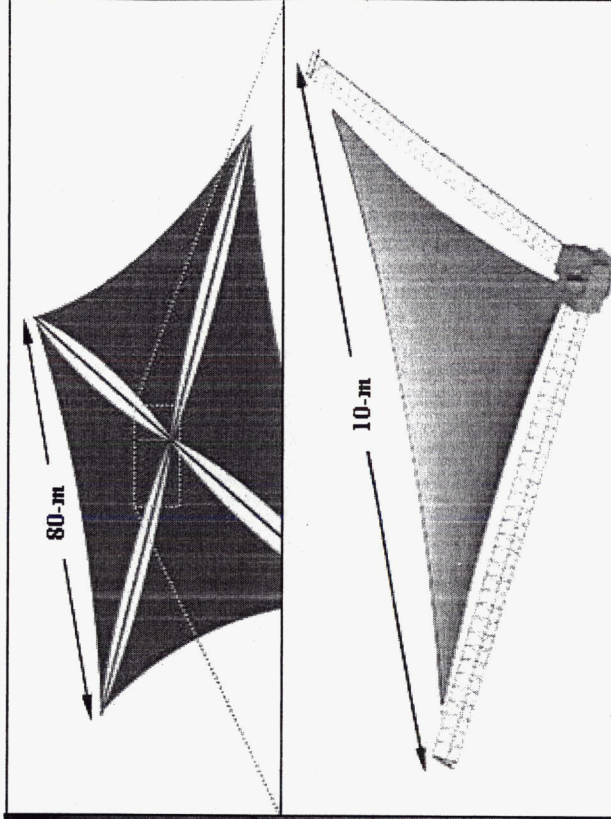




# 10-M QUADRANT



10-m S4 Quadrant in Vacuum  
Post Deployment (April 7, 2004)



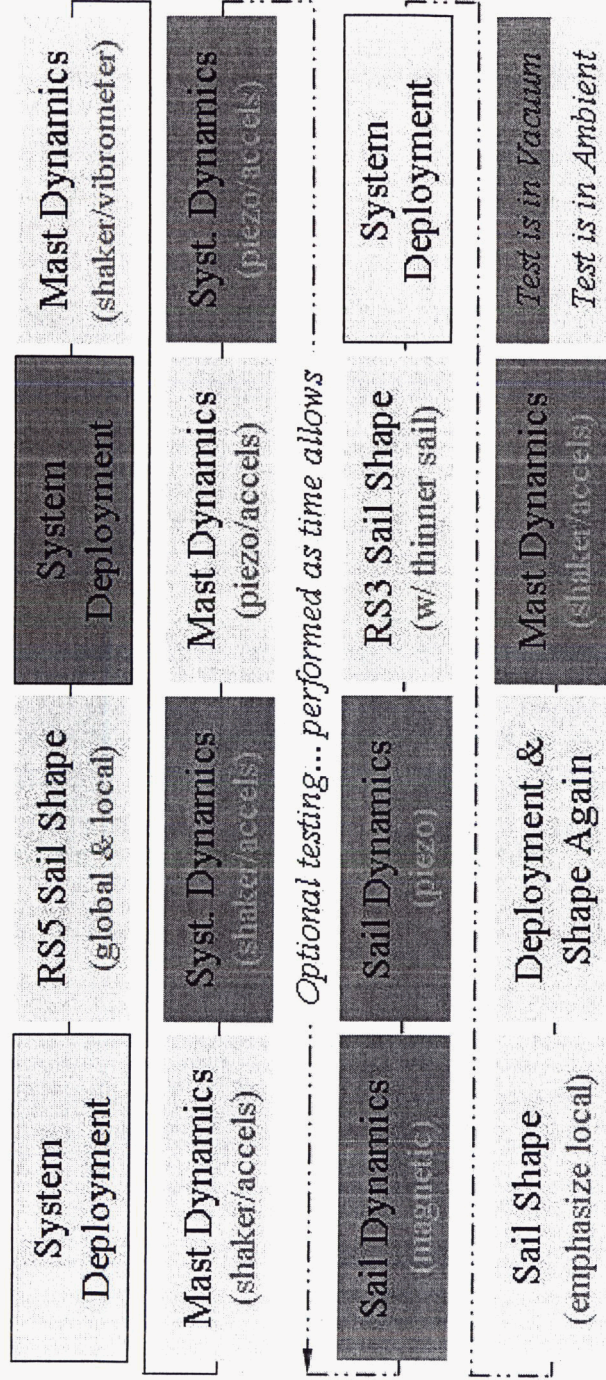
Demo Quadrant is 1/4 of a 80-m  
Scalable Square Solar Sail (S4)



# FLOW DIAGRAM FOR TESTING AT LARC

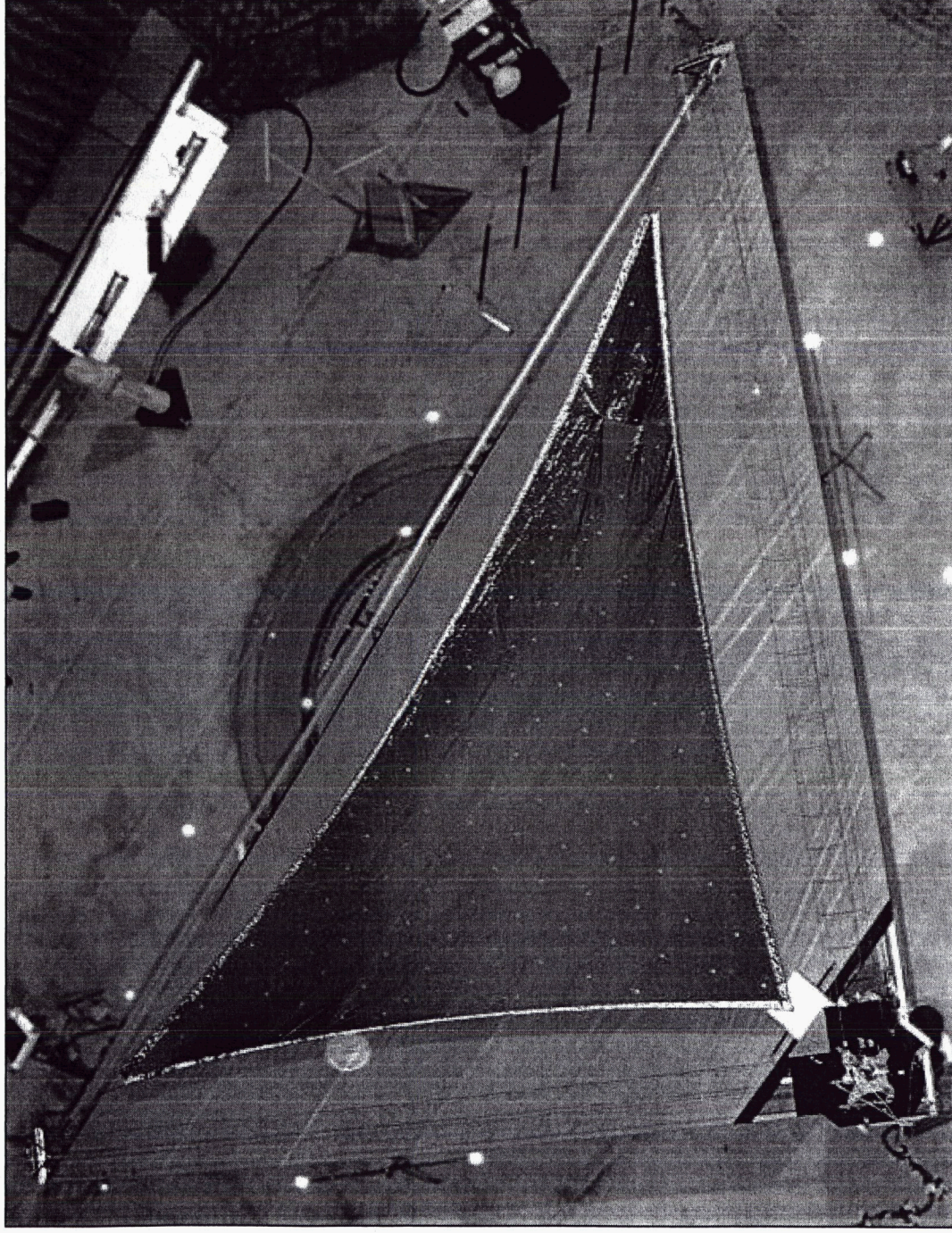
## Top-Level Test Goals

- ◆ Demonstrate deployment in vacuum of mast and sail system
- ◆ Provide data for modeling evaluation & correlation on:
  - Sail and mast shape and mast/sail/system dynamics



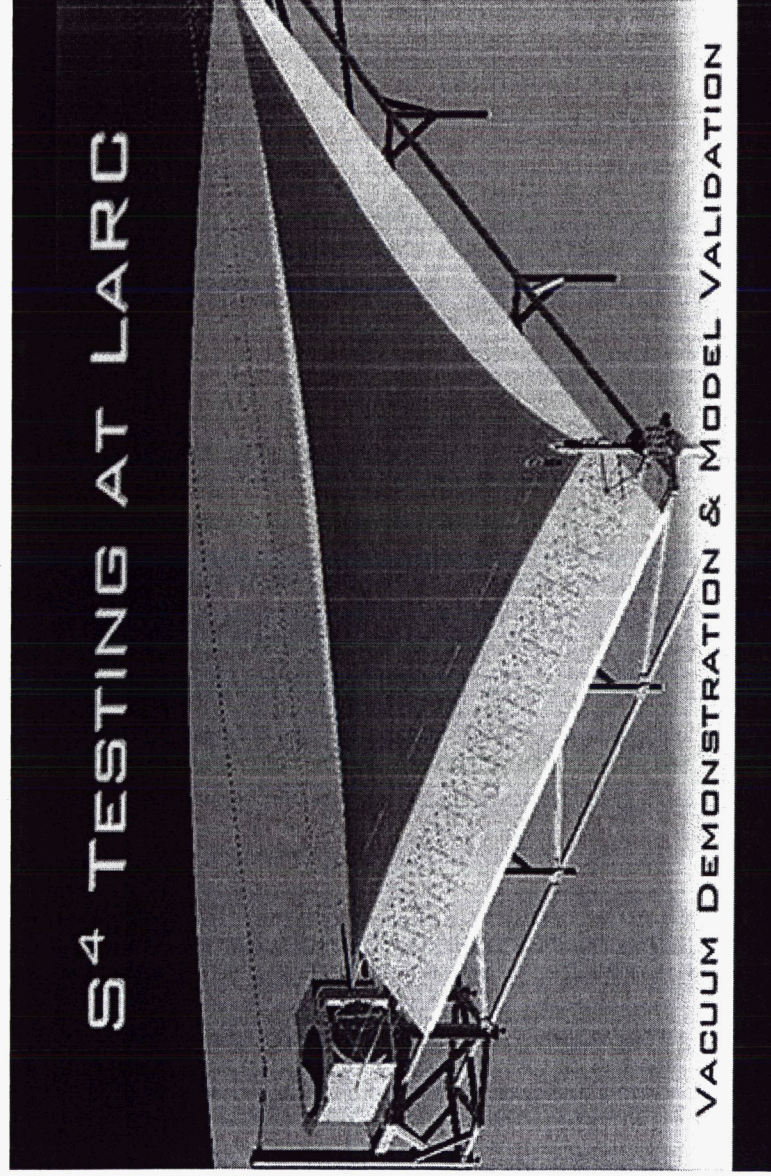


# 10-M QUADRANT IN LARC CHAMBER



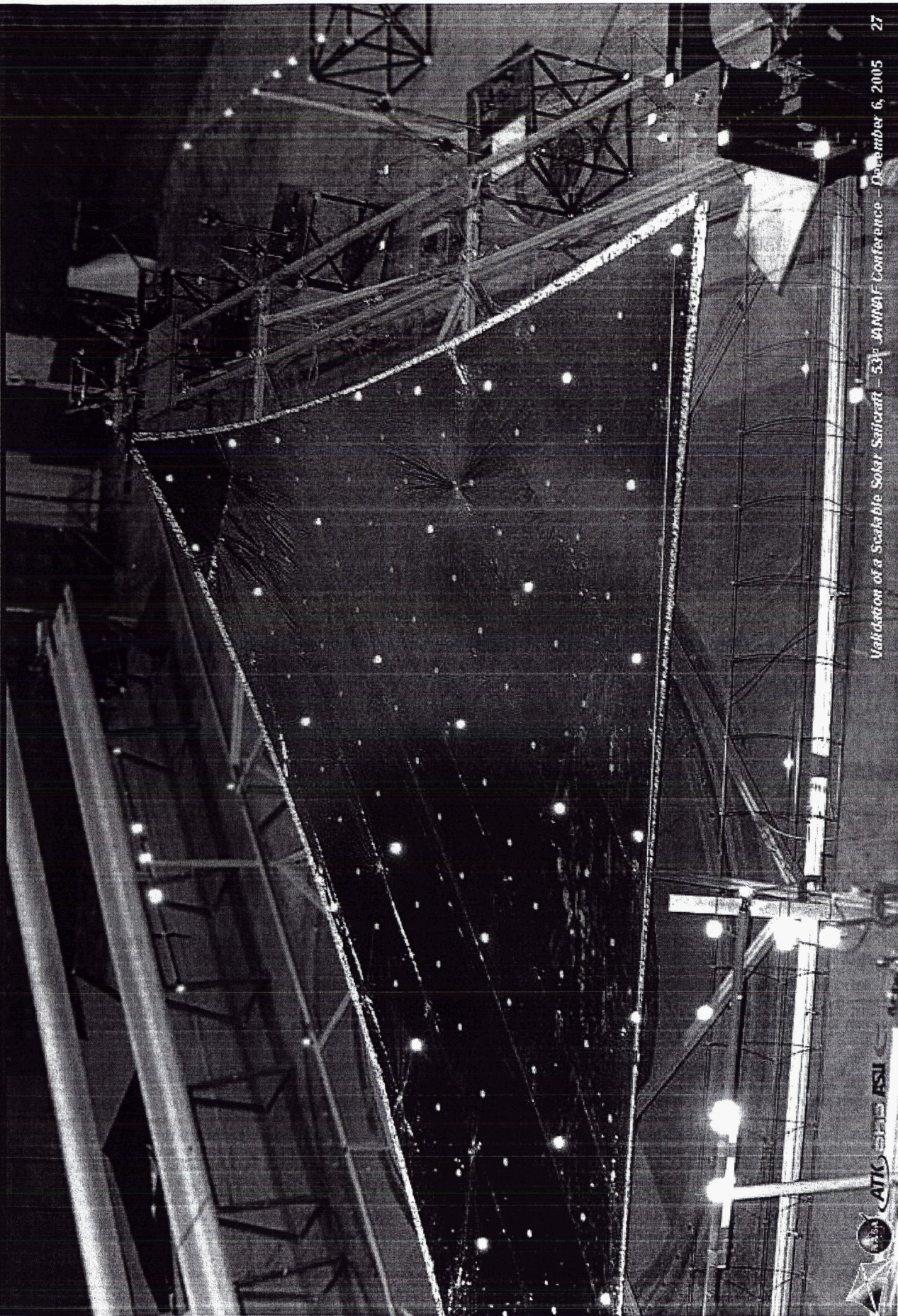


# 10-M QUADRANT IN LARC CHAMBER





# 10-M QUADRANT IN LARC CHAMBER





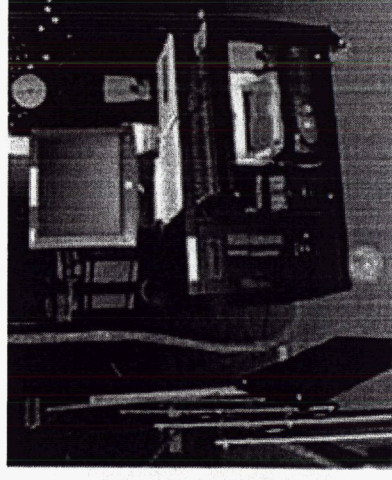
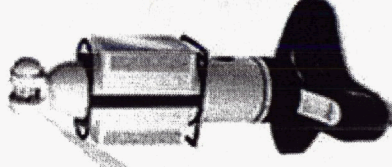
# SAIL SHAPE TESTING

Global and local shape measured

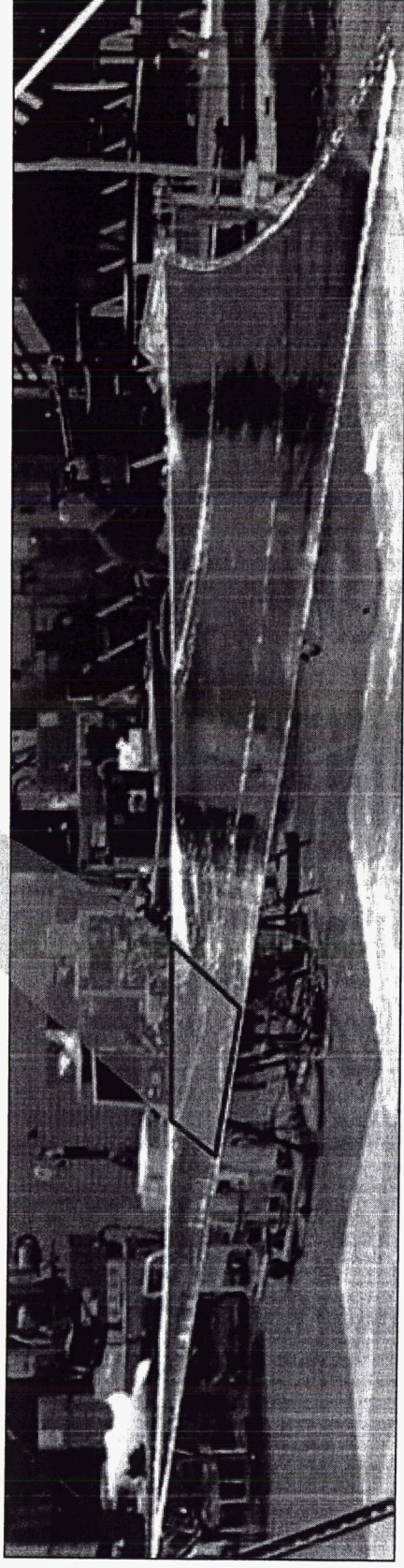
- ◆ Sag in 1-g correlated to FEA models

Local testing documented creasing effects from folding and rolling

- ◆ Allows identification of sail topology (propulsiveness) at 0-g stress levels

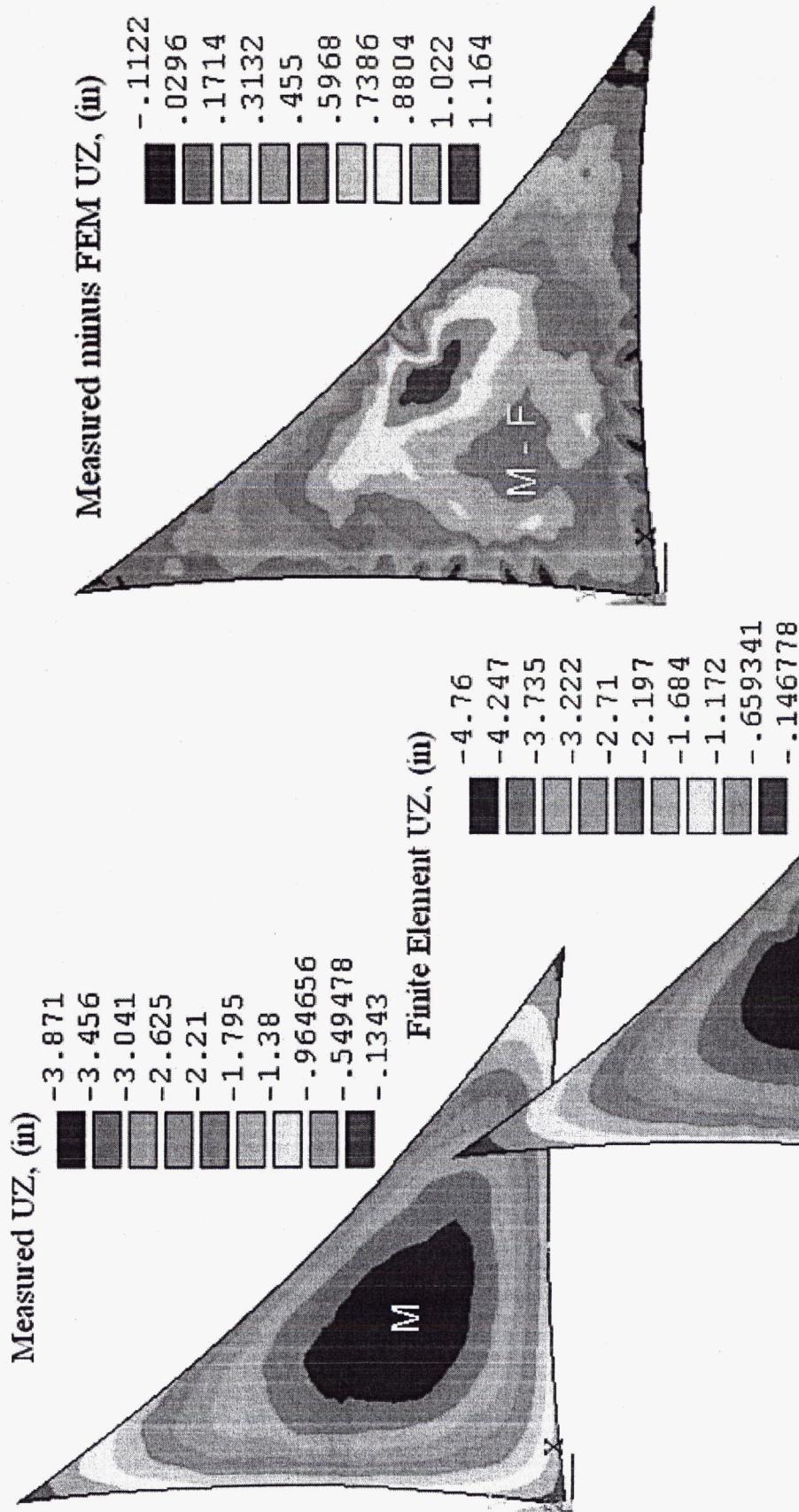


Leica Laser Radar



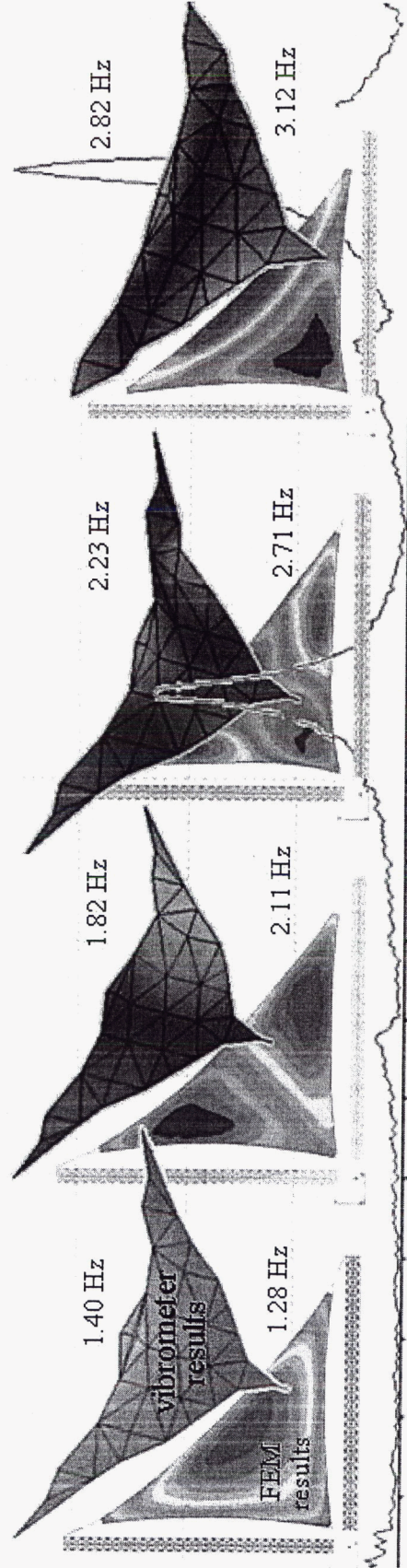
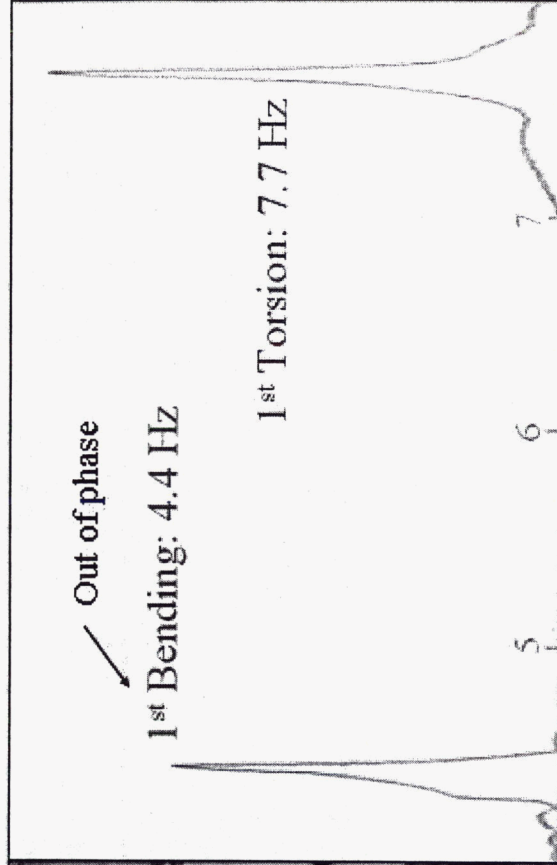
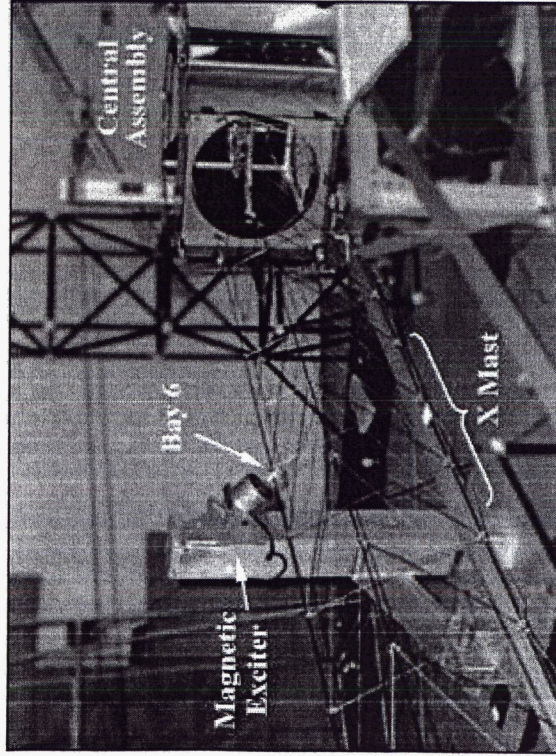


# SAIL DEFLECTIONS - CORRELATION



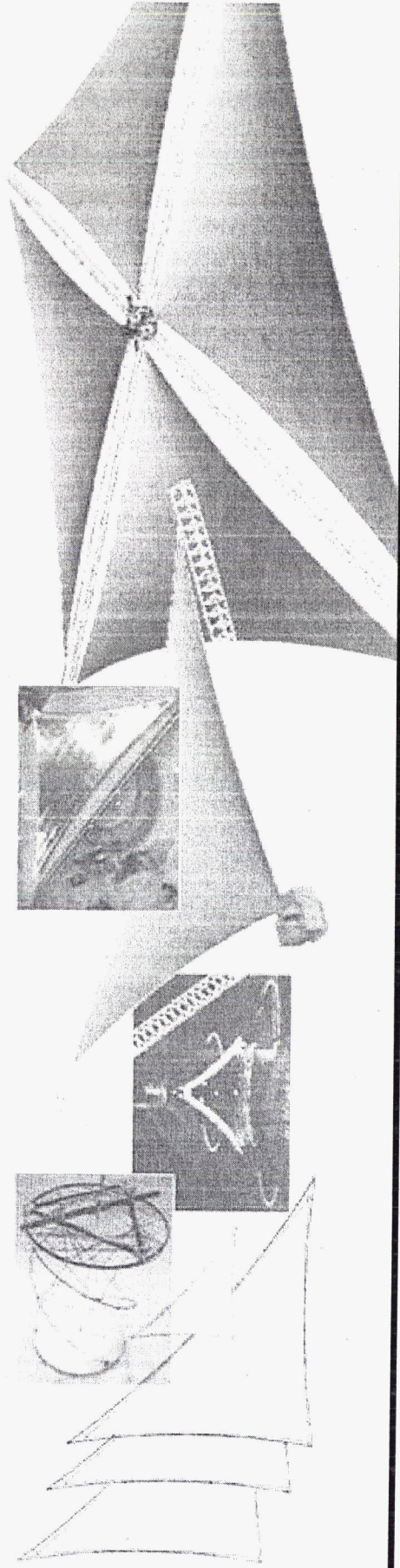


# DYNAMICS TESTING, MAST & SYSTEM

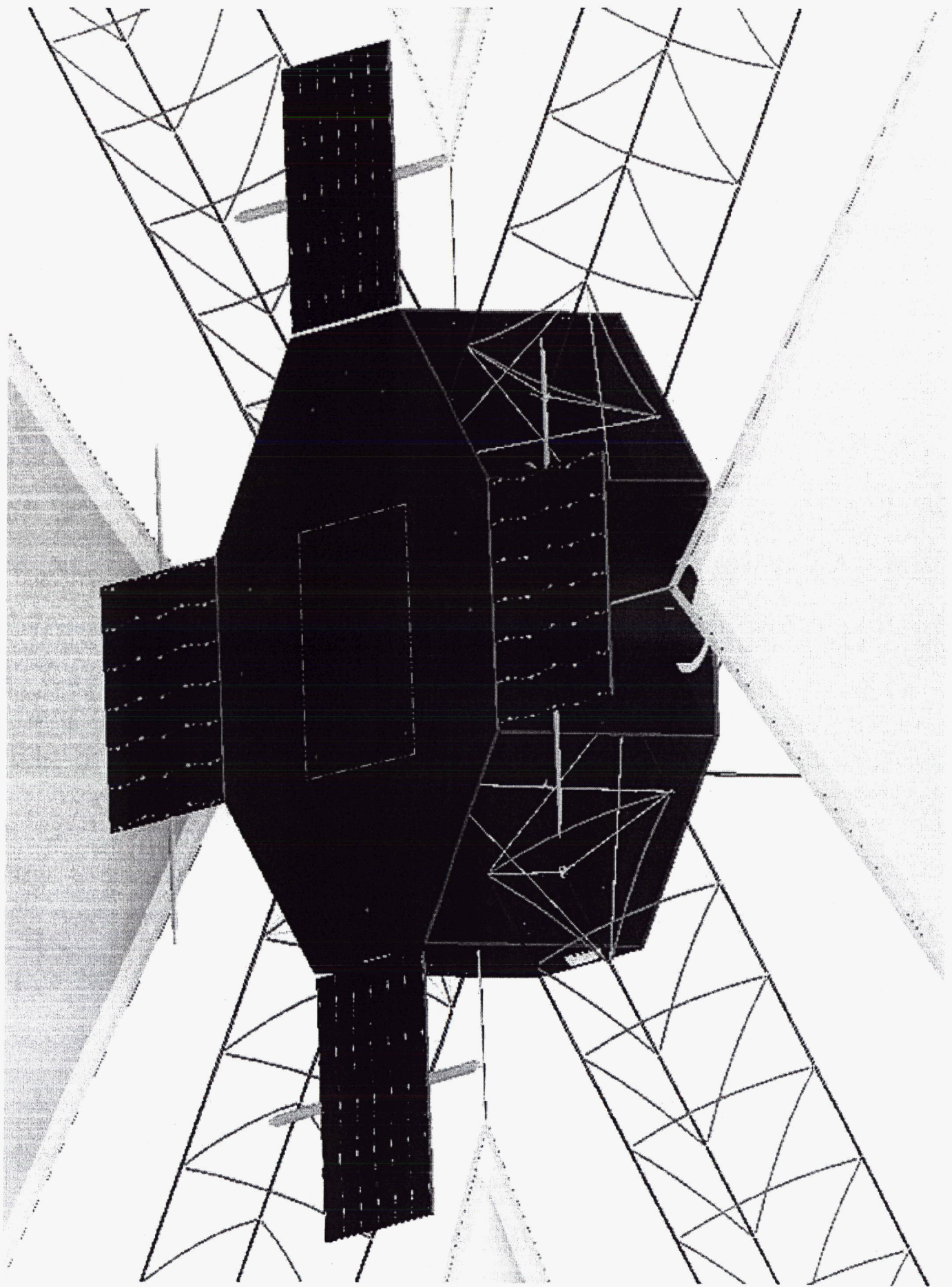




# PHASE 3- 20-M SYSTEM









# DESIGN EVOLUTION

*Primary components and functional changes from 10-m design:*

Central Assembly (CA) is flight-like (composite honeycomb)

- ◆ 10-m Quadrant CA was only a functional form
- ◆ Launch ties for mast tips, sail doors
- ◆ LV release structure

Added roll control

- ◆ Via sail "blade pitch" adjustment by tip spreaders

Hoisting sails from mast tips

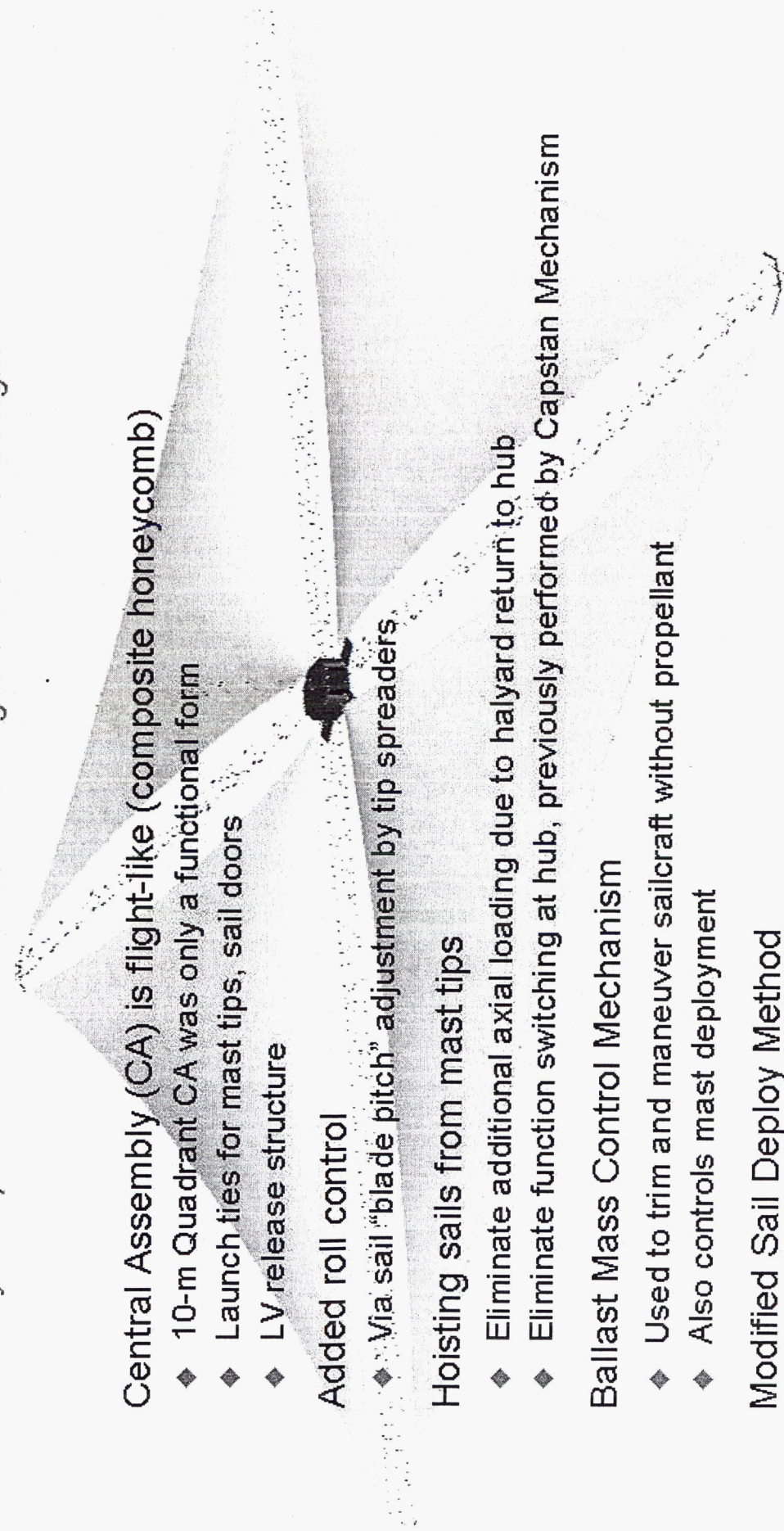
- ◆ Eliminate additional axial loading due to halyard return to hub
- ◆ Eliminate function switching at hub, previously performed by Capstan Mechanism

Ballast Mass Control Mechanism

- ◆ Used to trim and maneuver sailcraft without propellant
- ◆ Also controls mast deployment

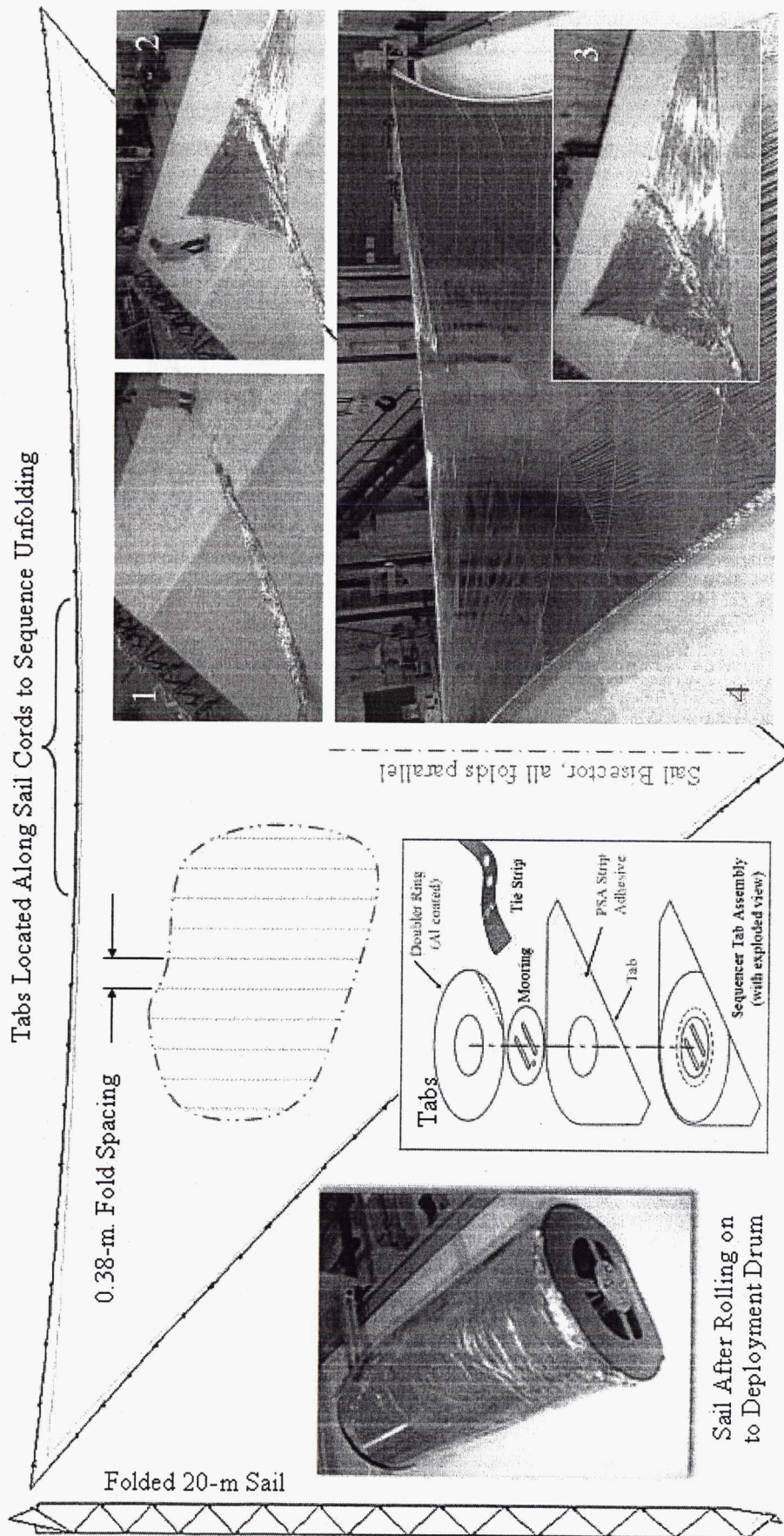
Modified Sail Deploy Method

- ◆ Folded parallel to hypotenuse, sequencers move to cords, break-away style



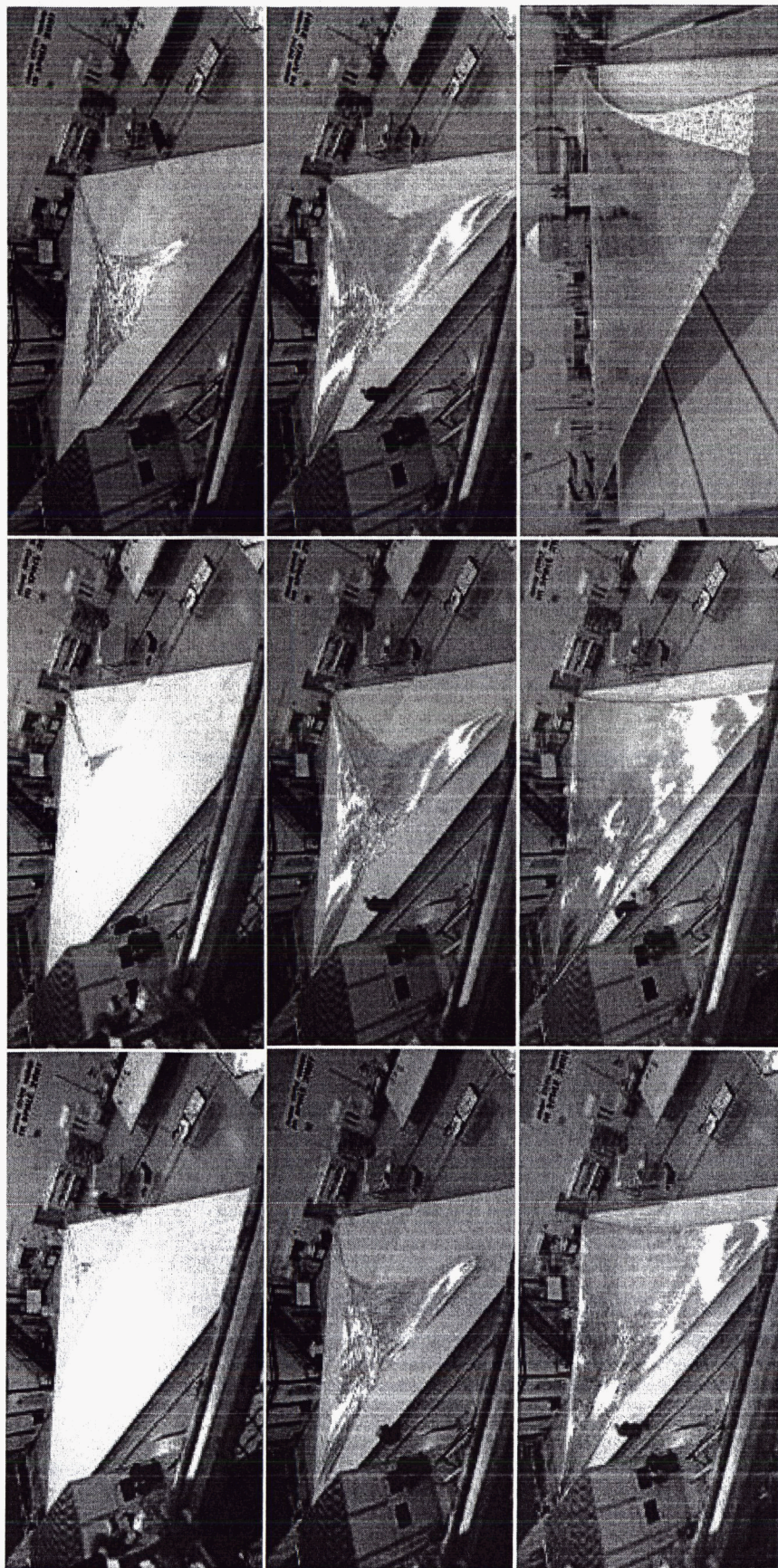


# SAIL PACKAGING & SEQUENCING



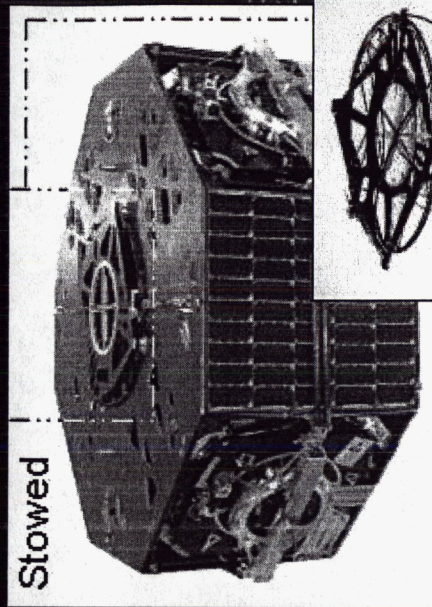
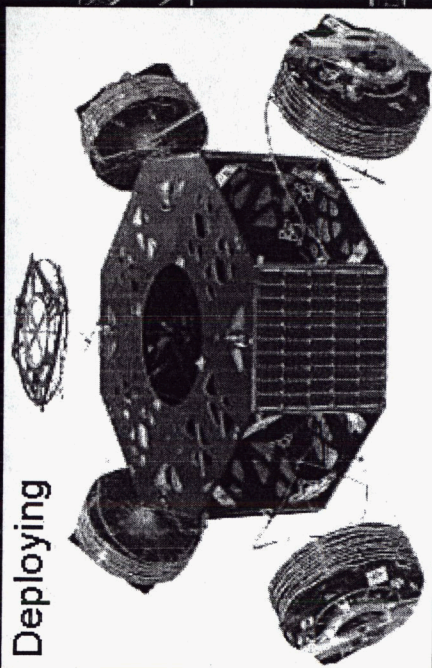


# PS20-1 1<sup>ST</sup> DEPLOYMENT

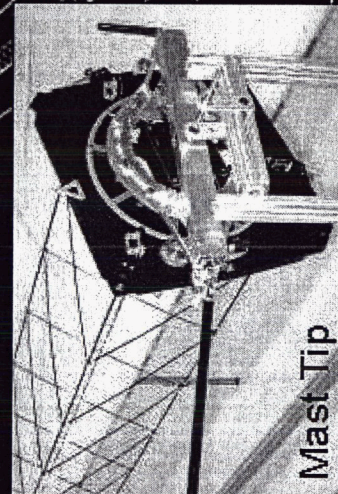
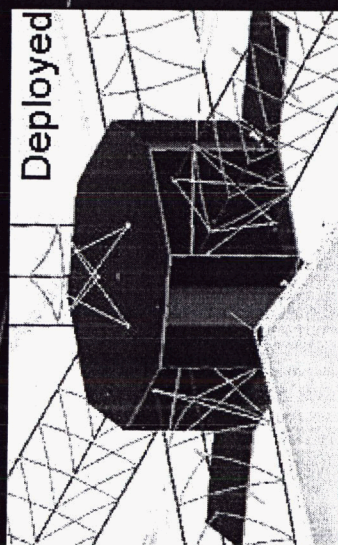
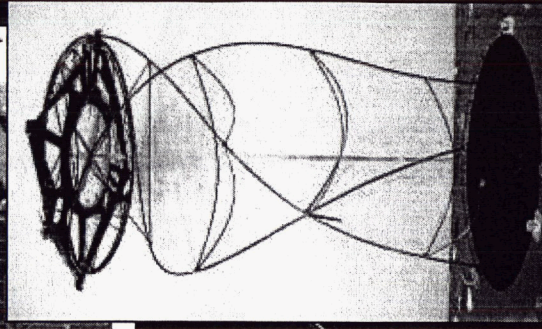




# VIEWS OF 20-M SYSTEM HARDWARE

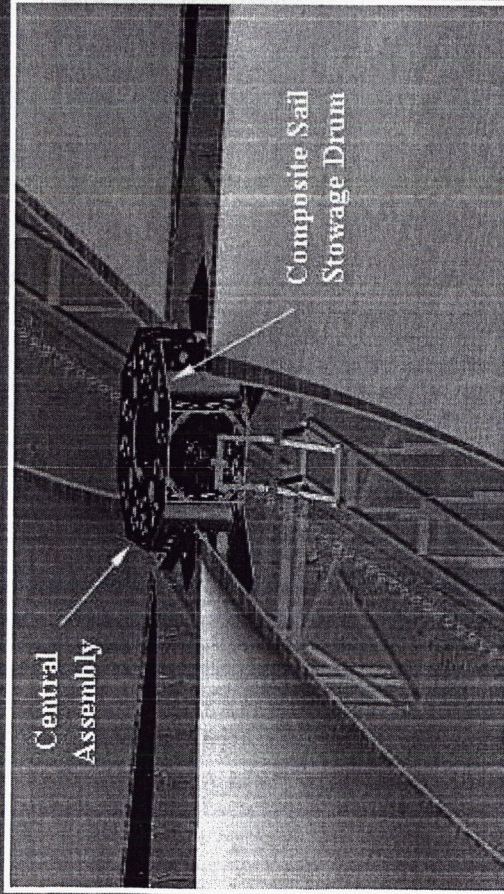


Instrument Boom, Deploying





# 20-M S<sup>4</sup> SYSTEM DEMONSTRATOR

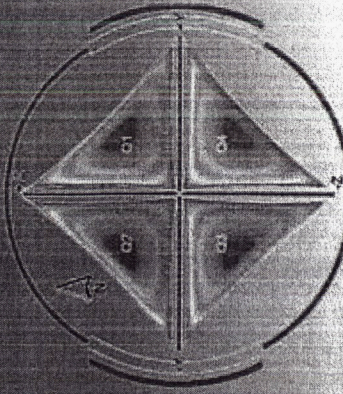


Central Assembly

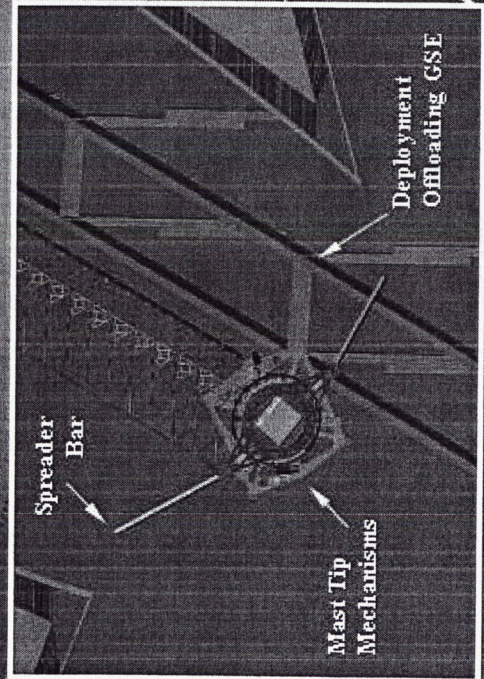
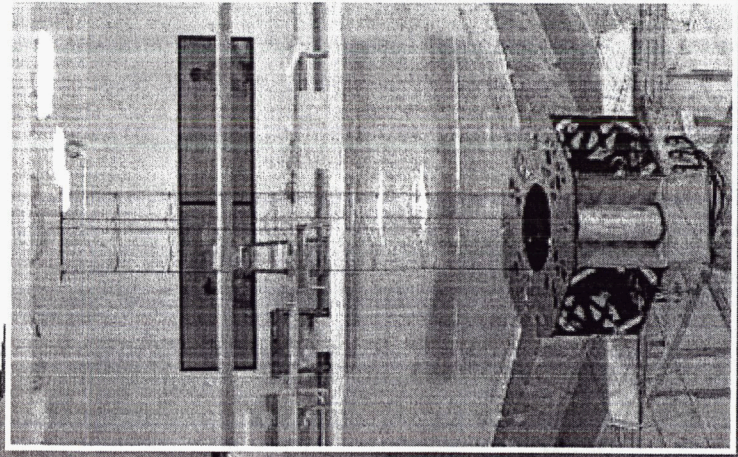
Composite Sail Stowage Drum

## In the Central Assy

Drive Mechanisms  
Motors / Drivers  
Electronics Controls  
Position Sensors  
Release Actuators  
Load Cells (Tack line)  
Piezo Actuators



20-m S<sup>4</sup> in 100-ft dia.  
Plum Brook TV Chamber



Spreader Bar

Mast Tip Mechanisms

Deployment Offloading GSE

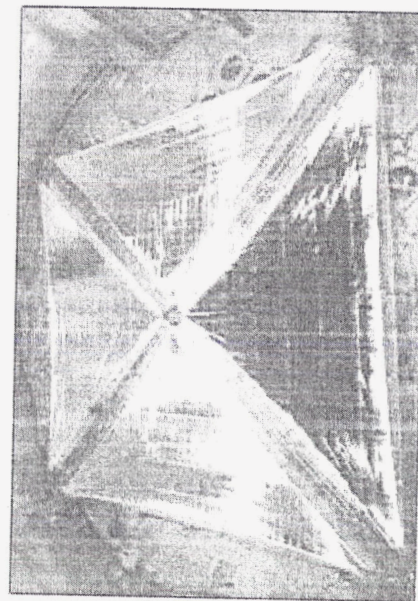
## In the Tip Assy

ACS Mechanism & Motor / Driver  
Accelerometers  
Load Cells  
Limit Switch





# SYSTEM TEST SERIES AT PLUM BROOK





# PLUM BROOK TESTING PRIORITIES

## ✓ Demonstrate Deployment Robustness

- ◆ 3 deployments were completed: The first in ambient, the second in high vacuum, and the third (also in a high vacuum) with a thermal gradient imposed across the stowed system.

## ✓ Capture Shape Data

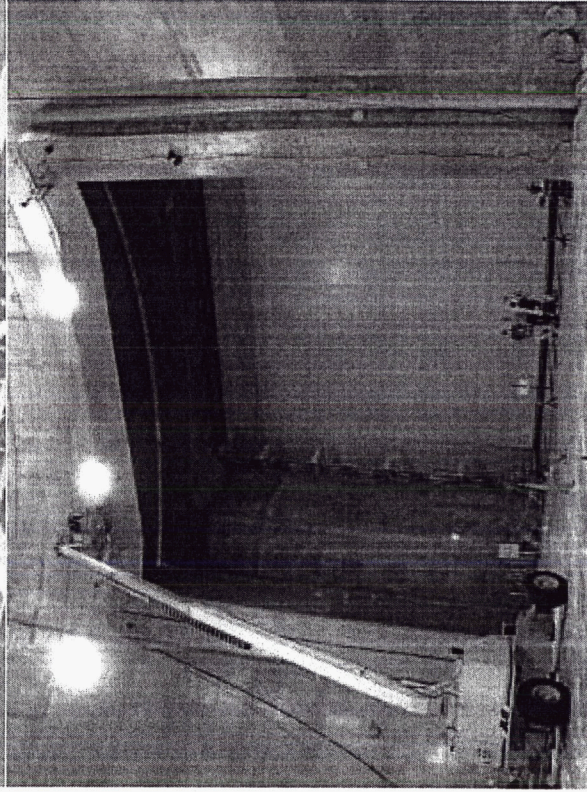
- ◆ Gravity effects on sail billow were measured by LaRC using five photogrammetry cameras at three spreader bar positions.

## ✓ Capture Dynamics Data

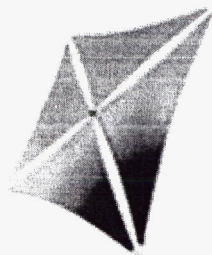
- ◆ The first modes and modal frequencies of the system were measured by LaRC using external inputs and response sensors, as well as embedded actuators and sensors that are applicable to a flight program.



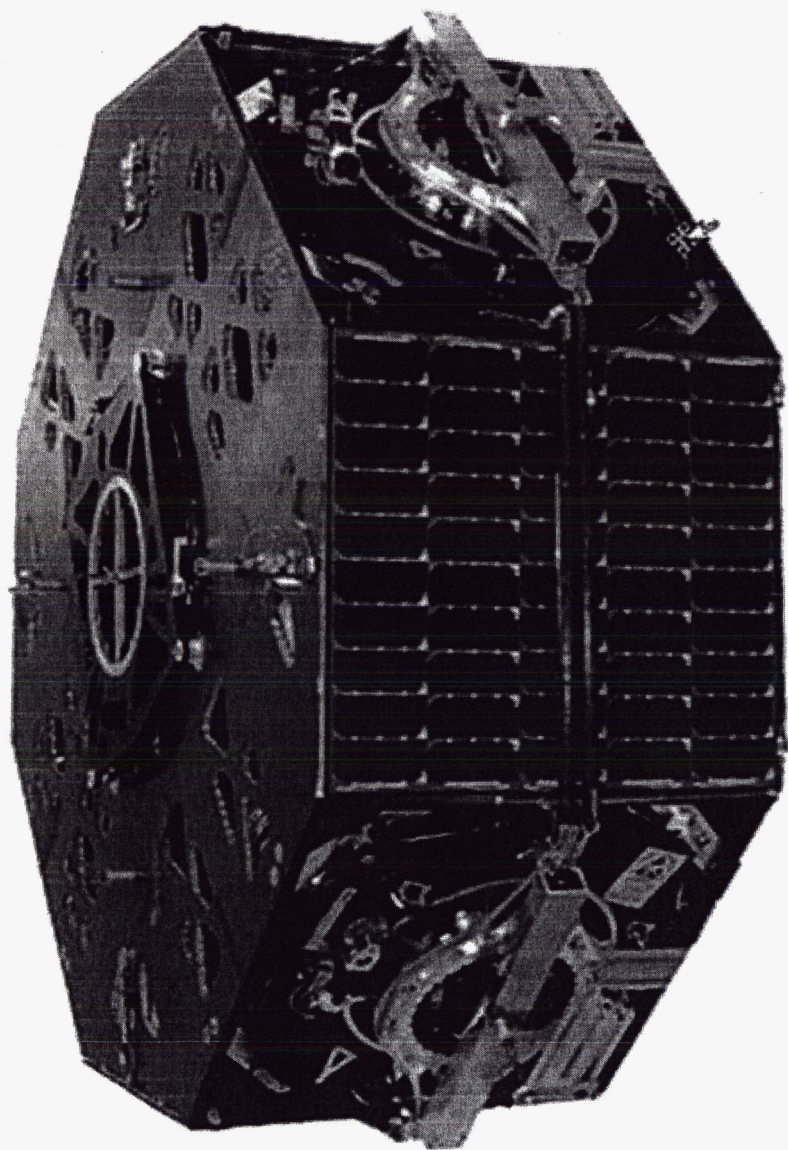
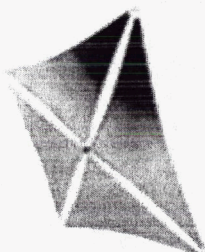
NASA GRC - PLUM BROOK





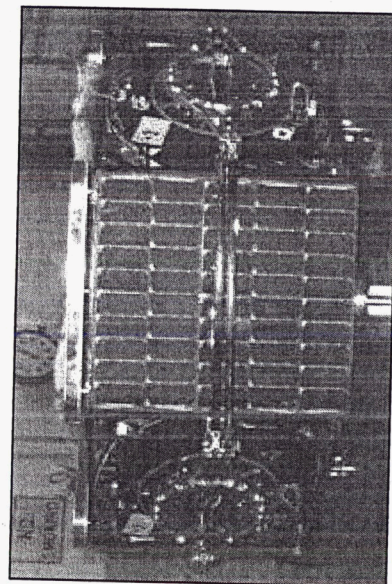
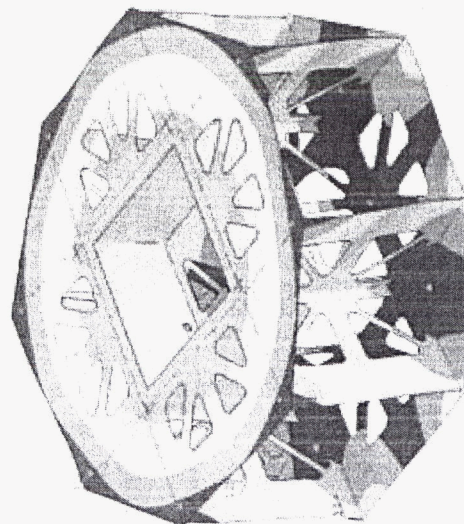


**SPS ASU**





# LAUNCH VIBRATION TEST / ANALYSIS





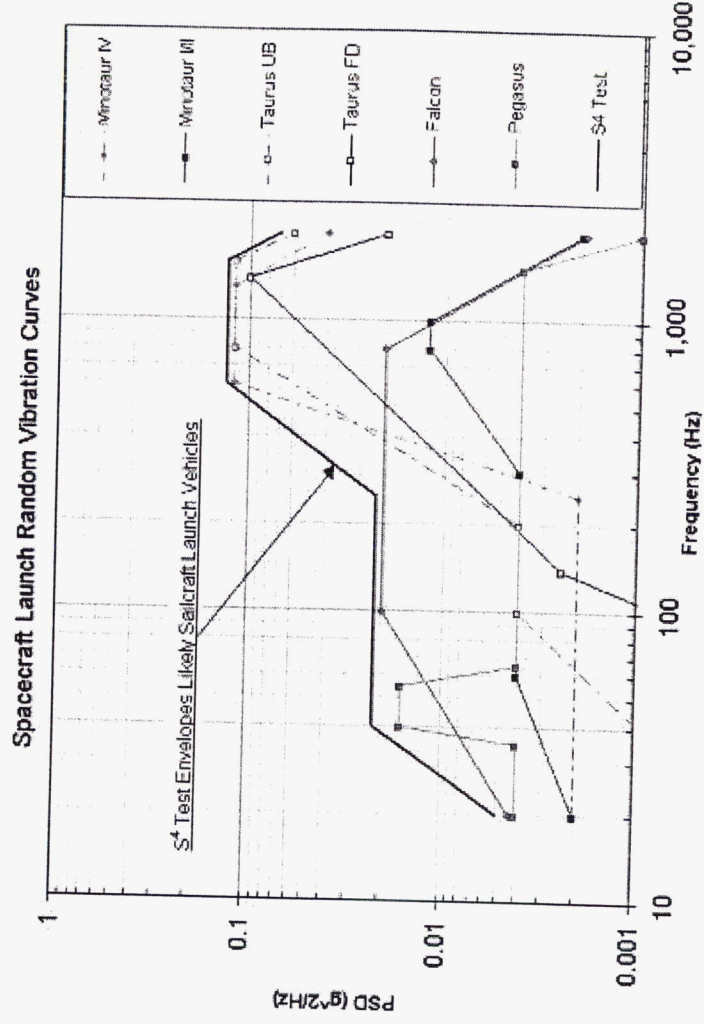
# VIBRATION TESTING

- ◆ Random spectrum to envelope all likely launchers
- ◆ Vibration Test performed in accordance with...
  - 3099D2239, System Test Plan
  - 3099D2254, Vibration Test Procedure

Hz	G <sup>2</sup> /Hz
20	0.005
40	0.022
250	0.022
600	0.130
1600	0.130
2000	0.070

$$G_{\text{rms}} = 14.04$$

- ◆ Test objectives:
  - Test flight-like S<sup>4</sup> in relevant environment
  - Determine structure resonant frequencies
  - Increase technology TRL

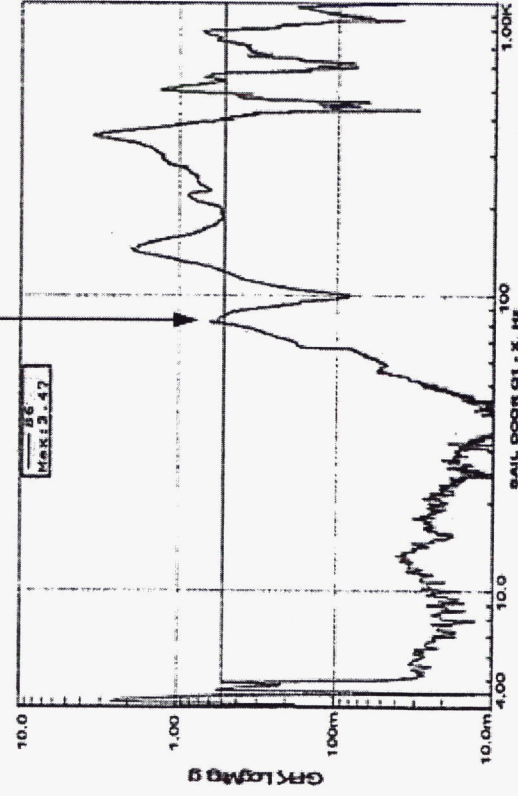




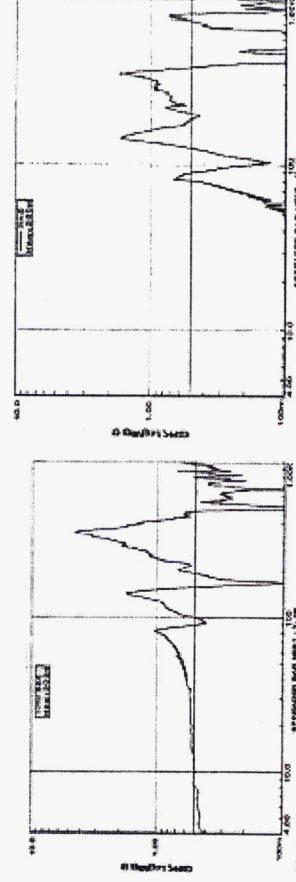
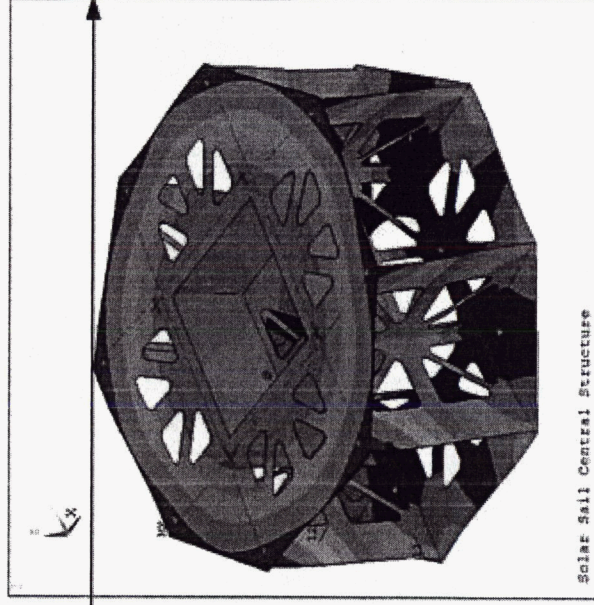
# MODE RESPONSE CORRELATION

- ◆ Fundamental Mode estimated as 83 Hz
  - Similar to response seen with several accels and for inputs along mast axis and 45° off that

81 Hz

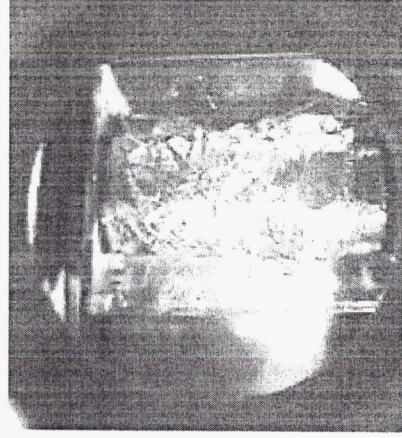
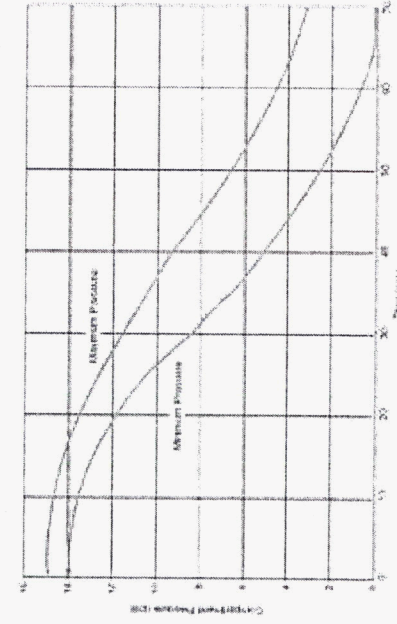
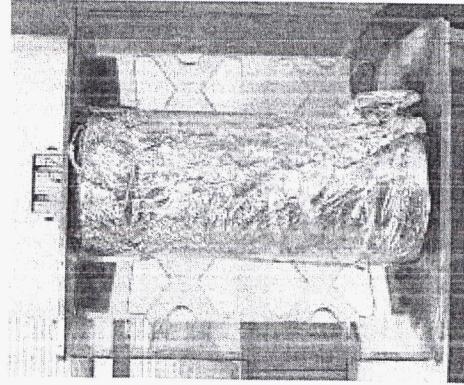


ANSYS 9.0  
SEP 7 2005  
14:51:21  
MODAL SOLUTION  
STEP=1  
SUB =1  
FREQ=83.404  
USUM (AVG)  
RMS=0  
POWERGRAPHIC  
EFFECT=1  
AVRES=mat  
DMX =3.121  
SMX =3.121





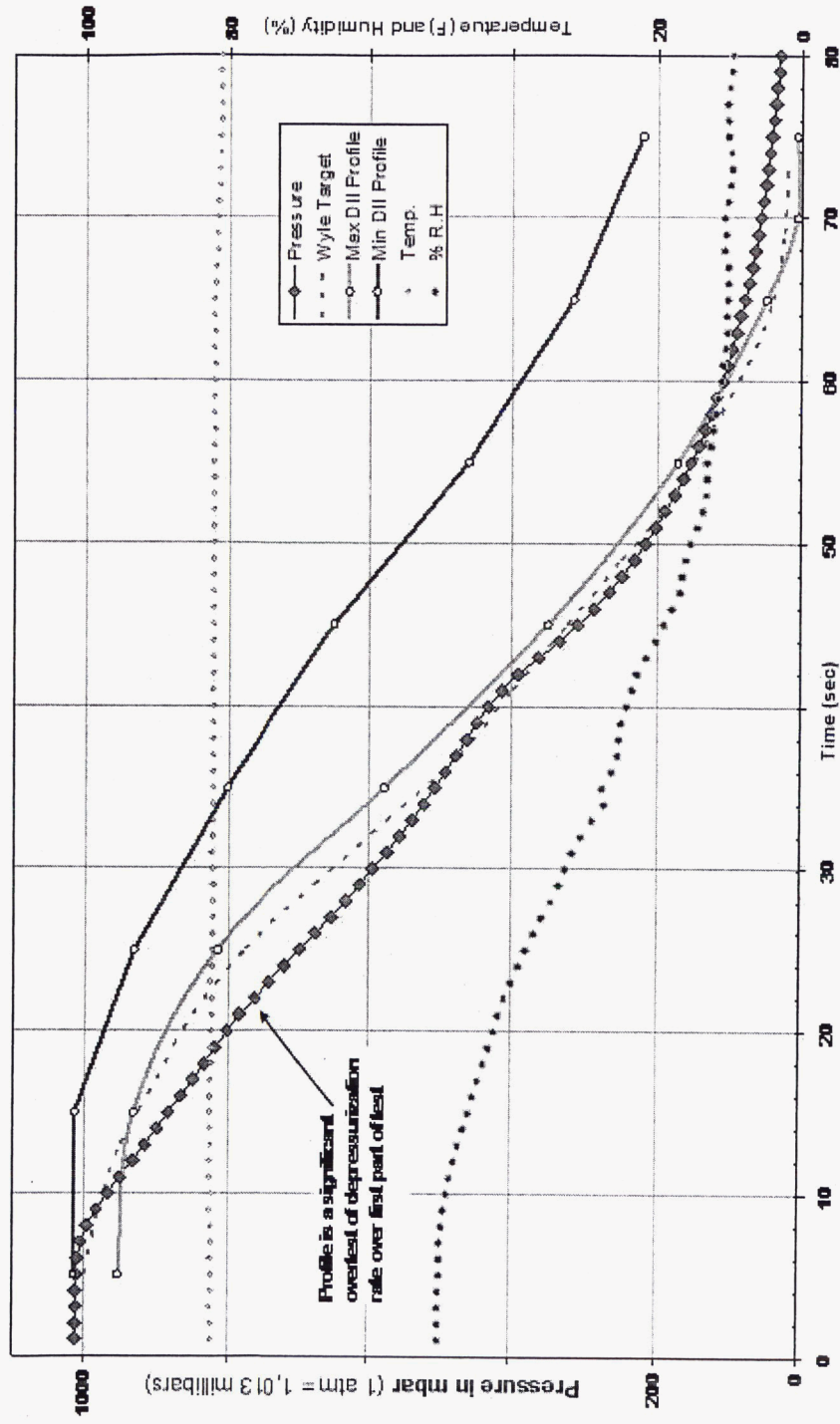
# LAUNCH ASCENT VENTING





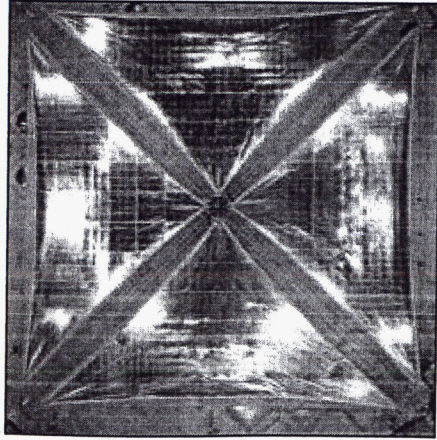
# ASCENT VENTING TEST PROFILE

Plot of pressure profiles desired and as tested

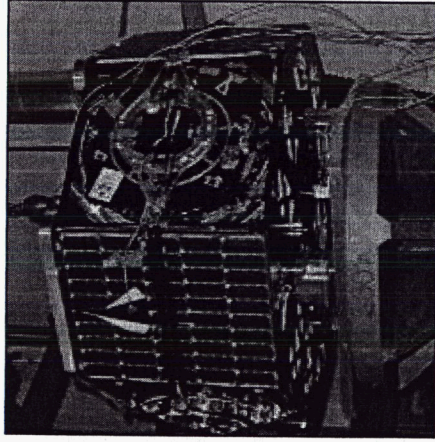




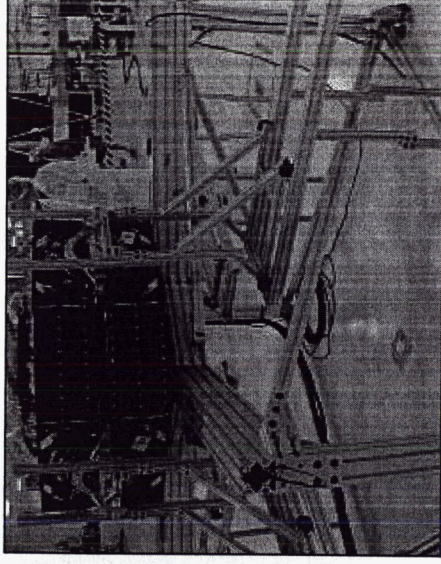
# ASCENT VENTING TESTING OVERVIEW



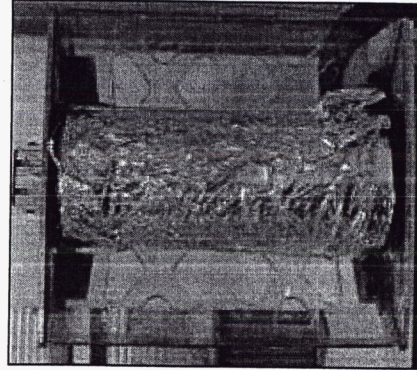
Final Stow May 23<sup>rd</sup>, Ohio



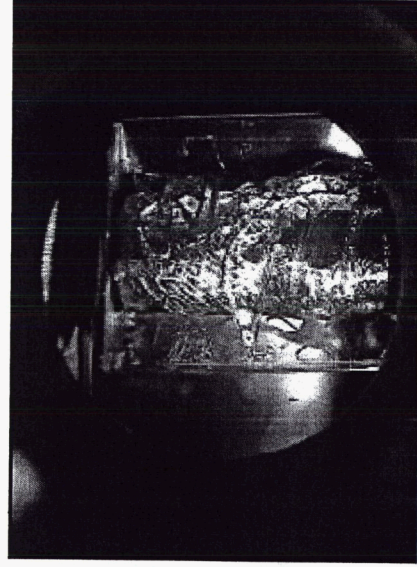
Vibration Testing  
Chatsworth, July 5<sup>th</sup> & 6<sup>th</sup>



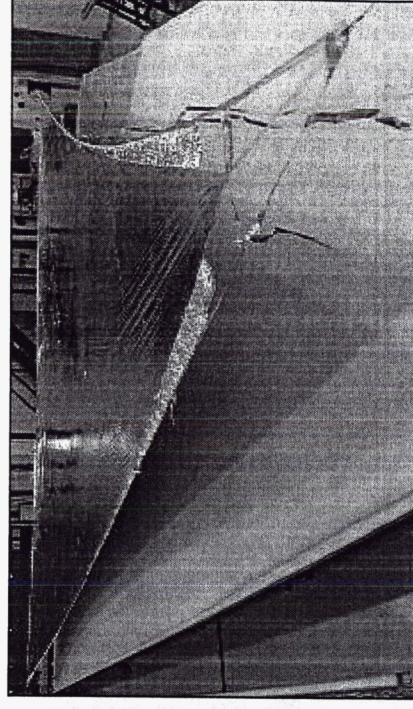
Post-Vibe Deploy,  
ATK, Goleta, July 14<sup>th</sup>



Venting GSE,  
ATK, Goleta, July 22<sup>nd</sup>



Venting Test  
El Segundo, CA, July 29<sup>th</sup>



Final Deploy,  
SRS, Huntsville, AL, Aug. 2<sup>nd</sup>

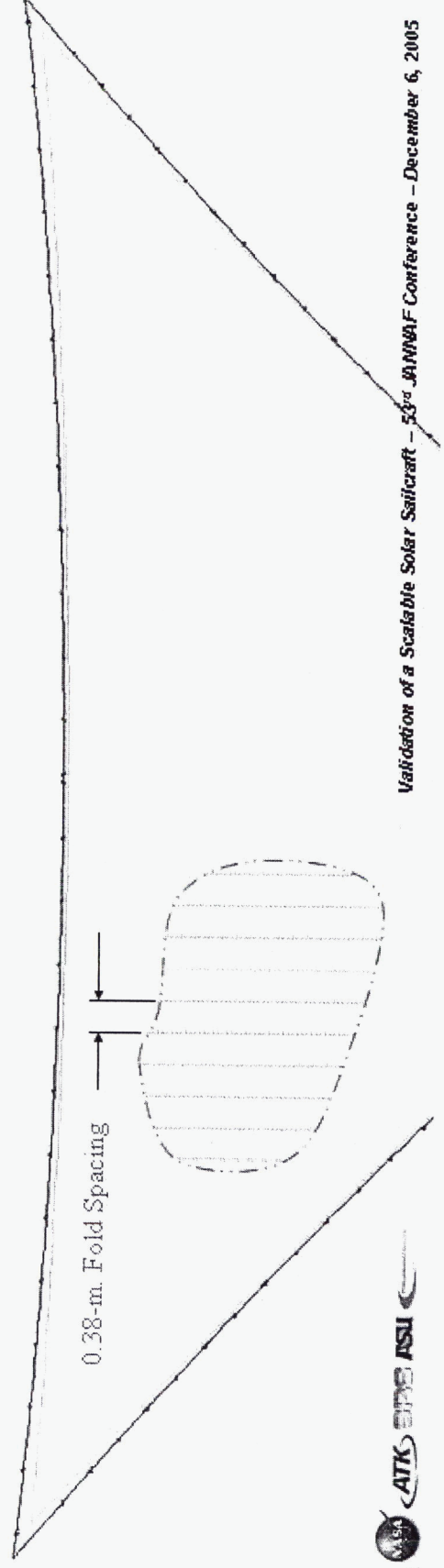
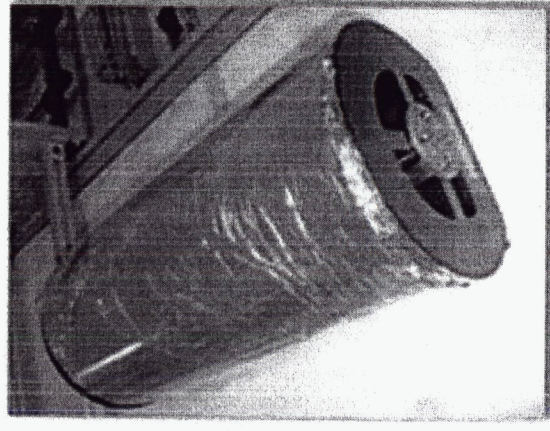




# ASCENT VENT TEST SUMMARY

## Launch Depressurization Test Findings

- ◆ Folded and rolled sail vents well under launch conditions
- ◆ Launch pressure change does not damage sail
- ◆ Deployment control unaffected by pressure change exposure





# PRESENTATION SUMMARY

The ISP S<sup>4</sup> GSD system development and hardware demonstration efforts were successfully completed

- ◆ A challenging technology has been advanced appreciably and is now well prepared for a demonstration in earth orbit

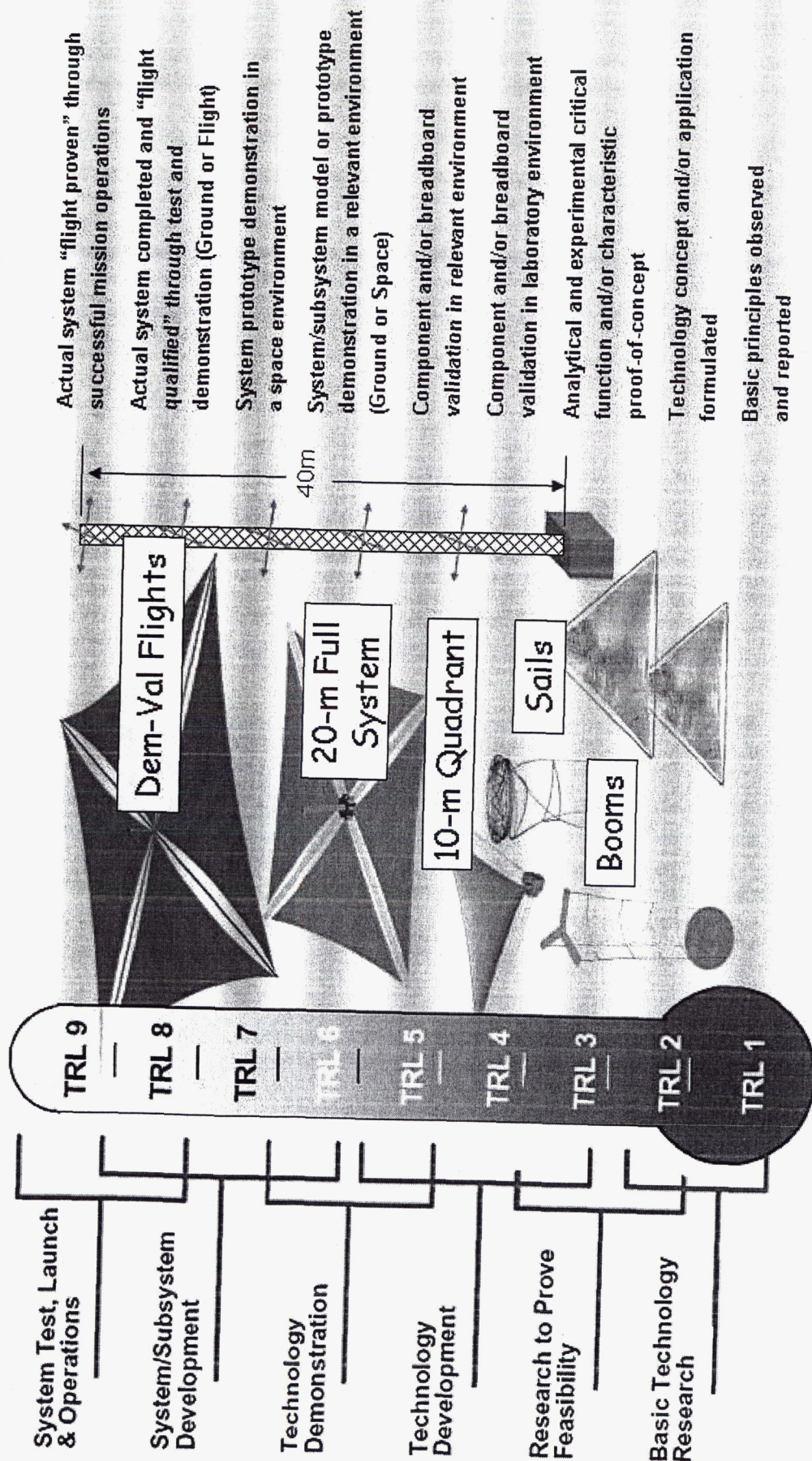
The S<sup>4</sup> sailcraft systems configuration demonstrated:

- ◆ Package: volumetrically efficient, robust to venting & vibration
- ◆ Integration: sharing of bus functions/structure = optimal sailcraft
- ◆ Deploy: kinematically determinate, reliable, and well controlled
- ◆ ACS: well controlled, embedded systems, robust fault recovery
- ◆ Propulsion: uniform tension, flat, propulsively efficient, predictable
- ◆ Scalability: meets roadmap missions, with affordable launchers



# TECHNOLOGY READINESS LEVEL (TRL)

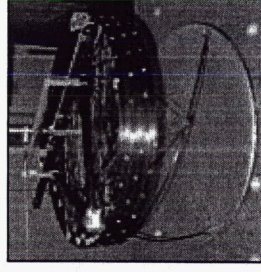
## Advancing the TRL to Prepare for Science Missions





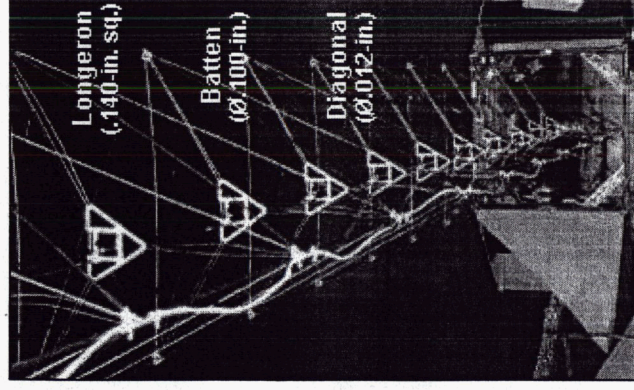
# S<sup>4</sup> SYSTEM 10,000 M<sup>2</sup> POINT DESIGN

- Operating Temperature
  - 25°C at 1.0 au
- First Natural Frequency
  - 0.03 Hz
- Stowed Package
  - 1.9 m dia. by 0.54 m
- Control Systems
  - Runners & Spreader Bars
- System Mass:
  - 113 kg
- Characteristic acceleration
  - 0.73 mm/s<sup>2</sup>
  - 0.35 mm/s<sup>2</sup> with 130 kg SC

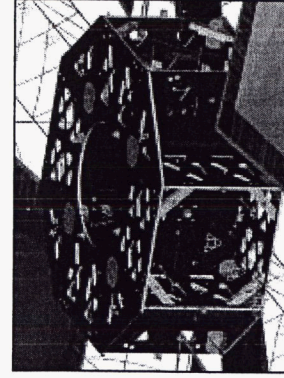
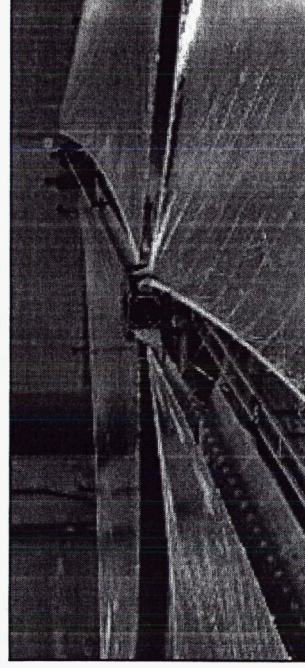


**Stowed  
Coilable**  
Ø20-in. (50.5 cm)  
25.7-in.-tall  
(<0.80% of length)

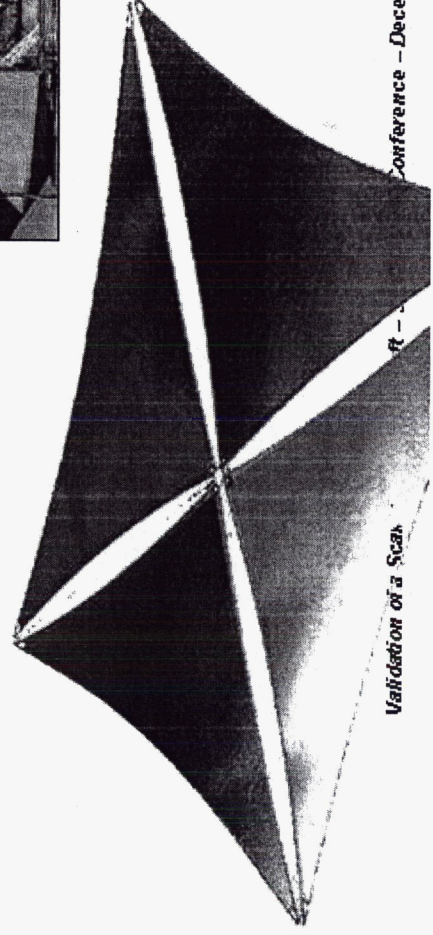
**Mast Linear Mass: 115 g/m  
(with 11 g/m harness)**



**Sail Thickness: 2.25 µm**



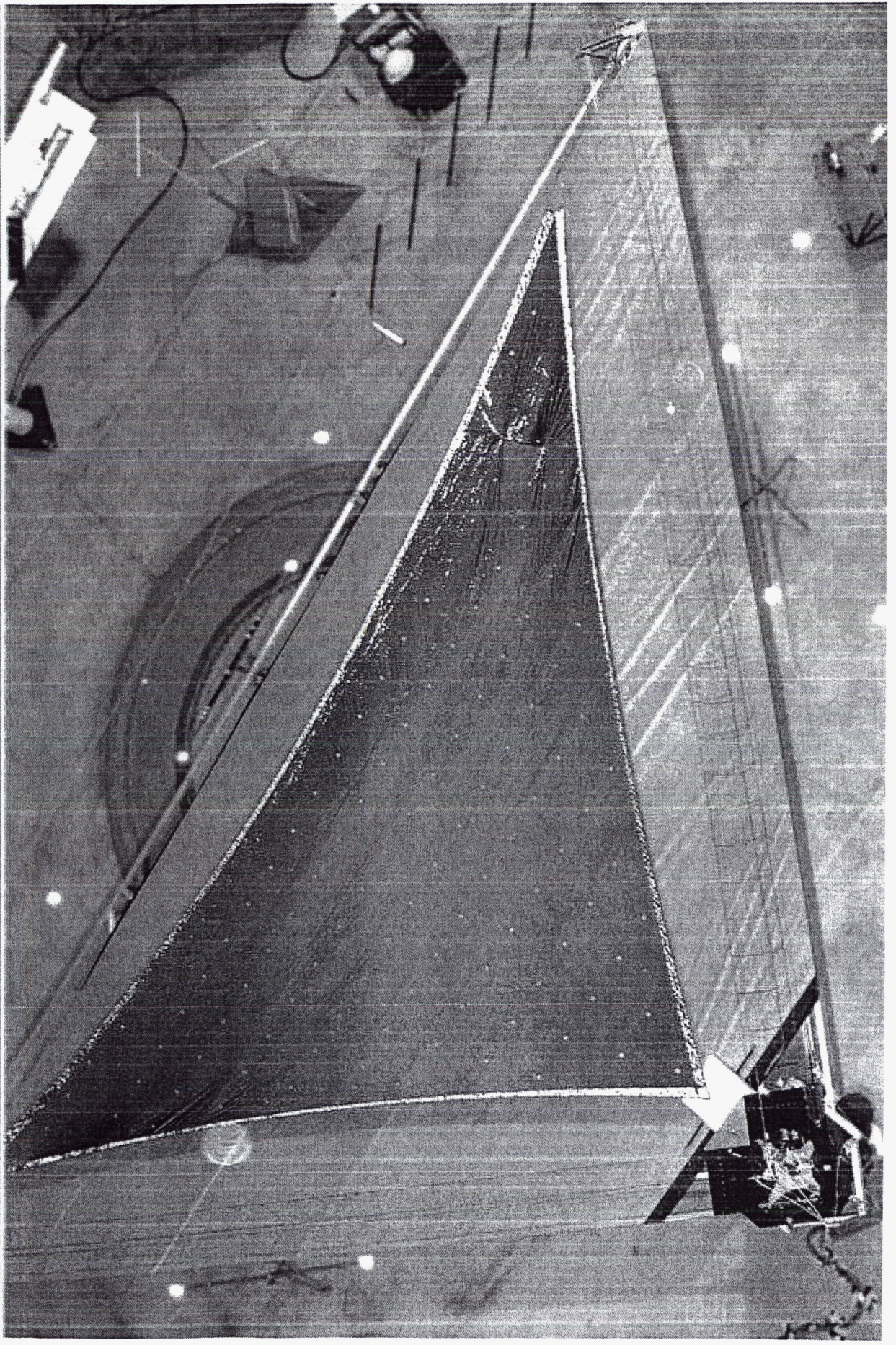
**Detail of  
Central  
Assembly**



**Validation of a Scan**

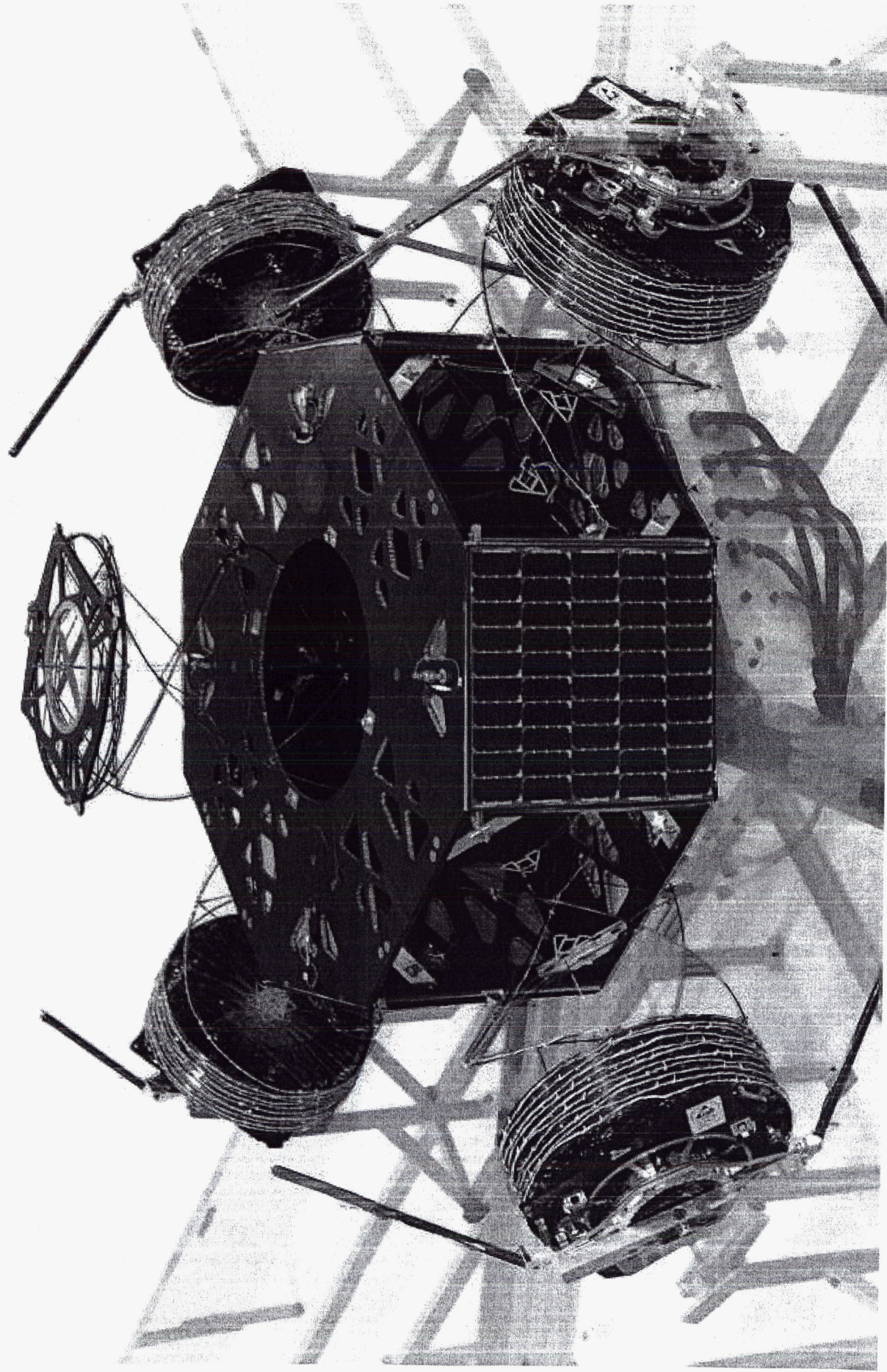


# PH. 2 10-M QUADRANT SYSTEM



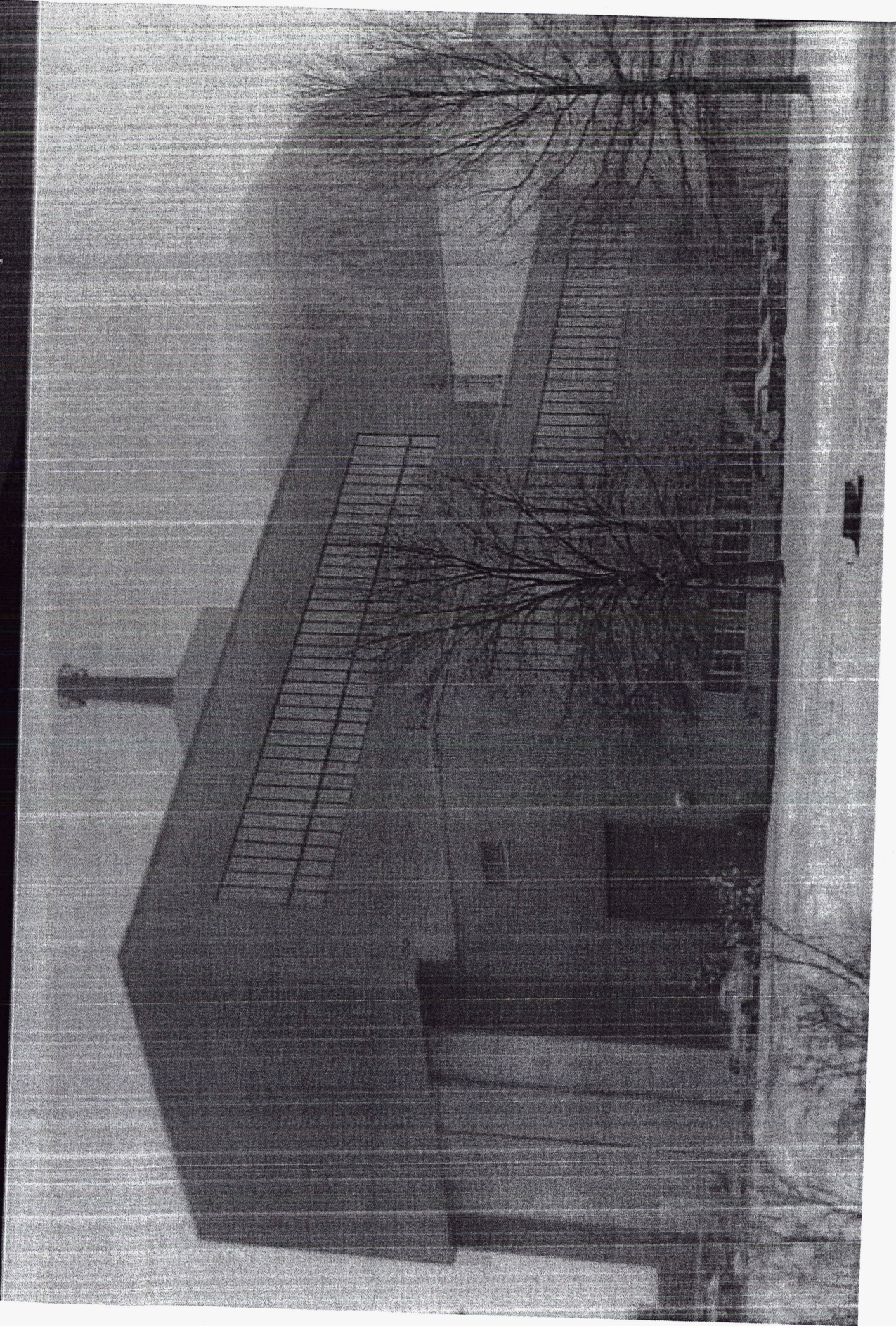


# S<sup>4</sup> • DEPLOYING AT ATK - GOLETA



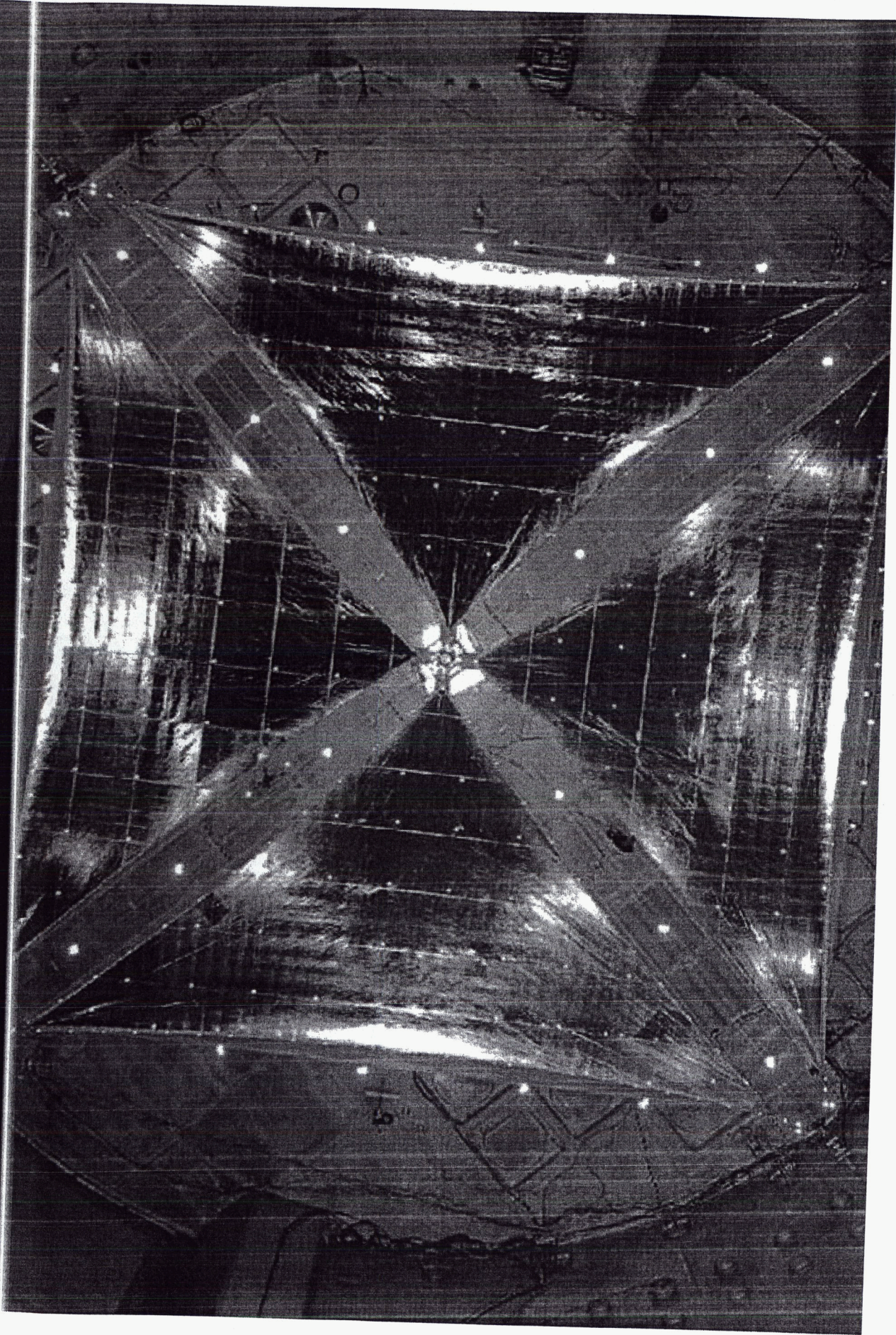


# NASA PLUM BROOK STATION, OHIO



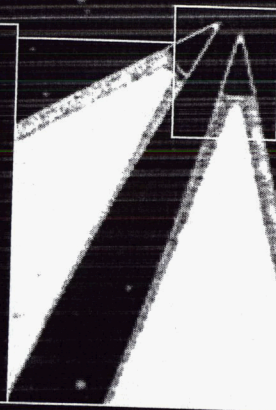
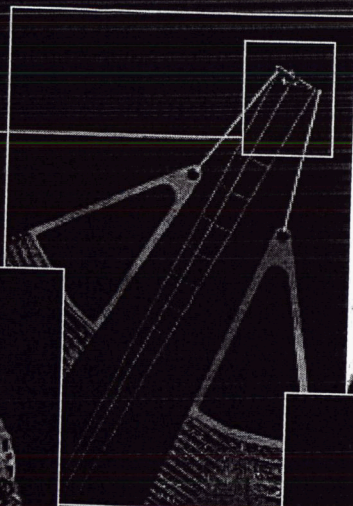
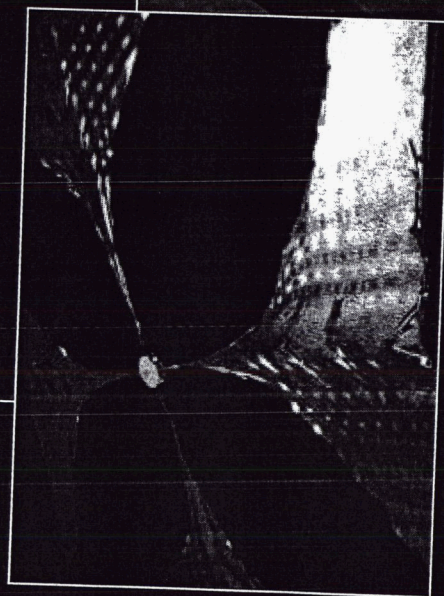
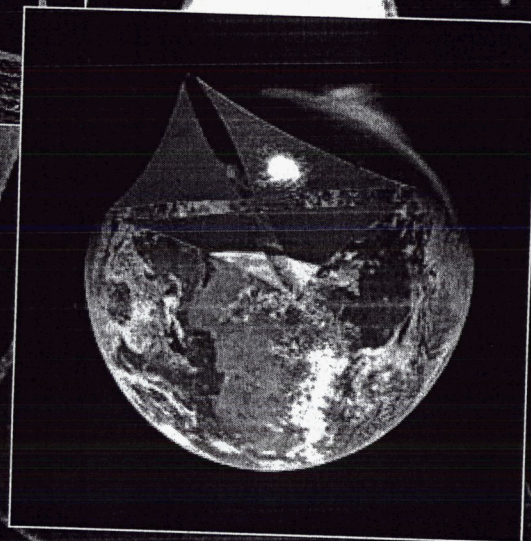
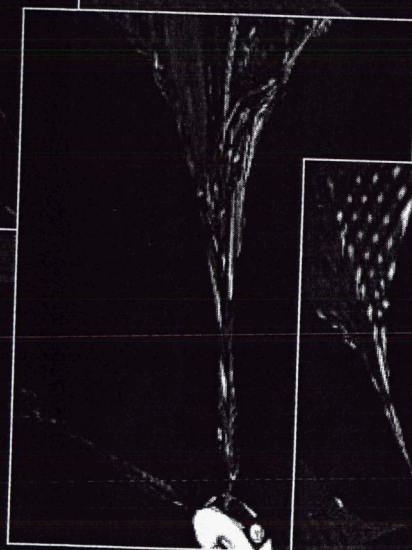
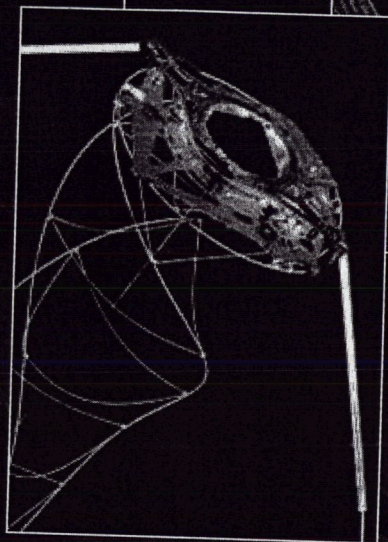
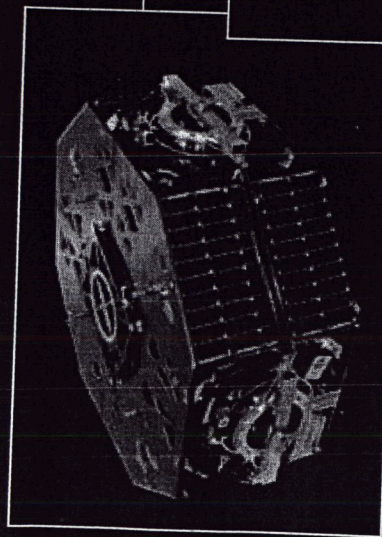


# PHASE 3 20-M SYSTEM





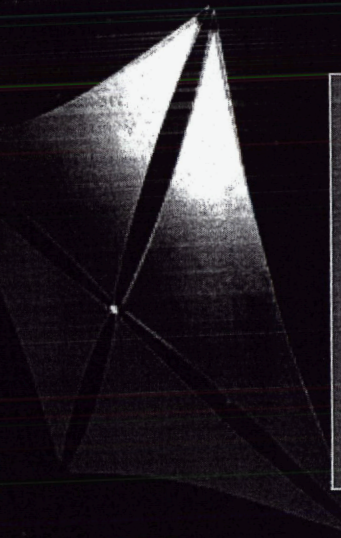
# S<sup>4</sup> • DEPLOYMENT IN ORBIT





# SCALABLE SQUARE SOLAR SAIL (S<sup>4</sup>)

## GROUND SYSTEM DEMONSTRATION TECHNOLOGY DEVELOPMENT TEAM



**NASA:** ISP Program Leadership

**MSFC:** ISP Project Management

**ATK Space Systems**  
Sail System Ground  
Demonstration Lead

**S. Montgomery**  
Project Manager

**D. Messner**  
Program Director

**SRS Technologies**  
Sail Assembly Provider  
Development & Validation

**A. English**  
COTR

**D. Murphy**  
PI - Technical Director

**G. Laue**  
Sail Lead

**ASU - PSS**  
ACS Trades, Modeling,  
and Implementation

**NASA - MSFC SEE**  
Materials Evaluation  
and Life Testing

**NASA - LaRC**  
Modeling and  
Dynamics Testing

**NASA - GRC**  
Plum Brook Test  
Facility Operations



# ISP - ATK 20-M GSD S<sup>4</sup> SYSTEM



**ATK** **SFS ASI**  
TECHNOLOGIES

